

# The Ecological and Evolutionary Drivers of Spatial Biodiversity Patterns

Alexander Skeels

---

Division of Ecology and Evolution

Research School of Biology

The Australian National University

---

A thesis submitted for the degree of Doctor of Philosophy

February 2020

© Copyright by Alexander Skeels 2020  
All Rights Reserved

# **Declaration**

This thesis contains no material which has been accepted for the award of any other degree or diploma in any university. Co-authored chapters are indicated, with order of authorship indicating the intellectual input and workload.

Alexander Skeels

February 2020

# Acknowledgements

First and foremost, biggest thanks go my supervisor Marcel for supporting my research interests as far back as 2014 when I signed on as an undergraduate in the Macroevoco lab. Thank you for actively encouraging me to pursue my (probably too) broad interests and to follow any random leads I had along the way. You are at least partially responsible for the jumble of topics covered here!

It has been a joy to be part of the eclectic Macroevoco Group so thank you to Lindell, Xia, Zoe, Russell, Andrew, Camille, David, Keaghan, Isaac, and Ollie, for all the cakes, crochet, and chats.

Thanks also to my panel, Craig Moritz, Dan Rosauer, and Nick Matzke, for help along the way and letting me tag along to lab meetings and coastal retreats. These thanks extend to all the macro-inclined people in E&E over the years (who really are a brilliant bunch) for help with lizards and statistics and other tricky things: Je, Leo, Marta, Ian, Iliana, Damien, Becky, Carlos, Octavio, and Renee.

Thanks to my family who I still don't think know what I do - but that's ok.

All my thanks and love to Bea.

Dedicated to Flip and Squiz

# Abstract

The form, function, and kinds of species that coexist together vary dramatically from place to place. These spatial patterns of biodiversity are the focus of biogeographical and macroecological research and offer us clues into the evolutionary processes shaping nature's variety. Finding general patterns and their underlying drivers, however, is not a straightforward task because a suite of ecological and evolutionary processes interact to shape patterns of biodiversity in the present-day. By integrating geographic, phylogenetic, phenotypic, and ecological data, and methods from the tool kits of community ecologists, macroevolutionists, and biogeographers, we can delve into the complexities shaping diversity patterns and get a more holistic understanding of their origin and maintenance.

In my opening chapter I briefly summarise the state of the field and introduce the outline of my thesis. The first two chapters forming the core of my thesis (Chapter Two and Chapter Three) present new methods to study spatial patterns of biodiversity. Chapter Two presents a process-based model of geographic range evolution and the geography of speciation. I use this model to make inferences about the history of speciation in thirty different plant and animal clades, highlighting some general taxonomic trends in speciation which have shaped biogeographic patterns in the present day. Then, in Chapter Three, I present a method to reconstruct temporal patterns in the evolution of biodiversity based on ancestral range estimates from historical biogeographic models.

The following three chapters present empirical studies which link community ecology, macroecology, and macroevolution to better understand spatial diversity patterns in plants and lizards. Chapter Four integrates phenotypic and spatial data to look at what drives global  
vi

patterns of species richness in ten different lizard clades, comprising over 6000 species. Chapter 5 and Chapter 6 explicitly investigate links between community ecology and macroevolution to look at the evolution of the Southwest Australian Biodiversity Hotspot flora, using a large genus of Australian plants, *Hakea* (family Proteaceae), as a case study. Chapter Five focuses on how macroevolutionary dynamics have led to a greater concentration of diversity of *Hakea* in the Mediterranean-climate-ecosystem of Southwest Australia compared to other biomes. Chapter Six narrows in on the Southwest biodiversity hotspot asking how pollination ecology in *Hakea* has evolved in response to high diversity of closely related species.

Finally, I conclude by highlighting how the preceding chapters, which cover a broad range of topics, are intertwined in the aim of linking ecological and evolutionary processes to better understand spatial diversity patterns, all forming pieces of the same puzzle. I also briefly highlight future directions. Together, my thesis investigates the evolution of diversity using different approaches, united by the common goal of finding a better understanding of the patterns of diversity we appreciate in the world today.

# Table of Contents

<b>Chapter 1:</b> Introduction .....	1
<b>Chapter 2:</b> Reconstructing the geography of speciation from contemporary biodiversity data .....	9
<b>Chapter 3:</b> Lineages through space and time plots: visualising spatial and temporal changes in diversity .....	56
<b>Chapter 4:</b> Alternative pathways to diversity across ecologically distinct lizard radiations .....	68
<b>Chapter 5:</b> Equilibrium and non-equilibrium phases in the radiation of <i>Hakea</i> and the drivers of diversity in Mediterranean-Type Ecosystems .....	106
<b>Chapter 6:</b> Ecological interactions shape the evolution of floral traits in communities across a temperate biodiversity hotspot .....	146
<b>Chapter 7:</b> Conclusion .....	176
<b>References</b> .....	187

# Chapter 1: Introduction

The uneven distribution of biodiversity around the globe is of perennial fascination to ecologists and evolutionary biologists alike. From spatial variation in the distribution of biodiversity, like the almost-ubiquitous trend for more species to be found at lower rather than higher latitudes, (the latitudinal diversity gradient, Fig. 1.1), to temporal variation in the origin of biodiversity, such as accelerating, decelerating, or constant rates of diversification through time seen in molecular phylogenies (Fig. 1.2), it has been a central aim in biology to identify general patterns, or ‘rules’, that govern the distribution of biodiversity across space and through time. Historically, however, different research programs have independently investigated the many different facets of biodiversity, and there has been a notable distinction between traditional ecological versus evolutionary approaches to understanding and explaining biodiversity.

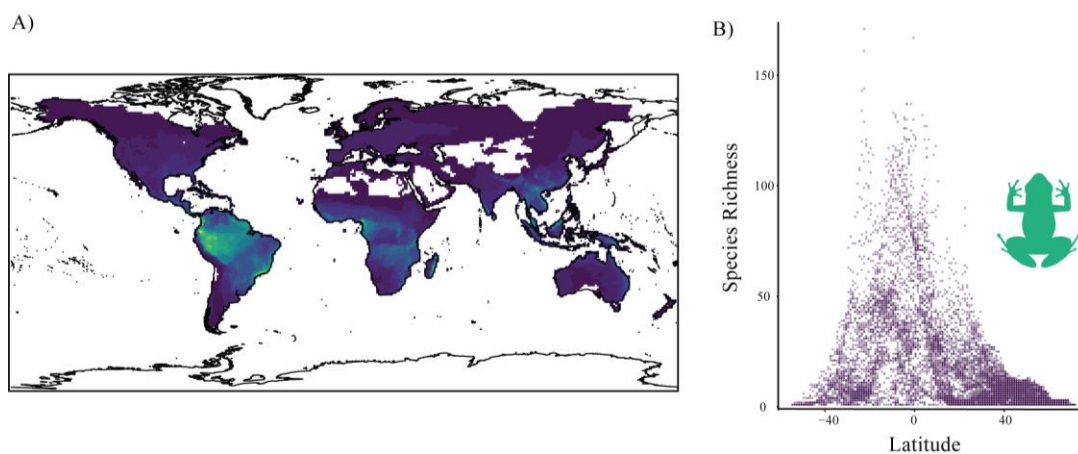


**Figure 1.1.** Spatial patterns of species richness of anurans in 1-degree grid cells (A) and the distribution of richness by latitude (B). Spatial data from the IUCN ([iucn.org](http://iucn.org)).

An ecological approach aims to understand the distribution of biodiversity by looking at how interactions between species and their environments shape their present-day distributions within ecological communities and across environmental gradients. One of the first naturalists

to not only document, but also try to explain large-scale patterns in biodiversity, was Alexander von Humboldt, who today is recognised as one of the founders of modern macroecology. He noted variation in species richness and composition along altitudinal gradients and tried to explain this in terms of environmental variation related to the physical geography of mountains (von Humboldt 1807). These observations laid the foundations for the most fundamental concept in the ecological approach to biodiversity studies; the definition of species' ecological niches. Pioneered by Grinnell (Grinnell 2008), Elton (Elton 1946), and Hutchinson (Hutchinson 1959, 1978), the niche concept defines the subset of resources that each species utilises in an environment. MacArthur (MacArthur and Levins 1967; MacArthur 1972), was one of the first to formalise how niche differences or similarities between species can facilitate coexistence (or lead to the exclusion) of species in ecological communities, which sets limits on the number and kind of species that can share the same geographic space. It was this work that laid the ground rules for community ecology, which seeks to explain community structure and richness in terms of governing ecological interactions between species such as competition or mutualisms.

Macroecology, in a sense, extended the aims of community ecology to explain broad scale patterns of biodiversity with respect to environmental and ecological factors (as was previously the focus) but differed in having a renewed focus of regional and historical processes, such as the biogeographic histories of regions and the evolutionary dynamics of clades. The aims of macroecology are to statistically describe broad scale patterns in the distributions of species (Brown and Maurer 1989), including many recurring facets of diversity, for example species-area relationships (Simberloff 1976), species-abundance distributions (Preston 1948), latitudinal diversity gradients (Blackburn and Gaston 1997), and broad scale patterns of functional and phylogenetic diversity (Weiher et al. 1998; Purvis et al. 2005). The premise of

macroecology is that general patterns, repeated across taxa and regions, may have general drivers and that statistically characterising these patterns may give additional insight into the local and regional processes that generated them (McGill 2019).

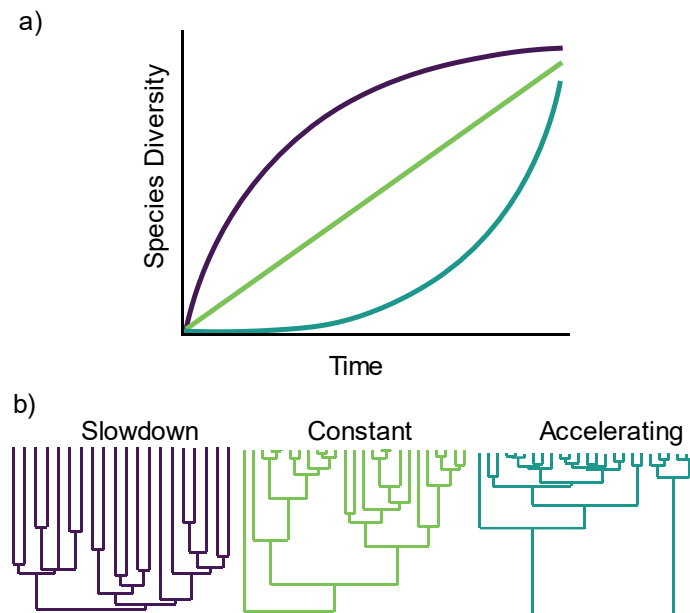


**Figure 1.2.** Lineages through time plots (a) from phylogenetic trees (b) simulated under three models of diversification with time-varying rates.

These ecological explanations for diversity generally differed from evolutionary ones, which primarily focused on the historical factors that lead to the origin (or extinction) of species, rather than patterns in the co-distribution of species in the present. Historical explanations place a greater weight on contingency as a factor that shapes the distribution and evolution of diversity, importantly recognising the roles of gradual and punctuated changes in earth's history as important drivers of diversity (e.g., plate tectonics and catastrophic mass extinction events). Wallace was perhaps one of the first to give a nuanced historical explanation for biodiversity patterns (Wallace 1876). He suggested that the stability of tropics allowed species to prosper

and become specialised through a variety of ecological interactions, whereas glaciation events destroyed diversity of higher latitudes. Wallace's hypotheses were extremely prescient, and this theory remains one of the major explanations for the latitudinal diversity gradient today.

The modern analytical macroevolutionary approach, however, has its roots in palaeontology, where the appearance and disappearance of different taxa from the fossil record presented evidence for how biodiversity has changed dramatically over time, with clades waxing and waning in diversity, punctuated by mass extinction events (Sepkoski 1978; Raup and Sepkoski 1982; Rohde and Muller 2005). The fossil record also presented evidence for evolutionary mechanisms behind periods of rapid diversification, adaptive radiations, in which the origin of key adaptation leads to the proliferation of species able to exploit a novel resource (Simpson 1953). The origin of molecular phylogenetics and divergence dating using molecular clocks and fossil calibrations gave rise to a complementary source of information on diversification dynamics and many predictions about the tempo and mode of evolution under different evolutionary scenarios were reformulated to make use of this new technology (Raup et al. 1973; Nee et al. 1992). For example, adaptive radiation was considered in terms of early-burst rates of evolution followed by a slowdown (Fig. 1.2; Harmon et al. 2010; Morlon 2014). More recently, we can fit complex models of lineage and trait diversification using molecular phylogenies (Morlon 2014), to better understand underlying processes, such as whether there are statistical associations between particular traits and rates of lineage diversification (Maddison et al. 2007; Caetano et al. 2018).

While evolutionary and ecological perspectives have traditionally been separated, it's hard to imagine a complete understanding of biodiversity without considering them in unison. We can think of species contemporary distributions as the result of two main processes, the geographic

context in which new species form and any subsequent range movement. Diversity itself, is then the outcome of any extrinsic or intrinsic factors that shape the rate in which new lineages form via speciation (and are lost to extinction) and the rate in which species co-occur (or no longer co-occur) via dispersal after diverging (Wiens and Donoghue 2004; Roy and Goldberg 2007). These two main processes are often considered evolutionary and ecological drivers of diversity respectively, however this is misleading because ecological and evolutionary factors shape both rates.

To coexist in geographic space species must share at least part of their abiotic niche, however species that share many aspects of their niche are likely to be in competition if resources are limiting (Elton 1946; Hutchinson 1959, 1978; MacArthur and Levins 1967; MacArthur 1972). Therefore, coexistence is thought to be driven by the interplay of convergent and divergent traits (Chesson 2000), allowing species to be similarly adapted to a geographic place, but not so similar to each other as to be in direct competition (Silvertown et al. 2006; Holt 2009). These interspecific interactions are shaped by the evolutionary history of clades (e.g., which niche differences already exist when two species come into contact; Webb et al. 2002b; Ackerly 2003; Kraft et al. 2007), but they also shape the future evolutionary landscape by changing the selective environment (Weber et al. 2017). This can drive the evolution of phenotypes (character displacement; Brown and Wilson 1956), ecological opportunities for population divergence and speciation (Schluter 2000), competitive exclusion and range contraction which may drive extinction (Rabosky 2013a), and the carrying capacities of environments (Cornell 2013; Rabosky and Hurlbert 2015a), all of which shape regional diversity patterns (Fine 2015a). Therefore, to understand spatial diversity patterns we need to understand the ecological context in which species are found today, the evolutionary context of lineage diversification and phenotypic evolution that has shaped the number and kind of species that exist in the

regional biota, and the interaction between the two over deep time – an extremely complex undertaking.

That ecological and evolutionary approaches to studying biodiversity are complementary, has long been acknowledged, and while part of the reason they have remained incompletely integrated is sociological (a trend of decreasing interdisciplinarity in academia), the other is conceptual: it is non-trivial to make predictions for patterns of phylogeny and the distributions of species and their traits, that link ecological and evolutionary processes. For example, ecological processes are often considered ephemeral, taking place over short time scales, and therefore unlikely to leave macroevolutionary signatures. However, more and more evidence suggests this is not the case, with competition and other ecological interactions shaping the evolutionary of phenotypes (e.g., Drury et al. 2018), the mode of speciation (e.g., Winkelmann et al. 2014), and diversification dynamics (e.g., Phillimore and Price 2008). As such, recent calls have been made to more holistically unify the study of biodiversity by bringing (back) together evolutionary and ecological approaches (Ricklefs 2004; Warren et al. 2014; Mittelbach and Schemske 2015; Pärtel et al. 2016; Weber and Strauss 2016; Weber et al. 2017; McGill et al. 2019).

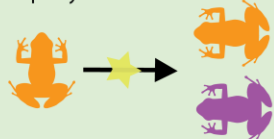
Here, I present five chapters which investigate biodiversity patterns across a diverse range of taxa, using different approaches and combining methods from different biodiversity sub-disciplines at the intersection of (macro)ecology and (macro)evolution (Box 1). In the first two chapters I present novel methods to make evolutionary inferences from phylogenetic and geographic range data. Firstly, I show how the geography of speciation leads to macroecological patterns in the geographic distributions of clades which we can use to make inferences about the prevailing mode of speciation. Then, I present a method to reconstruct

temporal patterns in the evolution of biodiversity based on ancestral range estimates from different historical biogeographic models. The following three chapters present empirical studies which link community ecology, macroecology, and macroevolution to better understand spatial diversity patterns in plants and lizards. Together, the chapters of my thesis are united by the common goal of finding a better understanding of the spatial patterns of diversity we appreciate across the world today.

### Box 1.3 Intersections between ecology and evolution

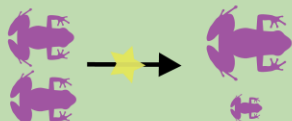
#### A. Speciation mode

Geographically separated populations can become new species by drift or local adaptation in isolation. Alternatively, intraspecific competition for resources can drive divergent selection which can lead to ecological speciation in sympatry or parapatry.



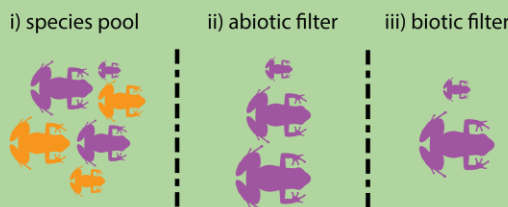
#### C. Trait evolution

Sympatric lineages that compete for resources may be under selection for ecological traits to diverge to minimize resource sharing and niche overlap. The availability of resources and number of competitors will impact the strength of selection.



#### D. Community ecology

The composition of species and traits in present-day assemblages is determined by evolved differences between species in the regional pool i) and their subsequent filtering into assemblages based on ii) suitability of the abiotic environment and iii) the absence of competitors.

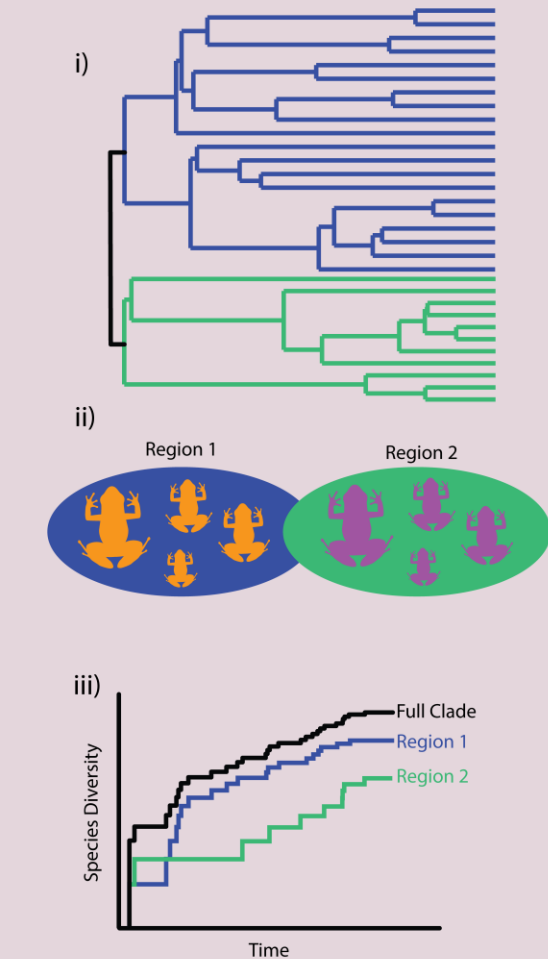


#### B. Lineage diversification

Ecological interactions can shape patterns of lineage diversification. This figure shows the diversification dynamics of a clade (i) split across two regions (green and blue; ii).

A diversity-dependent model of diversification predicts that as species diversity increases within a region so too does competition between interacting species which decreases ecological opportunities for speciation. This is predicted to leave a signature of diversification slowdown in the number of lineages present through time, as seen in the whole clade and in Region 1 (iii).

Placing diversification dynamics in their spatial context (iii) helps to explain differences in species diversity between regions.



## Chapter 2: Reconstructing the geography of speciation from contemporary biodiversity data



Skeels, A. & Cardillo, M. 2019. Reconstructing the Geography of Speciation from Contemporary Biodiversity Data. *American Naturalist*. 193 (2), 240-255.

## Abstract

Inferring the geographic mode of speciation could help reveal the evolutionary and ecological mechanisms that underlie the generation of biodiversity. Comparative methods have sought to reconstruct the geographic speciation history of clades using data on phylogeny and species geographic ranges. However, inference from comparative methods has been limited by uncertainty over whether contemporary biodiversity data retain the historic signal of speciation. We constructed a process-based simulation model to determine the influence of speciation mode and post-speciation range evolution on current biodiversity patterns. The simulations suggest that the signal of speciation history remains detectable in species distributions and phylogeny, even when species ranges have evolved substantially through time. We extracted this signal using a combination of summary statistics that had good power to distinguish speciation modes, then used these statistics to infer the speciation history of 30 plant and animal clades. The results point to broad taxonomic patterns in the modes of speciation, with strongest support for founder speciation in mammals and birds, and strongest support for sympatric speciation in plants. Our model and analyses show that broad-scale comparative methods can be a powerful complementary approach to more focused genomic analyses in the study of the patterns and mechanisms of speciation.

## Introduction

Speciation has an explicitly geographic context, as the spatial proximity of diverging populations will influence gene flow and the development of reproductive isolation (Mayr 1963; Coyne and Orr 2004; Wolf and Ellegren 2016). For example, populations bisected by physical barriers (vicariant speciation), or established by long distance dispersal (founder speciation) experience immediate reproductive isolation which may drive speciation (Mayr 1942, 1963; Coyne and Orr 2004). In diverging populations which are broadly overlapping (sympatric speciation), partially overlapping or adjacent (parapatric speciation), it is expected that ecological or phenotypic differentiation can drive divergence with gene flow by reducing contact between co-occurring populations in time or space, or by the development of genetic incompatibilities or decreased hybrid fitness (Turelli et al. 2001; Bolnick and Fitzpatrick 2007). Hence, particular geographic modes of speciation are likely to be associated with particular evolutionary processes, although the association may not always be clear-cut (Bolnick and Fitzpatrick 2007; Fitzpatrick et al. 2009).

Increasingly, detailed molecular and ecological data are being used to reconstruct mechanisms of population divergence within species or species-groups, with an emphasis on the genomic architecture underlying the inhibition of gene flow (Savolainen et al. 2006; Seehausen et al. 2008; Luebert et al. 2013; Jónsson et al. 2014; Egan et al. 2015; Li et al. 2015). However, there remains a great deal of interest in a more broad-scale, explicitly geographic approach that aims to reconstruct geographic speciation modes within clades, using comparative methods and readily-available, contemporary biodiversity data (Barraclough and Vogler 2000; Fitzpatrick and Turelli 2006; Phillimore et al. 2008; Anacker and Strauss 2014; Cardillo and Warren 2016). Comparative methods for reconstructing speciation modes are based on the expectation that

speciation history should leave a detectable signature in present-day patterns of phylogeny and species geographic distributions (Lynch 1989; Chesser and Zink 1994; Barraclough et al. 1998; Figure 2.1). For example, under both vicariant and founder speciation, recently-diverged sister species ought to show little or no overlap in their geographic ranges, whereas sympatric speciation is expected to produce sister species with complete or near-complete spatial overlap (Chesser and Zink 1994; Figure 2.1). Founder speciation is expected to result in highly asymmetric range sizes among sister species, because the process of speciation by long-distance dispersal is typically thought of as a daughter species with a very small initial population being seeded by a more widely distributed ancestral species (Gavrilets and Hastings 1996), and we would expect this to also lead to a greater geographic distance between sister species ranges at speciation (range isolation). Under vicariant and sympatric modes of speciation, on the other hand, the relative sizes of sister species ranges could range from very similar to highly asymmetric (Figure 2.1).

Speciation mode	Range overlap	Range asymmetry	Range isolation
Vicariant	low	no prediction	high
Parapatric	moderate	high	low
Founder	low	high	very high
Sympatric	high	no prediction	low

**Figure 2.1.** A graphical representation of four geographic speciation modes with *a priori* predictions of how these might affect key features of sister-species range geometries (range overlap, range-asymmetry, and range isolation).

Early comparative studies made use of these kinds of expectations to develop summary measures that attempted to provide diagnostic indicators of the prevailing geographic mode of speciation in a clade (Lynch 1989). For example, age-range correlations (ARC) fit a regression of divergence time against degree of range overlap among all pairs of species in a clade, with the expectation that both the intercept and the slope allow us to distinguish a primarily sympatric from a primarily allopatric speciation mode across the clade (Lynch 1989; Chesser and Zink 1994; Barraclough et al. 1998; Fitzpatrick and Turelli 2006). However, comparative approaches to reconstructing speciation history have often returned results that are equivocal, or do not strongly support any particular hypothesis (Fitzpatrick and Turelli 2006). The major criticism levelled at comparative approaches based on contemporary data is that species distributions are dynamic: the spatial configurations of geographic ranges soon after the time of speciation might be erased subsequently by the movement of species range boundaries (Losos and Glor 2003). This may (for example) lead to secondary transitions to sympatry from originally allopatric distributions (Pigot and Tobias 2014), or lead to more symmetrical sister-species range sizes as the smaller-ranged daughter species expands geographically (Barraclough and Vogler 2000). A critical question, which has remained largely unanswered by previous comparative studies, is to what extent do present-day geographic ranges of species retain the historic signal of speciation, and to what extent do they reflect post-speciation range movement and evolutionary processes? The answer to this question determines our confidence in the ability of comparative methods to reconstruct speciation history from contemporary biodiversity data.

In a large part this will depend on the extent, speed, and predictability of post-speciation range movement. The theoretical expectations are mixed. Closely-related species with conserved environmental niches might track changing climates in a similar way, maintaining the spatial

relationships of their distributions even as the distributions themselves change. Alternatively, niche evolution might lead species along divergent trajectories in response to climate changes (Ackerly 2003). In most cases, empirical testing of these processes is limited to inferences from indirect evidence, and the evidence to date is also mixed. On the one hand, geographic range positions tend to show strong phylogenetic signal, suggesting that species current distributions reflect distributions at the time of speciation, modified by gradual drift of range boundaries (Cardillo 2015). On the other hand, it has been shown that range shifts in response to changing climate, such as during Pleistocene glacial cycles, have sometimes been both rapid (Hewitt 2000), and idiosyncratic (Jackson and Overpeck 2010).

The aims of this study are twofold. The first aim is to investigate the degree to which the true speciation history of clades is detectable, and different geographic speciation modes distinguishable, from contemporary data on species distributions and phylogeny. To do this we construct a process-based simulation model of dynamic range evolution and diversification (the DREaD model), in a way that reflects our expectations of how species ranges evolve and shift following speciation events. Our model incorporates some of the most likely determinants of range movement into the simulation framework; dispersal, niche evolution, and environmental change (Holt 2003; Sexton et al. 2009). By incorporating these processes and exploring the way they interact to determine present-day species ranges, our simulation model extends previous efforts to model the geography of speciation, which have focused primarily on random drift (Phillimore et al. 2008; Cardillo 2015). The second aim of this study is to use simulation-based inference methods to classify the geographic mode of speciation in 30 real clades of plants, vertebrates and invertebrates, to survey patterns in speciation mode across a broad range of taxonomic groups, biogeographic regions, and ecologies. We also ask whether clades show evidence of a predominant geographic mode of speciation (when most divergences in the

clades' history can be classified as a particular speciation mode), or if clades show evidence of multiple modes in their divergence history. We use simulation-based inference methods that allow us to perform model selection in a statistically rigorous framework (Csilléry et al. 2010) to let the data tell us, in a way that incorporates the complexity and stochasticity of evolutionary and biogeographic processes, whether we can reliably distinguish different geographic modes of speciation in real clades.

## Methods

### Simulation model parameters

The DREaD model simulates the diversification of a clade and the evolution of geographic ranges in between speciation events, against the background of a gridded, heterogeneous landscape, in which each grid cell contains a value for a single, continuously-varying, hypothetical environmental variable (for a detailed description of the simulation model see the expanded methods in Appendix A). We modelled four distinct speciation modes; vicariant, sympatric, parapatric, and founder speciation (Figure 2.1), and one mixed model of speciation including all four modes. The simulation begins by randomly generating the grid values for the environmental variable, with a specified degree of spatial autocorrelation across the whole landscape using unconditional Gaussian simulation. We then seed the clade with an ancestral species, drawing its attributes (geographic range boundaries, niche position, and niche breadth) randomly from uniform distributions. At each time step the species is able to expand its range via dispersal into new grid cells that lie within the range determined by the clade's dispersal capacity ( $D$ ), and which have environmental values that fall within the bounds of the species niche (niche position  $\pm$  niche breadth). Dispersal occurs against a background of environmental

change through time, modelled in two ways: 1) cyclical, with environmental change modelled as a sine wave with parameters for amplitude, ENV<sub>A</sub> and frequency ENV<sub>F</sub>; and 2) directional, with environmental change modelled as a linear increase with a parameter for the slope, ENV<sub>S</sub>. Each environmental change model was either spatially homogenous, where each grid cell changes by the same amount at each time step, or spatially heterogeneous, where the degree of change of each cell is a linear function of its latitude. Hence, we model four different environmental change scenarios. Environmental change had the effect of reducing a species geographic range if the environmental values of occupied cells changed so that they no longer fall within the niche of the species.

Concurrently, at each time step, one of six different events is able to occur: vicariant, sympatric, parapatric, or founder speciation, extinction, or no-event. Speciation probability is modelled as a Gaussian function of range size, in which the per-lineage speciation rate is greatest at intermediate range sizes (Rosenzweig 1978; Gaston 1998). The probability of stochastic extinction decreases logarithmically with range size, so the per-lineage extinction rate is greatest in narrowly distributed species and reaches zero in species with range sizes equal to or larger than a minimum range size threshold  $m$  (Rangel et al. 2007; Appendix A). The predominance of a particular speciation mode is enforced by setting the values of the speciation rate constant ( $\lambda$ ) separately for each speciation mode. A mixed model of speciation is determined by setting equal  $\lambda$  values to all modes.

The basic geographic modes of speciation in the simulation model are sympatric, parapatric, founder and vicariant. Each of these modes is modelled as follows:

*Sympatric:* Under the sympatric model, one daughter species maintains the range of the parent and the other occupies a range that lies completely within the boundaries of the parent

species. This is chosen by randomly drawing four coordinates from within the parent species range, which form the boundaries of the daughter species range.

*Parapatric:* Parapatric speciation occurs via budding at the range periphery. The new species is formed by creating an abutting range that may partially overlap the parent range. This is done by selecting a cell within dispersal distance,  $D$ , from the parent species range boundary and drawing four distances from a uniform distribution (from 1 to  $D$ ) from this point to be the range boundaries of a new quadrant.

*Founder:* Founder speciation follows a founder-event model where dispersal events can found a new species in non-contiguous geographic space. Founder speciation proceeds by selecting a cell within the domain to be colonized with a probability inversely related to the shortest distance from the parent species range. The range boundaries are drawn by selecting 4 distance values from a uniform distribution (from 1 to  $D$ ) from the colonized cell.

*Vicariant:* Vicariant speciation is modelled in two different ways depending on the geometry of the species range. Firstly, if the species range is a single contiguous area, vicariant speciation will occur via bisection of this range, whereby a line is drawn randomly through the species range dividing it into two. The bisection is ambiguous with respect to the range size asymmetry of the daughter species ranges. The second method of vicariant division is used if a species range is fragmented. In this case, the parent species range is split so that each daughter species is composed of a cluster of range fragments that are in closer spatial proximity to each other than to the sister species. Clustering is performed with a k-means method (Hartigan and Wong 1979) on the x-y coordinates of the range fragments.

We model phylogenetic signal of the niche at speciation as follows. Under vicariant speciation, immediately following speciation both daughter species niche positions are recentred towards the mean environmental value of the species new range. Under founder, parapatric, or sympatric

speciation, the niche position of the budded daughter species (the smaller ranged daughter species) is recentered. The degree to which the species shifts its inherited niche position value towards this new value is modelled with the parameter PS, the proportion of the step between the current niche position and the mean environmental value that the new species will take. A PS value of 1 means the species will move completely towards the mean, while a value of 0 means the new species will inherit the same niche position as the parent . In this way, the PS parameter controls the strength of “punctuational” evolution of the niche at speciation events. We also model evolution of the niche along the branches of the phylogeny by allowing a species niche position and niche breadth to drift independently under a modified random walk model of trait evolution, controlled by the rate parameters NE<sub>P</sub> (for niche position) and NE<sub>B</sub> (for niche breadth). Species niche positions and breadths drift randomly under the single condition that the environmental value of at least one grid cell within the species range must remain within the species niche (niche position ± niche breadth).

## Running the simulation model

We simulated range evolution and speciation under different scenarios of environmental change, niche evolution, dispersal rate, clade size, and geographic speciation modes. Parameters were sampled from uniform prior distributions, using Sobol sequences to efficiently explore parameter space (Burhenne et al. 2011; Appendix A), reducing the number of simulation replicates required to effectively explore parameter space. We ran the simulation 36000 times until a clade of size  $n$  was generated (Table A2.1), discarding 269 simulations which could not be completed because the parameter combination led to total clade extinction more than five times successively. This lead to roughly 7200 replicates for each speciation scenario, which is considered adequate for model selection in an ABC framework (Pudlo et al.

2016). At the completion of each simulation we retained the resulting phylogeny, each tip species final geographic range, the environmental grid, and a data frame containing information on the final niche position, niche breadth, range size, and mode of speciation at each node in the phylogeny. From this output we generated 30 summary statistics that describe aspects of species geographic range overlap, range size asymmetry, range isolation, range size, and phylogenetic tree shape, within each clade. We reduced these 30 summary statistics to a set of 14 using a variable selection procedure (Appendix A; Table 1). Our simulations were written and implemented in R version 3.4.2.

**Table 2.1.** List of summary metrics used for the study of the geographic mode of speciation with description and supporting references.

Summary metric	Description	Abbreviation
Age-Range Correlation	Slope and intercept of regression between phylogenetic node age and geographic range overlap among nodal descendants (Fitzpatrick and Turelli 2006).	ARC <sub>slope</sub> , ARC <sub>intercept</sub>
Sister species overlap x divergence times	Intercept of regression between sister species range overlap and divergence times. Similar to ARC but using only sister species.	RO <sub>intercept</sub>
Mean range overlap of sister species	Range overlap = proportion of range of the smaller ranged sister species found within the larger ranged sister species.	RO <sub>mean</sub>
Sister species sympathy proportions	Proportion of species which have values of range overlap $\geq 0.9$ , or 1.0	RO <sub>90</sub> , RO <sub>100</sub>
Difference between sister species overlap and sister – outgroup overlap	The mean of the difference in the overlap between sister species and the overlap of each sister species with an outgroup species. Scaled between -1 where species overlap completely with outgroups and not at all with each other, and 1 where sisters completely overlap with each other and not at all with outgroups (Cardillo 2015).	TO <sub>mean</sub>
Range asymmetry x divergence times	Slope and intercept of regression between range asymmetry and divergence times.	Asym <sub>slope</sub> , Asym <sub>intercept</sub>
Mean and standard deviation of standardised range size	Standardised range size for each species = range size / largest range size in clade. Measured across all tip species in the phylogeny.	RS <sub>mean</sub> , RS <sub>SD</sub>

---

SD of standardised distance between sisters species ranges	Standardised range distance = minimum distance between sister species ranges / maximum distance between two species in the clade.	$RD_{SD}$
Range isolation x divergence times	Intercept of regression between standardised range distance and divergence times.	$RD_{intercept}$
Sackin's Index	Phylogenetic tree imbalance (Blum and Francois 2005).	SI

---

## Analysis of simulation outputs

We compared the distributions of each summary statistic for simulated clades generated under different geographic speciation modes, using pairwise Kolmogorov-Smirnov tests (KSt). Our simulations generated large sample sizes (~7,200 replicates for each speciation scenario), which may return significant p-values even when the effect sizes are small. To reduce the chance of misinterpreting significant differences we ran the analysis across 500 randomly subsampled simulation replicates 100 times, and took the mean values of the test statistic and p-value. Next, we asked whether the signal of speciation is stronger than the signal of geographic range evolution in present-day (simulated) data, by exploring which model parameters explained the greatest amount of variation in the summary statistics independent of all other model parameters. To do this we used a hierarchical partitioning protocol (Chevan and Sutherland 2017) which assesses all possible combinations of independent variables (model parameters) on the response (summary statistics) in a generalized linear modelling framework and partitions the variance according to a goodness of fit statistic ( $R^2$ ). This allows for the independent assessment of each parameter's contribution while removing the effects of multicollinearity. Hierarchical partitioning was implemented in the R package hier.part (Walsh and MacNally 2013).

## Empirical data collection

We used the outcomes of the simulation model to infer speciation modes in a selection of empirical datasets. We collected spatial and phylogenetic data for 30 clades (six plant, two fish, one invertebrate, four amphibian, four reptile, five mammal, and eight bird clades), selected to cover a range of taxonomic groups and levels, clade sizes, and geographic regions (Table A2.3). All selected clades were monophyletic and densely sampled, with >80% of known species included, and the majority with >90%. Spatial data for species distributions were obtained, where possible, as spatial polygons from the IUCN (<http://www.iucnredlist.org>) or BirdLife (BirdLife 2016), which depict species range extents based on both occurrence data and expert assessment of species contemporary distributions. Where range polygons were not available we used point occurrence records downloaded from GBIF (<http://www.gbif.org>) and cleaned of obvious outliers, or supplied from the supplementary materials of an associated article relating to the clade. Spatial polygons were estimated from occurrence points using a fixed-k convex hull method (Getz and Wilmers 2004). From the spatial and phylogenetic data we obtained the same summary statistics as for the simulated data.

## Model Selection

To infer the predominant speciation mode in the empirical data sets we used three likelihood-free model selection and model classification techniques: a machine-learning Linear Discriminant Analysis (LDA), and two Approximate Bayesian Computation (ABC) approaches. We tested the discriminatory ability of our candidate summary statistics to distinguish speciation modes for each method using a leave-one-out cross validation procedure, calculating the rate of model misspecification for each geographic speciation mode (the

reclassification accuracy). We then inferred the geographic mode of speciation in the 30 empirical datasets using LDA, implemented using the caret (Kuhn 2016) package in R, and two ABC methods (multinomial logistic regression, and neural net), implemented with the abc package (Csilléry et al. 2012). An illustrated example of the simulation and model selection pipeline can be seen in Figure 2.2. Derived summary statistics for both empirical and simulated data are deposited in the Dryad Digital Repository, DOI: doi:10.5061/dryad.d9j09bm (Data Table A and Data Table B respectively).

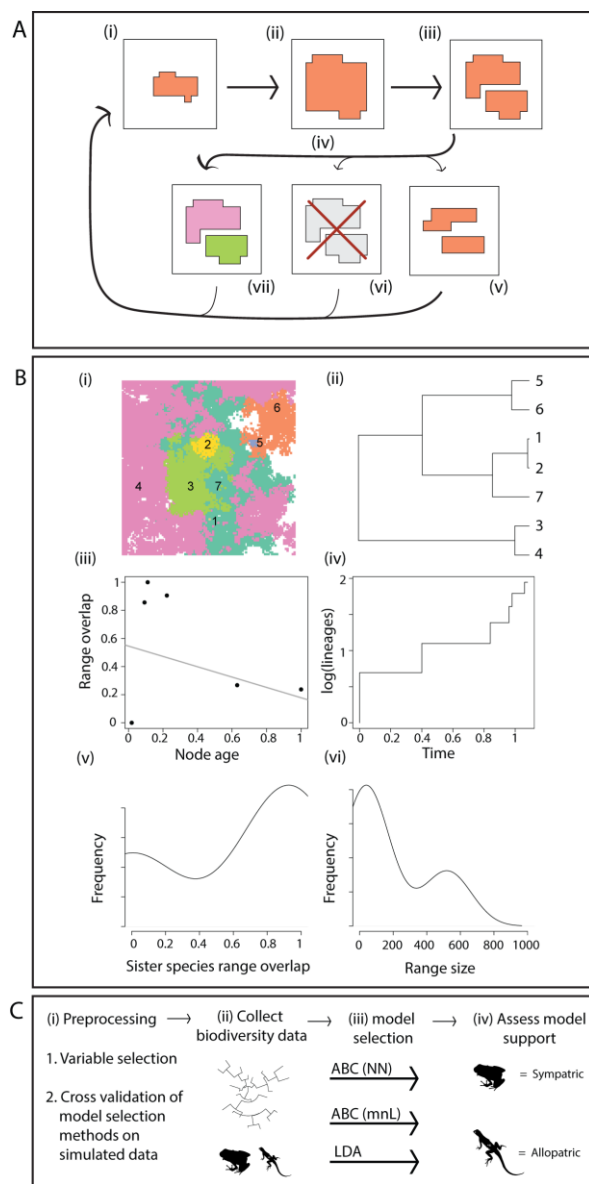


**Figure 2.2.** Schematic of the simulation procedure (A), simulation output (B), and model selection procedure (C). (A) Simulation workflow: at each time step (i) each species geographic range can (ii) expand via dispersal, (iii) change due to changes in the distribution of suitable habitat; (iv) probabilities of each event are assessed and one event is selected from: (v) niche evolution; (vi) extinction; and (vii) speciation. This algorithm is repeated until a clade of a given number of species is generated. (B) Simulation output: the simulation generates (i) a set of species distributions and (ii) a phylogenetic tree. Summary metrics are then derived from the final output, including (iii) range overlap x node age, (iv) temporal distribution of nodes ( $\gamma$ ), and (v) distribution of sister species overlap and range size. (C) Model selection procedure: (i) data processing and model validation, (ii) generating summary statistics for clades of interest, (iii) implementing model selection procedures, and (iv) identifying support for different geographic speciation modes based on posterior probabilities.

## Results

Simulation results: speciation mode, range evolution and biodiversity summary statistics

Across our simulated dataset, many of the summary statistics exhibited enough variation between speciation modes to provide discriminating power. Variance partitioning showed that, of the parameters included in the simulations, the geographic mode of speciation had the largest independent effect on 12 of the 14 summary statistics (Figure 2.3A), while the rate of niche position evolution explained more of the variation in two summary statistics,  $RD_{intercept}$  and  $TO_{mean}$ . Pairwise KSt confirmed that distributions of the 14 retained summary statistics were significantly different between speciation modes (Figure 2.4). The KSt identified two summary statistics ( $RO_{intercept}$ ,  $Asym_{intercept}$ ) that were able to distinguish between nine of the ten pairwise comparisons among the five speciation models, and a further two ( $ARC_{slope}$ ,  $TO_{mean}$ ) that were able to distinguish between at least eight comparisons.

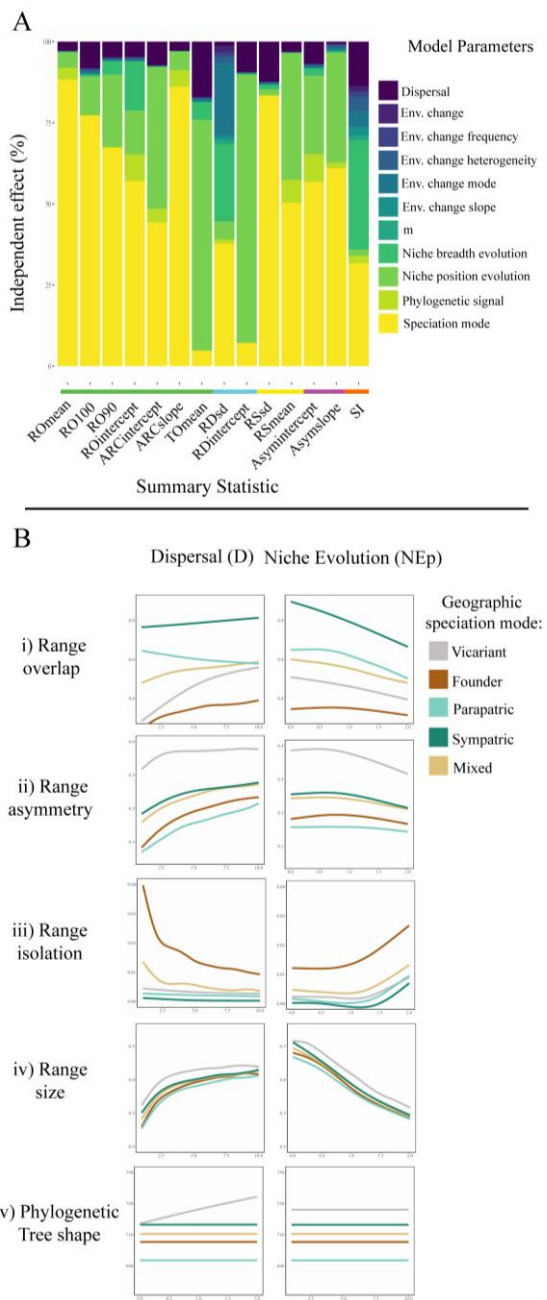


**Figure 2.3.** (A) Independent effect (% of variance explained) of each simulation model parameter on 14 summary statistics describing spatial and phylogenetic biodiversity patterns; and (B) relationship between five summary statistics and two key model parameters, niche position evolution ( $NE_P$ ) and dispersal rate ( $D$ ), for each of the five speciation modes. Summary statistics can be classified as describing either measures of range overlap (horizontal green line in 3A), range isolation (blue line), range size (yellow line), range asymmetry (purple line), or phylogenetic tree shape (orange line). 3B depicts the loess curves for one summary statistic from each of these categories to give a graphical impression of the general trends. i)  $RO_{\text{intercept}}$ , a measure of range overlap, ii)  $Asym_{\text{intercept}}$ , a measure of range size asymmetry, iii)  $RD_{\text{intercept}}$ , a measure of the distance between sister species ranges, iv)  $RS_{\text{mean}}$ , a measure of the average range size, and v) Sackin's index (SI), a measure of phylogenetic tree imbalance.

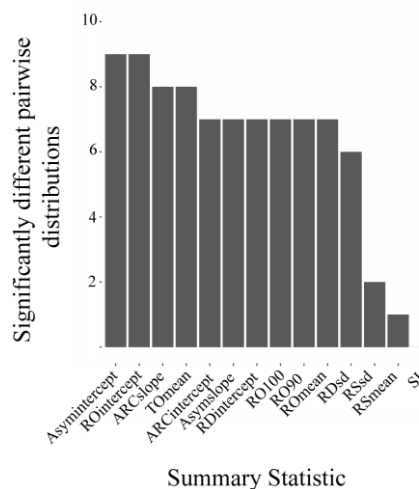


**Figure 2.4.** The number of significantly different comparisons of the distribution of 14 summary statistics between each pair of speciation modes in the simulated dataset. 10 pairs in total. Significance was tested using Kolmogorov-Smirnov tests

There were a number of broad patterns evident in the summary statistics generated from our simulated dataset: (1) Founder speciation led to the highest degree of range isolation and lowest range overlap; (2) Vicariant speciation resulted in larger absolute range sizes, low rates of range asymmetry, and more balanced phylogenetic branching; (3) Sympatric speciation resulted in the highest degree of range overlap and lowest range isolation; (4) Parapatric speciation resulted in highly imbalanced phylogenetic trees and asymmetrical range sizes (Figure 2.3B).

The relative difference between summary statistics for different speciation modes was generally consistent for different values of key model parameters (e.g., the degree of range overlap was higher in sympatric than vicariant speciation modes at different rates of niche position evolution; Figure 2.3B). However, variance partitioning showed that both the rate of niche position evolution ( $NE_p$ ) and rate of dispersal ( $D$ ) both explained a considerable amount of variance in a number of summary statistics (Figure 2.3A). Other parameters, including the rate of niche breadth evolution and the environmental change model, also explained a considerable

amount of variance in some parameters though this was less consistent across summary statistics (Figure 2.3A). Investigating relationships between estimated summary statistics and parameter values for key range evolution parameters, for each speciation mode separately, we found that the same values for several summary statistics could be produced by different speciation modes at different values of niche position evolution ( $NE_P$ ) and dispersal (D). This shows the interactive effect of speciation mode and range/niche evolution (e.g., range size asymmetry is similar when speciation is sympatric and dispersal rates are low, compared to when speciation is parapatric and dispersal rates are high; Figure 2.3B). Higher rates of niche evolution led to increased range isolation, decreased range size and range overlap, and greater asymmetry of range sizes. Dispersal rate, on the other hand, had an opposing effect, increasing range overlap and range size, while decreasing range isolation and range asymmetry. Furthermore, some summary statistics did not show clear directional trends with model parameters or shift in parallel across speciation modes. For example, phylogenetic tree shape (SI) showed an increasing trend with dispersal rate for the vicariant speciation model but no trend for other speciation models (Figure 2.3B).

### Empirical results: The geography of speciation across plants and animals

We asked if biodiversity summary statistics for 30 different clades, spanning a broad range of plant and animal taxa, are consistent with a single predominant mode of speciation within clades. We used three alternative model selection methods to infer the support for different speciation modes. We found that mammal clades tended to show strongest support for a founder mode of speciation, with two clades, the Madagascan lemurs (Lemuridae) and Australian Diprotodont marsupials (Diprotodontia), also showing strong support for vicariant speciation, especially under the two ABC methods, mnL and NN (Figure 2.5). Similarly, bird clades

showed strongest support for founder speciation, except for the Australian robins (Petroicidae), which showed equivalent levels of support for vicariant, mixed, and founder speciation, and the indigobirds/whydahs (*Vidua*) which showed strongest support for vicariant using mnL, and both mixed and vicariant speciation modes with LDA and NN. Founder speciation was also strongly supported in three of the four reptile clades, while support for different speciation modes was more variable among the amphibian, fish, and insect clades. Among plant genera, three (*Protea*, *Hakea*, *Bursera*) showed support for sympatric speciation under all three methods, one (*Sidalcea*) for parapatric speciation, and two (*Banksia*, *Mimulus*) for a mixed model of speciation, although LDA strongly supported sympatric speciation in these two genera. In only one of the 30 clades we tested (Myobatrachidae) was there strong support for an vicariant speciation mode across all three methods. Relative levels of support for different speciation modes tended to be consistent among the three methods (LDA, mnL and NN), although in general, the LDA method more frequently attributed strong support to a single speciation mode, while NN was more likely to apportion support more evenly among several modes.

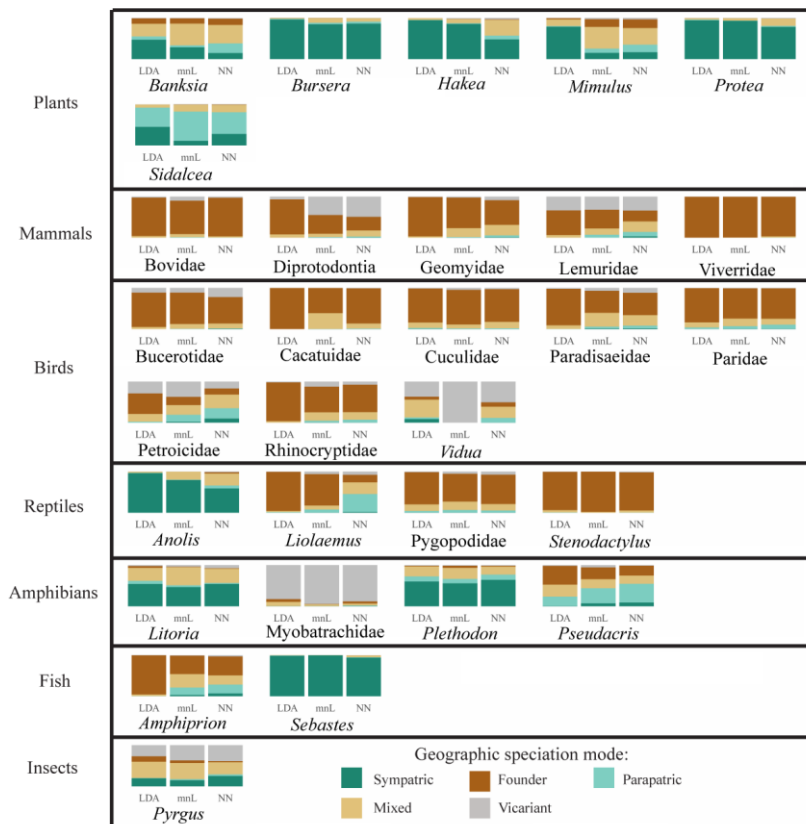


**Figure 2.5.** Posterior probabilities for inferred geographic speciation mode for 30 plant and animal clades. The height of the coloured bars indicates the relative support for each speciation mode under each of three model-selection methods: LDA = linear discriminant analysis, mnL = multinomial logistic regression, NN = neural net. Clades are grouped by higher taxa: mammals, birds, reptiles, amphibians, plants, fish, and invertebrates. Founder speciation shows the strongest support in birds, mammals, and reptiles, whereas sympatric, parapatric and mixed speciation modes tend to prevail in amphibians and plants.

Model classification accuracy was assessed using a cross-validation procedure for each method (LDA, mnL, NN). We found that reclassification accuracy was significantly better than random ( $\text{Kappa} > 0.6$ ,  $p < 0.001$  across three methods), and we were able to predict the correct model of speciation geography in 69%-71% of simulations. Vicariant speciation had the highest reclassification accuracy of all speciation models (>84%), followed by sympatric (>78%), founder (>73%), parapatric (>61%), and finally the mixed model (<46%). Model adequacy was assessed graphically by plotting the predicted values for the first two axes of a linear discriminant analysis for the empirical datasets onto the simulated datasets (Figure 2.6). The

empirical datasets fall within the range of our simulated data in all cases, so we can conclude that our simulations generated realistic biogeographic patterns (Pudlo et al. 2016).

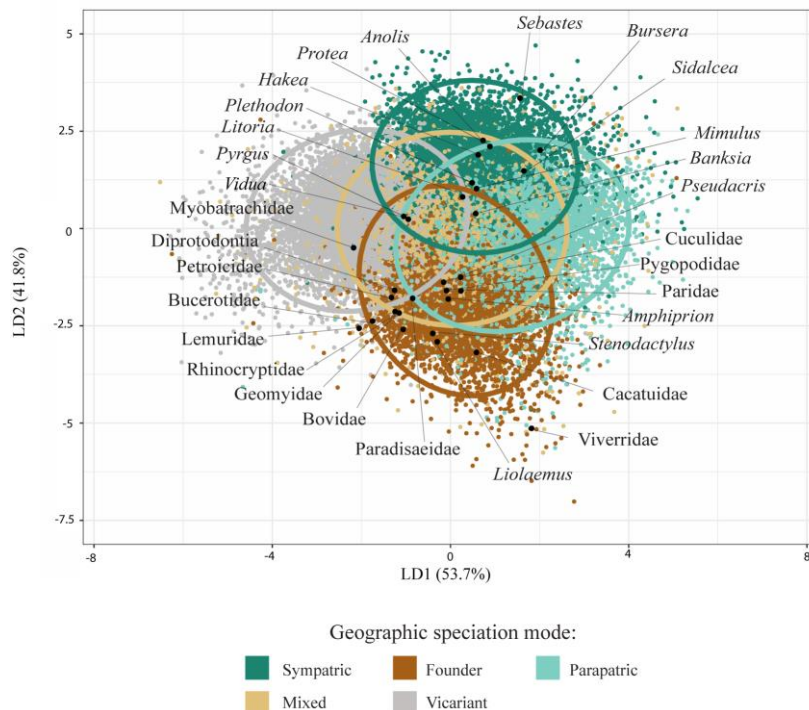


**Figure 2.6.** Projection of the first two axes of a Linear Discriminant Analysis (LDA) performed on simulated and empirical datasets. Coloured points show bivariate distributions of the first two axes of a LDA constructed from 14 biodiversity summary statistics. The summary statistics are derived from clades simulated under 5 geographic modes of speciation. Coloured ellipses contain 90% of all simulated datasets for a given speciation mode. Black points represent predicted values of 30 empirical plant and animal clades.

## Discussion

### Detecting the geographic mode of speciation

Comparative analyses to recover the prevailing geographic mode of speciation in clades have been limited by uncertainty over how much of the historic signal of speciation is retained in contemporary biodiversity data, and how much is eroded by post-speciation geographic range movement (Losos and Glor 2003). Previous attempts to model these processes have gone some

way to reducing the uncertainty, but their interpretation has remained rather ambiguous because models have been based on a limited set of processes, have typically applied only one or two summary statistics to recover signal from contemporary data, and have focused on hypothesis testing rather than model comparison and selection (Barraclough and Vogler 2000; Fitzpatrick and Turelli 2006; Phillimore et al. 2008; Cardillo and Warren 2016). Figure 2.3B illustrates why previous studies, based on one or two biodiversity summary statistics, have often lacked power to discriminate geographic speciation modes. Interactive effects between speciation mode and range evolution mean that models with different speciation modes can return similar values for summary statistics, depending on the range of dispersal and niche evolution parameters.

Our simulation model (DREaD), together with model selection methods based on 14 summary statistics that capture aspects of species range sizes, proximity, overlap, and phylogeny, show that the signal of speciation mode can indeed be detected in contemporary biodiversity data. Several of our analysis results point to this conclusion. First, the geographic mode of speciation had the strongest independent effect on the majority of summary statistics, compared to other simulation model parameters (Figure 2.3A). Second, simulations under different speciation modes produced summary statistics with consistently different distributions (e.g., Figure 2.3B, Figure 2.4). Third, the cross-validation procedures under both LDA and ABC methods had a considerably higher than random reclassification accuracy. This allowed us to infer the geographic modes of speciation in 30 empirical clades across a broad range of plant and animal taxa. The results point to a predominance of founder speciation in animals and of sympatric speciation in plants.

## Broad-scale patterns in speciation mode

Our reconstructions of geographic speciation modes for plant and animal clades reveal broad-scale taxonomic patterns in speciation mode across a wide range of organisms. For much of the 20<sup>th</sup> century allopatric speciation was widely considered the most likely mode of speciation, at least in animals, because of the theoretical requirement for disruption to gene flow in order to generate reproductive isolation (Mayr 1963). This idea has been supported by several comparative studies of speciation mode in mammals and birds (Fitzpatrick and Turelli 2006; Phillimore et al. 2008) and is supported for many vertebrate clades in our study. Despite the importance of allopatry in the formation of incipient species, debate over the relative importance of vicariance versus dispersal has been of interest in biogeography as these different mechanisms relate to fundamentally different processes - geographic isolation is environmental in the case of vicariant speciation (e.g. mountains, rivers, coastlines), and essentially biological in the case of founder speciation, since dispersal is associated with the mobility of individual organisms. Our result is consistent with recent evidence for the frequency of founder-event speciation in model-based biogeographic analyses (Cowie and Holland 2006; Matzke 2014), suggesting that the preponderance of allopatric speciation might be explained by the continual dispersal “attempts” being made by individual organisms being driven beyond their range limits (propagule pressure; Levin 2006), compared to the relative infrequency of the geological events that cause a population to be subdivided (Gaston 1998).

More recent theoretical developments have shown that speciation can occur with geographic range overlap and the opportunity for gene flow (Gavrilets et al. 2000; Baack et al. 2015a). A number of studies have demonstrated this empirically (e.g. Barluenga et al. 2006; Savolainen et al. 2006; Seehausen et al. 2008; Peakall et al. 2010) and suggest it may be common, especially

in higher taxa such as plants (Anacker and Strauss 2014; Grossenbacher et al. 2014), and under certain conditions, in animals (Bush 1994; Via 2001; Nosil 2008; Rosser et al. 2015). Our results support this suggestion by inferring a prevailing sympatric mode of speciation for many of the plant clades we examined, as well as in several herptile clades (*Anolis*, *Litoria*, and *Plethodon*), and the rockfish genus *Sebastodes*. Many of these groups are hypothesised to have diversified by mechanisms of ecological divergence, a key step in establishing a unique species identity in the face of gene flow. The Caribbean lizard genus *Anolis* is, in fact, a textbook case study for repeated speciation by the divergence of co-occurring island populations into habitat-specific ecomorphs (Mahler et al. 2010). In plants, sympatric speciation has always been considered to be more prevalent than in animals, because of strong divergent or disruptive selection that can be exerted by ecological mechanisms such as differences in flowering times or soil-type specialization (Savolainen et al. 2006), and because plants are considered prone to speciation by genome duplication leading to polyploidy (Rieseberg and Willis 2007).

## Geographic range evolution

Although the mode of speciation was the major driver of spatial and phylogenetic patterns in our simulated data, there were strong interactive effects of niche evolution and dispersal with the mode of speciation. Niche position evolution was negatively correlated, and dispersal positively correlated, with range overlap, such that low rates of niche evolution (i.e. niche conservatism: Wiens 2004) and a high rate of dispersal were both associated with a higher degree of range overlap between closely related species. The explanation of this effect in our simulation model also suggests a plausible biological scenario in the real world, as follows: if allopatric sister species inherit a similar environmental niche from their common ancestor, then in a spatially autocorrelated landscape the most suitable habitat for a species is likely to be

found within the range of its sister species. A high dispersal capacity will offer many opportunities for sister species ranges to move back into sympatry (Pigot and Tobias 2014). This suggests that the degree of spatial autocorrelation in key environmental niche variables for a given clade may be important: if niches are conserved, stronger spatial autocorrelation should exert a pressure for distributions of sister species to overlap. A further process that could counteract this pressure for sister species to overlap is biotic interaction. We did not incorporate biotic interactions (such as interspecific competition) into our model because it adds a substantial layer of complexity and is probably best tackled as a separate question, but it is conceivable that in some cases, competition serves to minimize range overlap and maintain allopatric distributions (Pigot and Tobias 2013; Wisz et al. 2013; Pigot et al. 2018). We suggest this should be an important avenue for further development of our model.

Environmental change parameters did not exert a strong influence on the distribution of the summary statistics, possibly because of a filtering effect. If a species cannot disperse rapidly enough to track environmental change, there will be a high probability of it going extinct, leaving no record in contemporary phylogenetic and geographic data. Furthermore, species that are severely affected by climatic change may be a phylogenetically biased sample, if closely-related species inherit from their common ancestors a similar capacity to disperse, similar ecological traits that put them at risk of extinction, or occupy habitats that are differentially threatened (Parmesan 2006). Depending on the phylogenetic conservatism of key environmental niche traits, we might therefore expect closely related species to show similar responses to environmental fluctuations. In some cases, this could elevate the probability of extinction of the entire clade, while in others it may serve to maintain the relative spatial relationships of species ranges.

## Model assumptions and caveats

Like any model of complex systems, the DREaD model necessarily makes a number of simplifying assumptions. As already mentioned, we omit the possible role of biotic interactions in limiting species range boundaries. Additionally, our modelling approach follows, *a priori*, the simplifying assumption that speciation can be categorized into a set of discrete geographic modes. The geography of speciation, however, could instead be described by a continuum from complete spatial separation to complete overlap (Fitzpatrick et al. 2009). There is empirical evidence to suggest that many speciation events may be best explained with varying degrees of range overlap along this continuum (Pinho and Hey 2010). Furthermore, each individual speciation event may involve a protracted process in which populations pass through various stages of allopatry and sympatry. For example, gene flow between populations may recur at different stages of the speciation process (Rundle and Nosil 2005; Nosil 2008) with genetic variation accumulating in allopatry, then becoming sorted into sympatric populations through introgression (Feder et al. 2005; Poelstra et al. 2018). In such cases, whether we can identify the one predominant geographic mode of speciation is unclear. Our model is phenomenological and simulates divergence at the lineage level rather than the population level, so we cannot rule out more complex speciation histories of the clades we have investigated. We believe there is some value in classifying speciation modes into discrete categories at this level of investigation. For example, if speciation is completed in sympatry, then a spatial model of sympatric speciation may adequately capture the spatial patterns of divergence even if the processes by which those patterns emerge are not explicitly considered. Nevertheless, we acknowledge that definitions of allopatry and sympatry often fall in a grey area that defies simple categorisation.

We treat speciation mode as a categorical parameter in our model to compare whether one particular speciation mode predominates in the evolutionary history of each clade, or a mixed model of speciation better explains the data in a model selection framework. However, as the mixed model had poor reclassification accuracy in the simulation analysis there may be a bias towards under-representation in the posterior probabilities of our model selection procedure. This may partially explain the tendency for greater support for single speciation modes in the clades we investigated. We suggest that a future avenue of research should be to allow the frequencies of different speciation modes ( $\lambda$  parameter) within a clade to be estimated from the data. In fact, several model-based methods for reconstructing ancestral ranges already do this (e.g., DIVA: Ronquist 1997; DEC: Ree and Smith 2008). However, these methods differ from DREaD in that they treat geographic ranges as the occupancy of discrete biogeographical regions, they do not explicitly model speciation as a function of the configuration of species ranges in continuous space and are aimed at reconstructing large-scale biogeographic shifts rather than the geographic mode of speciation.

As well as the relative values of  $\lambda$  between modes, the absolute rate of speciation and the function linking range size to the probability of speciation require further exploration. The justification of a peaked relationship between range size and speciation is largely based on theory regarding the placement of barriers and likelihood of vicariant speciation (Rosenzweig 1978; Gaston 2003), however, whether we expect the same relationship to hold with other speciation modes is unclear as there is little empirical evidence on which to base the parameterisation of this model component. It is possible that different relationships between speciation mode, range size (and other features of species biogeography), and speciation rate may lead to patterns in summary statistics different from those we observed. The rate of speciation relative to other rates in DREaD (e.g., niche evolution, dispersal, or environmental

change) may also affect the relative impact of these parameters on biogeographic patterns, although we did not explore this in depth. There are still relatively few spatially explicit studies which have integrated multiple macroevolutionary and biogeographic processes (but see, for example, Qiao et al. 2016; Rangel et al. 2018), so there is much work to be done to understand how these dynamics interact to influence present day patterns in species distributions (Weber et al. 2017).

Another area of uncertainty is the sensitivity of our results to the way species geographic ranges are defined. In particular, the use of polygons that define a species extent of occurrence may overestimate the degree of range overlap between two species, and hide the micro-allopatry that may occur at much finer spatial scales (Cardillo and Warren 2016). For example, although we found strong support for a sympatric model of speciation in *Sebastodes* rockfish, previous studies have suggested that species in this group have partitioned geographic space in three-dimensions along a depth gradient and their distributions may be better explained by a parapatric model of speciation (Ingram 2011). Furthermore, there may be a difference between using polygons that have been determined by expert assessment (e.g., IUCN) versus those that are modelled from species occurrence records (e.g., convex hulls), as these may infer range boundaries at different resolutions potentially biasing hull methods towards non-allopatric speciation modes. However, it is far from clear what the appropriate spatial resolution is for the measurement of geographic range overlap to infer speciation mode, and we suspect the answer is context-dependent, depending on the patterns of habitat use and dispersal capabilities of the species involved. The application of simulation models such as DREaD, may allow this to be tested *in silico* to inform future studies.

## Conclusions

Losos and Glor (2003) asked the question: “Can a null hypothesis that speciation was not sympatric be rejected if sympatric species are found to be sister taxa?” As allopatric speciation is typically considered the “null model” of speciation (Coyne and Orr 2004), the burden of evidence has been on finding strong support for non-allopatric speciation (Bolnick and Fitzpatrick 2007). Comparative approaches to understanding speciation geography have stalled in the past decade, partly because existing methods have had relatively little discriminatory power. We have shown that by adopting an approach based on simulation and model selection, increasingly advocated in biogeography (Goldberg et al. 2011; Matzke 2014; Qiao et al. 2016; Sukumaran et al. 2016; Cabral et al. 2017), Losos and Glor’s question can be rephrased as “given the observed data and a model of geographic range evolution, what is the support for allopatric speciation relative to other models?” Our results suggest that a broad-scale comparative approach to understanding speciation processes can indeed be powerful and informative.

In recent years, much of the research on speciation has shifted away from tests with an explicitly geographic focus, towards questions about regions of the genome that show evidence of divergence among populations in the context of gene flow and selection (Feder et al. 2012, 2013; Seehausen et al. 2014; Wolf and Ellegren 2016; Foote 2018). We see broad-scale comparative methods, and taxonomically-focused genomic and population genetic studies, as complementary. At present, a broad taxonomic overview of inferred speciation modes can only be achieved using geographic and phylogenetic data, and the outcomes of such analyses can serve to generate hypotheses about speciation mechanisms that might then be testable in particular species groups using genomic data.

## Appendix

### Expanded methods

We develop a model of dynamic range evolution and diversification (DREaD), which simulates the diversification of a clade and the evolution of geographic ranges in between speciation events. The model is spatially-explicit and takes place against a background of a gridded, heterogeneous landscape, in which each grid cell contains a value for a single, continuously-varying, hypothetical environmental variable. Each species in the model is defined by three key attributes: their geographic range, niche position, and niche breadth. The geographic range is defined by the species occupancy of grid cells, and species are able to occupy space and disperse through the landscape as they track cells that fit their niche (niche position  $\pm$  niche breadth) through space and time. Our model builds on previous simulation studies of the evolution of geographic ranges (e.g., Rangel et al. 2007; Colwell and Rangel 2010; Qiao et al. 2016), but differs in that it explicitly models range movement in dynamic environmental space under different initial range overlap conditions at the point of speciation (geographic speciation modes). R Code to perform the simulation and an accompanying vignette can be found in the supplemental file, deposited in the Dryad Digital Repository, DOI: doi:10.5061/dryad.d9j09bm, and the functions used to perform different parts of the simulation model are referenced throughout this expanded methods.

### Simulating landscape and seed species

Our simulation (*DREaD* function) begins by generating a background environment. Each simulation generates a new landscape with a single hypothetical environmental layer on

a grid of 100 x 100 cells ( $n = 10,000$ ) using unconditional Gaussian simulation, in the `gstat` package in R (Pebesma 2004). The layer is spatially autocorrelated using kriging to represent a heterogeneous environmental layer with no defined direction in the spatial gradient and values of the cells are scaled between a range of 0 and 20 for consistency (`generateEnv` function). The degree of spatial autocorrelation is held constant between simulations, but the environmental values of each grid cell differs for each simulation replicate.

The simulation proceeds by seeding an initial species (the ancestor to all species for that simulation replicate), which has an initial niche position, niche breadth, and occupied range (`seedSpecies` function). The initial species is seeded by randomly selecting a grid cell in the domain. A boundary is drawn around this cell by sampling the distance from the selected cell to each range boundary (north, south, east, and west) from a uniform distribution between 1 and 10 cells. The species niche position is given as the environmental value of the selected cell and the species niche breadth is drawn from a uniform distribution between 1 and 10. All cells within the range boundaries that fall within this breadth define the initial species range. The simulation then progresses in discrete time steps.

## Dispersal and Environmental change

At each time step each species is able to expand its range via dispersal into new grid cells that lie within its inherent dispersal capacity ( $D$ , a clade-wide value which is shared by all species within each simulation replicate, and drawn from a uniform distribution, Table A2.1), and which have environmental values that fall within the species niche (niche position  $\pm$  niche breadth). If no cells within the dispersal distance contain suitable habitat, the species will not expand its range (`rangeDispersal` function).

Concurrently, the environment changes at each time step by changing the value of the environmental variable in each grid cell according one of two models of environmental change.

1) Cyclical model where environmental change modelled as a sine wave with parameters for amplitude,  $\text{ENV}_A$  and frequency  $\text{ENV}_F$  (Rangel et al. 2007); and 2) directional model, with environmental change modelled as a linear increase with a parameter for the slope,  $\text{ENV}_S$ .

Each environmental change model was either spatially homogenous, where each grid cell changes the same amount at each time step, or heterogeneous, where the degree of change of each cell is a linear function of its latitude, so that the magnitude of environmental change follows a latitudinal gradient. Whether, a simulation uses a directional or cyclical model of environmental change, as well as whether or not environmental change varies spatially are defined by two binary parameters ( $\text{ENV}_{\text{mode}}$ ,  $\text{ENV}_{\text{hetero}}$  respectively). In total, we model four different environmental change scenarios: 1) cyclical homogenous, 2) cyclical heterogeneous, 3) directional homogenous, and 4) directional heterogeneous (*environmentalChange* function).

In response to environmental change, at each time-step a species will reposition its geographic range. If environmental change causes some occupied cells to contain values that are no longer within the species niche breadth, these cells are no longer part of the species range. This may lead to range contraction or range fragmentation, and at its extreme, if environmental change removes all cells with suitable habitat from the species range, then the species is considered extinct.

## Event selection

After dispersal and environmental change occur, for each species at each time step, one of six events can occur: vicariant, sympatric, parapatric or dispersal speciation, extinction, or no-event. Each speciation and extinction event are assigned a probability (described below), and

the probability of no-event is 1- the sum of these probabilities. At each time step one event is sampled in proportion to these probabilities. In the case of no-event, niche evolution proceeds. Probabilities for each event are defined as follows:

## Speciation

We explicitly model four different geographic modes of speciation (vicariant, sympatric, parapatric, and founder). Although the geographic mode of speciation is now considered to be a continuum from complete vicariant isolation to complete sympatric overlap (Fitzpatrick et al. 2009), here we treat the geography of speciation as taking place within discrete modes in order to simplify the process of speciation and more easily pull apart complex interactions. We believe these speciation modes, though not exhaustive, cover a majority of the overlap conditions likely at the point of speciation. In DREaD, speciation is a stochastic process that is a peaked function of range size. The probability of speciation for each species at each time step is modelled by the function:

$$\lambda * e^{-\frac{(r-B)^2}{2C^2}}$$

where  $r$  is the range size of the species,  $\lambda$  is the probability of speciation when  $r = B$ , and  $C$  defines the peak of the curve.  $B$  was set to 5000 which is the range size of a species that occupies half of the total domain, and  $\lambda$  was set so that the sum of speciation probabilities is equal to 0.0415 when a species range size is equal to  $B$ .

We simulated five different models changing the predominant mode of speciation: one each where a given speciation mode is predominant (vicariant, founder, sympatric, and parapatric) and a mixed model where each of these four modes had equal probability of occurring. For a

mixed model of speciation  $\lambda$  was fixed at 0.010375 equally for each speciation mode. When enforcing a predominant mode,  $\lambda$  was set to 0.04 for the predominate mode, and for all other speciation modes  $\lambda$  was set to 0.0005. The per-lineage speciation rate, therefore, is dynamic and greater in intermediate ranged species (Figure A2.1).

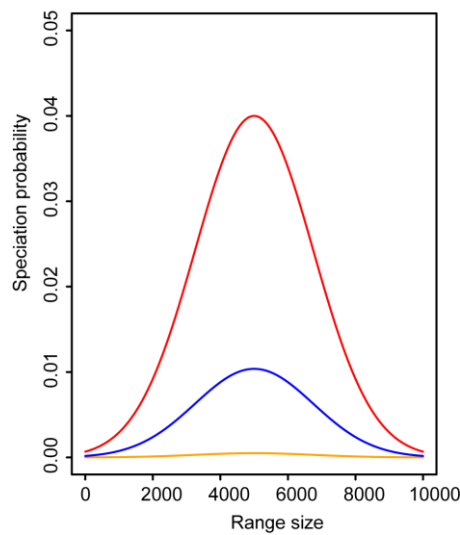


**Figure A2.1.** Relationship between speciation rate and range size. Speciation rate is a peaked function of range size. For a predominant speciation mode (red), the speciation rate is greatest when range size = 5000, and the probability of speciation with a non-predominant speciation mode is low (yellow). When the speciation mode model is mixed, all speciation modes have equal probability (blue) which sum to 0.0415 when range size = 5000.

Each of the four modes is modelled as follows:

*Sympatric:* Under the sympatric model, one daughter species maintains the range of the parent and the other occupies a range that lies completely within the boundaries of the parent species. This is chosen by randomly drawing four coordinates from within the parent species range, which form the boundaries of the daughter species range (*speciateSympatric* function).

*Parapatric:* Parapatric speciation occurs via budding at the range periphery. The new species is formed by creating an abutting range that may partially overlap the parent range. This is done by selecting a cell within dispersal distance from the parent species range boundary and drawing

four distances from a uniform distribution from this point to be the range boundaries of a new quadrant (*speciateParapatric* function).

*Founder:* Founder speciation follows a founder-event model where founder events can found a new species in non-contiguous geographic space. Founder speciation proceeds by selecting a cell within the domain to be colonized with a probability inversely related to the shortest distance from the parent species range. The range boundaries are drawn by selecting 4 distance values from a uniform distribution (from 1 to D) from the colonized cell (*speciateFounder* function).

*Vicariant:* Vicariant speciation is modelled in two different ways depending on the geometry of the species range. Firstly, if the species range is a single contiguous area, vicariant speciation will occur via bisection of this range, whereby a line is drawn randomly through the species range dividing it into two. The bisection is ambiguous with respect to the range size asymmetry of the daughter species ranges. The second method of vicariant division is used if a species range is fragmented. In this case, the parent species range is split so that each daughter species is composed of a cluster of range fragments that are in closer spatial proximity to each other than to the sister species. Clustering is performed with a k-means method on the x-y coordinates of the range fragments (*speciateVicariant* function).

## Extinction

Extinction is modelled in two ways in our simulation. Firstly, there is deterministic extinction which occurs if a species range collapses entirely. Secondly, there is a probabilistic rate of extinction that is a function of range size. Extinction probability is modelled by the function (following Rangel et al. 2007):

$$-\log \frac{(r/m)}{(1/\mu)^2}$$

Where  $r$  is the species range size,  $m$  is the extinction range size threshold, and  $\mu$  adjusts the magnitude of the function, which was fixed at 0.2. Here, extinction from stochastic processes is possible only in species with  $r < m$ , such that there is a point at which a species range is large enough that it can no longer go extinct from stochastic processes and is able to speciate (Figure A2.2).

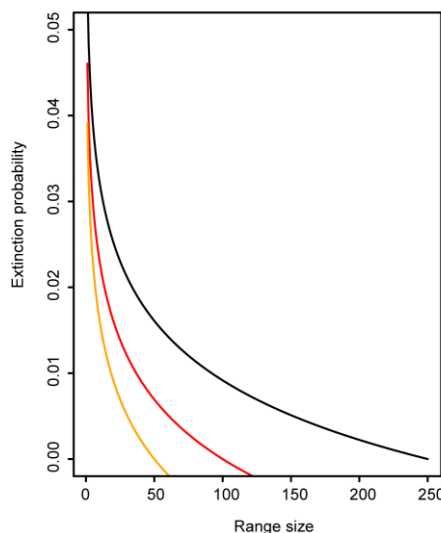


**Figure A2.2.** Relationship between range size and extinction rate. Extinction probability is highest in small range species, and becomes 0 when a species range size =  $m$ .  $m$  was drawn from a uniform distribution between 50 and 250 in our simulation study. Here shows the relationship when  $m=50$  (orange),  $m=100$  (red),  $m=250$  (black).

## Niche evolution and phylogenetic signal in the niche

Niche evolution is modelled by allowing a species niche position and niche breadth to drift independently under a modified random walk model of trait evolution, controlled by the rate parameters  $NE_P$  (for niche position) and  $NE_B$  (for niche breadth). Species niche positions and

breadths drift randomly under the single condition that the environmental value of at least one grid cell must remain within the species niche ( $\text{niche position} \pm \text{niche breadth}$ ), which ensures species do not evolve an environmental niche that causes their immediate extinction (*nicheEvolution*).

We model phylogenetic signal of the niche at speciation as follows. Under vicariant speciation, immediately following speciation both daughter species niche positions are recentered towards the mean environmental value of the species new range. Under founder, parapatric, or sympatric speciation, the niche position of the budded daughter species (the smaller ranged daughter species) is recentered. The degree to which the species shifts its inherited niche position value towards this new value is modelled with the parameter PS, the proportion of the step between the current niche position and the mean environmental value that the new species will take. A PS value of 1 means the species will move completely towards the mean, while a value of 0 means the new species will inherit the same niche position as the parent. In this way, the PS parameter controls the strength of “punctuational” evolution of the niche at speciation events (*nicheRecenter* function). We also model evolution of the niche along the branches of the phylogeny by allowing a species niche position and niche breadth to drift independently under a modified random walk model of trait evolution (*nicheEvolution* function), controlled by the rate parameters  $\text{NE}_P$  (for niche position) and  $\text{NE}_B$  (for niche breadth). Species niche positions and breadths drift randomly under the single condition that the environmental value of at least one grid cell within the species range must remain within the species niche ( $\text{niche position} \pm \text{niche breadth}$ ).

## Model parameters

We simulated range evolution and speciation under different scenarios of environmental change, niche evolution, dispersal rate, clade size, and geographic speciation modes, by sampling parameters from prior distributions. Priors were informed with preliminary simulations to qualitatively determine a match to broadly plausible evolutionary scenarios. For example, the rate of niche evolution was drawn from a uniform distribution between 0.005 - 2, these extreme values represent cases of strong environmental niche conservatism and of strong environmental niche lability that would be rare in many real clades (for example, if the environmental variable is considered to represent temperature, then values of niche evolution  $\approx 2$  could lead to shifts between tropical and temperate niche positions in relatively few time steps). Environmental change parameters on the other hand, were constrained by the mechanics of the simulation model, as high values of the slope of the directional model and amplitude of the cyclical model led to repeated mass extinction as species could not keep pace with the changing climate. This set an upper limit on the bounds of environmental change parameters. Due to the computational cost of running the simulation model and the potentially inefficient method of sampling parameter space in a Monte Carlo simulation framework, we sampled parameter space using Sobol-sequences (Burhenne et al. 2011), a type of quasi-random low-discrepancy sequence which aims to prevent any one region of parameter space from being disproportionately over- or under-sampled (Table A2.1).

**Table A2.1.** Sampling range of each parameter in the simulation model. A range of parameter values were sampled to explore parameter space and observe the effect on the patterns displayed by each clade. Dispersal capacity is modelled as a dispersal distance (D). Environmental change is modelled as both a frequency (ENV<sub>F</sub>) and amplitude (ENV<sub>A</sub>) of a sine wave under the cyclical model of environmental change, and as a slope (ENV<sub>S</sub>) in the directional model of environmental change. The model of environmental change is set by a binary parameter (ENV<sub>mode</sub>), and whether the model of environmental change is spatially homogenous, or varies across a spatial gradient, is defined by another binary parameter (ENV<sub>hetero</sub>). Niche evolution is modelled as both a niche position (NE<sub>P</sub>) and niche breadth (NE<sub>B</sub>) evolution rate, and phylogenetic signal in the niche is controlled by a single parameter (PS). The simulation proceeds until the phylogeny of the clade reaches a specified number of tips, with clade size (Tips). We modelled five different geographic speciation scenarios (Speciation mode): one each where a particular mode was predominant (vicariant, sympatric, parapatric, founder) and one mixed speciation scenario.

Parameter	Description	Sampling range
D	Distance of cells from occupied cells available during dispersal. Dispersal kernel.	1, 10
NE <sub>B</sub>	Niche breadth evolution rate	0.0025, 1
NE <sub>P</sub>	Niche position evolution rate	0.005, 2
PS	Phylogenetic Signal	0.25, 1
ENV <sub>A</sub>	Amplitude of the environmental change sine wave	0.25, 2
ENV <sub>F</sub>	Frequency of the environmental change sine wave	0.25, 2
ENV <sub>S</sub>	Slope of linear environmental change	0.001, 0.5
n	Simulated clade size	10, 150
m	Range size at which the risk of stochastic extinction = 0	50, 250
ENV <sub>hetero</sub>	Binary parameter controlling whether environmental change is spatially heterogeneous.	0,1
ENV <sub>mode</sub>	Binary parameter controlling the model of environmental change	0,1
Speciation mode	Discrete parameter controlling whether speciation model is vicariant, founder, sympatric, parapatric, or mixed.	1,2,3,4,5

We ran the simulation 36000 times until a clade of size  $n$  was generated (Table A2.1), discarding 269 simulations which could not be completed because the parameter combination led to total clade extinction more than five times successively. This lead to roughly 7200

replicates for each speciation scenario, which is considered adequate for model selection in an ABC framework (Pudlo et al. 2016). For each simulation we recorded the phylogenetic relationships of taxa, the polygons of each tip species range, the environmental grid, and a data frame containing information on the niche position, niche breadth, range size, and mode of speciation for all tip species and internal nodes. Our simulations were written and performed in R version 3.4.2 using the packages: ape (Paradis et al. 2004), raster (Hijmans 2016), sp (Bivand et al. 2013), rgeos (Bivand and Rundel 2016), and fpc (Hennig 2015).

## Data analysis

At the completion of each simulation, we calculated a 30 summary metrics that have been used, or might be used to help reconstruct the predominant mode of speciation. These fall into four main categories, 1) range overlap metrics, 2) range asymmetry metrics, 3) range size and position metrics, 4) range isolation metrics, and 5) phylogenetic tree shape metrics. More details on each metric are provided within Table A2.2. All summary statistics were generated in R version 3.4.2. (*generateSummaryStatistics* function).

**Table A2.2.** List of summary metrics used for the study of the geographic mode of speciation with description and supporting references.

Summary metric	Description	Abbreviation
Age-Range Correlation	Slope and intercept of regression between phylogenetic node age and geographic range overlap among nodal descendants (Fitzpatrick and Turelli 2006)	ARC <sub>slope</sub> , ARC <sub>intercept</sub>
Sister species overlap x divergence times	Slope and intercept of regression between sister species range overlap and divergence times. Similar to ARC but using only sister species.	RO <sub>slope</sub> , RO <sub>intercept</sub>
Mean range overlap of sister species	Range overlap = proportion of range of the smaller ranged sister species found within the larger ranged sister species	RO <sub>mean</sub>

Sister species sympathy proportions	Proportion of species which have values of range overlap $\geq 0, 0.5, 0.75, 0.9,$ or $1.0$ (Cardillo and Warren 2016)	$RO_{50}, RO_{75}, RO_{90}, RO_{100}$
Sister species range overlap skew	Degree of bias in the distribution of sister species range overlap towards higher or lower values	$RO_{\text{skew}}$
Sister species range overlap kurtosis	Degree of clustering or dispersion of sister species range overlap values	$RO_{\text{kurt}}$
Difference between sister species overlap and sister – outgroup overlap	The mean and standard deviation of the difference in the overlap between sister species and the overlap of each sister species with an outgroup species. Scaled between -1 where species overlap completely with outgroups and not at all with each other, and 1 where sisters completely overlap with each other and not at all with outgroups (Cardillo 2015)	$TO_{\text{mean}}, TO_{\text{SD}}$
Bimodality of sister species overlap	Degree to which sister species overlap distributions are either unimodally sympatric or vicariant, or evenly distributed between vicariant and sympatric (Phillimore et al. 2008). Sympathy $\geq 0.5, 0.75, 0.9,$ or $1.0.$	$Bimod_{50}, Bimod_{75}, Bimod_{90}, Bimod_{100}$
Mean sister species range size asymmetry	Mean ratio of range sizes between sister species.	$Asym_{\text{mean}}$
Range asymmetry x divergence times	Slope and intercept of regression between range asymmetry and divergence times (Grossenbacher et al. 2014).	$Asym_{\text{slope}}, Asym_{\text{intercept}}$
Mean and standard deviation of standardised range size	Standardised range size for each species = range size / largest range size in clade. Measured across all tip species in the phylogeny.	$RS_{\text{mean}}, RS_{\text{SD}}$
Skew of range size distribution across all tips	Degree to which clades show bias in the distribution of range sizes towards higher or lower values (Pigot et al. 2010).	$RS_{\text{skew}}$
Mean standardised distance between sisters species ranges	Standardised range distance = minimum distance between sister species ranges / maximum distance between two species in the clade	$RD_{\text{mean}}$
Range isolation x divergence times	Slope and intercept of regression between standardised range distance and divergence times.	$RD_{\text{slope}}, RD_{\text{intercept}}$
$\beta$ tree-splitting parameter	Phylogenetic tree imbalance = measure of the uneven distribution of species between clades descended from nodes across a phylogeny (Aldous 1996; Blum and François 2006; Pigot et al. 2010)	$\beta$

---

Colless's Index	Phylogenetic tree imbalance (Blum and Francois 2005)	CI
Sackin's Index	Phylogenetic tree imbalance (Blum and Francois 2005)	SI
$\gamma$	Distribution of node heights through time, indicating degree to which phylogeny conforms to temporally constant diversification rates (Pybus and Harvey 2000)	$\gamma$

---

We compared the distributions of each summary statistic for simulated clades generated under different geographic speciation modes, using pairwise Kolmogorov-Smirnov tests. Our simulations generated large sample sizes (~7,200 replicates for each speciation scenario), which may return significant p-values even when the effect sizes are small. To reduce the chance of misinterpreting significant differences we randomly subsampled 500 simulation replicates 100 times, and took the mean values of the test statistic and p-value.

Next we asked whether the signal of speciation is stronger than the signal of geographic range evolution in present-day (simulated) data, by exploring which model parameters explained the greatest amount of variation in the summary statistics, independent of all other model parameters. To do this we used a hierarchical partitioning protocol (Chevan and Sutherland 2017) which assesses all possible combinations of independent variables (model parameters) on the response (summary statistics) in a Generalized Linear Modelling framework and partitions the variance according to a goodness of fit statistic ( $R^2$ ), allowing for the independent assessment of each parameter's contribution while removing the effects of multicollinearity (MacNally 2000). Hierarchical partitioning was implemented in the R package `hier.part` (Walsh and MacNally 2013).

## Empirical Data Collection

We collected spatial and phylogenetic data for 30 empirical case studies (six plant, two fish, one invertebrate, four amphibian, four reptile, five mammal, and eight bird clades), selected to cover a range of taxonomic groups and levels, clade sizes, and geographic regions (Table A2.3). We selected monophyletic clades based on the availability of well-sampled phylogenetic data, with all clades having >80% of known species included, and most with >90%. Phylogenies were obtained where possible from the public databases TreeBase (treebase.org) and Data Dryad (datadryad.org), while one trees was obtained from unpublished sources – the South American *Liolaemus* (Esquerre et al. *unpublished work*). For bird and mammal clades, we used subsets of large composite supertrees constructed from multiple smaller phylogenies (Fritz et al. 2009; Jetz et al. 2012). Phylogenies for two clades (*Amphiprion* fish and *Stenodactylus* lizards) were not time-calibrated and were made ultrametric (with node heights scaled to a relative timescale) using the chronos function in the ape package in R. When phylogenies contained more than one representative from each species, these were pruned to species level by randomly selecting one sub-specific lineage to represent the species.

Spatial data for some clades were obtained as spatial polygons from the IUCN (<http://www.iucnredlist.org>) or BirdLife (BirdLife 2016), which depict species range extents based on both occurrence data and expert assessment of species contemporary distributions. For other clades we used point occurrence records from GBIF (<http://www.gbif.org>) and cleaned of obvious outliers, and in five cases we obtained spatial data supplied from the supplementary materials of the associated article presenting the phylogeny (*Pyrgus* butterflies, Pitteloud et al. 2017; *Mimulus* plants, Grossenbacher et al. 2014) or relating to the clade

(*Banksia*, *Hakea*, and *Protea* plants, Skeels and Cardillo 2017). Spatial polygons were estimated from occurrence points using a fixed-k convex hull method (following Getz and

**Table A2.3.** Details of clades used in empirical analysis. Columns indicate the major taxonomic group each clade belongs to; the total number of described species; the number of species included in the phylogeny; number of species with spatial occurrence record data from GBIF; number of species with spatial polygon data from IUCN or Birdlife; and the source of each phylogeny.

Clade	Higher taxon	Total species	Species in phylogeny	Species with occurrence records	Species with polygons	Reference
<i>Banksia</i>	plant	170	157	157	0	(Cardillo and Pratt 2013)
<i>Hakea</i>	plant	149	136	136	0	(Cardillo et al. 2017)
<i>Protea</i>	plant	110	90	85	0	(Valente et al. 2009)
<i>Mimulus</i>	plant	120	114	90	0	(Grossenbacher et al. 2014)
<i>Sidalcea</i>	plant	25	24	24	0	(Sabath et al. 2016)
<i>Bursera</i>	plant	100	85	83	0	(Sabath et al. 2016)
<i>Sebastes</i>	fish	110	95	92	0	(Ingram and Kai 2014)
<i>Amphiprion</i>	fish	30	27	17	10	(Litsios et al. 2012)
<i>Pyrgus</i>	invertebrate	37	36	35	0	(Pitteloud et al. 2017)
Myobatrachidae	amphibian	129	117	39	76	(Vidal-García et al. 2014)
<i>Pseudacris</i>	amphibian	18	17	1	15	(Pyron and Wiens 2013)
<i>Litoria</i>	amphibian	65	64	0	63	(Rosauer et al. 2009)
<i>Plethodon</i>	amphibian	55	45	6	36	(Wiens et al. 2006)
<i>Anolis</i>	reptile	119	100	81	17	(Mahler et al. 2010)
Pygopodidae	reptile	172	155	125	18	(Brennan and Oliver 2017)
<i>Liolaemus</i>	reptile	225	189	16	125	(D. Esquerre unpublished data)
<i>Stenodactylus</i>	reptile	12	12	9	3	(Metallinou et al. 2012)
Lemuridae	mammal	21	17	0	17	(Fritz et al. 2009)
Bovidae	mammal	143	143	0	137	(Fritz et al. 2009)
Diprotodontia	mammal	146	146	0	136	(Fritz et al. 2009)
Geomyidae	mammal	39	39	0	39	(Fritz et al. 2009)
Viveridae	mammal	33	33	0	33	(Fritz et al. 2009)
<i>Vidua</i>	bird	19	19	0	19	(Jetz et al. 2012)
Cuculidae	bird	126	126	0	126	(Jetz et al. 2012)

Petroicidae	bird	45	45	0	45	(Jetz et al. 2012)
Paradisaeidae	bird	42	42	0	42	(Jetz et al. 2012)
Bucerotiformes	bird	64	64	0	64	(Jetz et al. 2012)
Rhinocryptidae	bird	54	52	0	52	(Jetz et al. 2012)
Paridae	bird	53	53	0	53	(Jetz et al. 2012)
Cacatuidae	bird	21	21	0	21	(Jetz et al. 2012)

Wilmers 2004; Cardillo and Warren 2016). Finally, for consistency with our simulated data, all spatial polygons were transformed into gridded raster format with a grid resolution of 10 arc seconds to perform data analysis. From the spatial raster and phylogenetic data we obtained the same summary statistics as for the simulated data.

### Inferring the mode of speciation in empirical datasets using model selection

For many complex biogeographic models, determining a likelihood function for the purpose of model selection becomes intractable. However, there are multiple likelihood-free model selection and model classification techniques available. Here we use both a machine-learning Linear Discriminant Analysis (LDA) and two Approximate Bayesian Computation (ABC) approaches; multinomial logistic regression (mnL), and neural net (NN). Unlike traditional Bayesian or maximum likelihood inference, ABC avoids the calculation of a likelihood function by simulating data from prior distributions of the simulation parameters and summarizing this data using well-informed summary metrics (Csilléry et al. 2010; Blum et al. 2013). A simple ABC algorithm rejects or accepts sampled parameters based upon the distance between the simulated and observed summary statistics (Csilléry et al. 2010). However, to account for the discrepancy between accepted and observed summary metrics, local linear regression techniques or non-linear neural network machine learning methods can be used to

better approximate the true posterior (Blum and François 2010; Csilléry et al. 2010). Model selection can then be performed by estimating the proportion of each model in the posterior.

To perform model selection, first we removed highly correlated variables (Pearson correlation coefficient,  $r > 0.9$ ) and applied a variable selection procedure to reduce the number of summary statistics used in model selection, using the ‘stepclass’ function in R package *klaR* (Weihs et al. 2005). We then tested the discriminatory ability of our candidate summary statistics to distinguish between speciation modes for each method using a leave-one-out cross validation procedure, calculating the rate of model misspecification for each geographic speciation mode (the reclassification accuracy). After cross-validating each methods ability to reclassify the simulated data given the summary statistics, we then inferred the geographic mode of speciation in the 30 empirical datasets using LDA, implemented using the *caret* (Kuhn 2016) package in R, and two ABC methods (*mnl*, *NN*), implemented with the *abc* package (Csilléry et al. 2012). To examine model adequacy we plotted each empirical dataset in two dimensions along the first two axes of a LDA on the simulated dataset (Figure 2.6 in the main text). A schematic of the workflow for simulation-based model selection can be found in Figure 2.2 in the main text.

# Chapter 3: Lineages through space and time plots: visualising spatial and temporal changes in diversity



**Skeels, A.** 2019. Lineages through space and time plots: visualising spatial and temporal changes in diversity. *Frontiers of Biogeography*. 11 (2), e42954.

## Abstract

During the radiation of a clade, diversification rates can show temporal patterns such as a speedup or slowdown which might relate to different ecological and evolutionary mechanisms. The temporal dynamics of diversification of whole clades are often visualised as a lineage-through-time (LTT) plot, which traces the number of reconstructed lineages at different time points. However, clades do not radiate evenly across space and may show different temporal dynamics in different regions. As such, a biogeographic approach is required to more completely understand temporal diversification dynamics. Here, I present a tool to extract temporal diversity information across different biogeographic regions from the output of commonly used ancestral range estimation models implemented in the R package BioGeoBEARS. The lineages through space and time (LTST) plot allows for visualisation of diversification dynamics in different regions, formatted in an accessible way which can be used for further quantitative analysis.

## Introduction

The temporal dynamics of the build-up of diversity in different regions is key to understanding the emergence of biogeographic patterns in diversity. A common method to explore temporal patterns of diversification within whole clades is to plot the logarithm of the reconstructed number of lineages in different time-slices drawn through a time-calibrated molecular phylogeny; a lineages-through-time plot (LTT; Figure 3.1A; Nee et al. 1992; Harvey et al. 1994). LTTs can be used to visually explore when diversification is deviating from a straight line as expected under a constant rates model, for example as the net diversification rate of a clade slows down during the late stages of an adaptive radiation (Nee et al. 1992; Phillimore and Price 2008). Temporal diversification information can be analysed quantitatively to see when diversification deviates from the expectation of constant rates (e.g., Pybus and Harvey 2000) and the shape of LTT curves have recently been shown to be a useful summary metric for diversification diagnostics (Janzen et al. 2015). LTTs have been used extensively in evolutionary biology, forming a standard visualisation procedure in the toolbox of evolutionary biologists. However diversification dynamics are not spatially homogenous, and within a single clade diversity may accumulate more or less rapidly in different regions. To visualise the spatial context of diversification through time first requires an estimate of the geographic distribution occupied by each reconstructed lineage in the phylogeny.

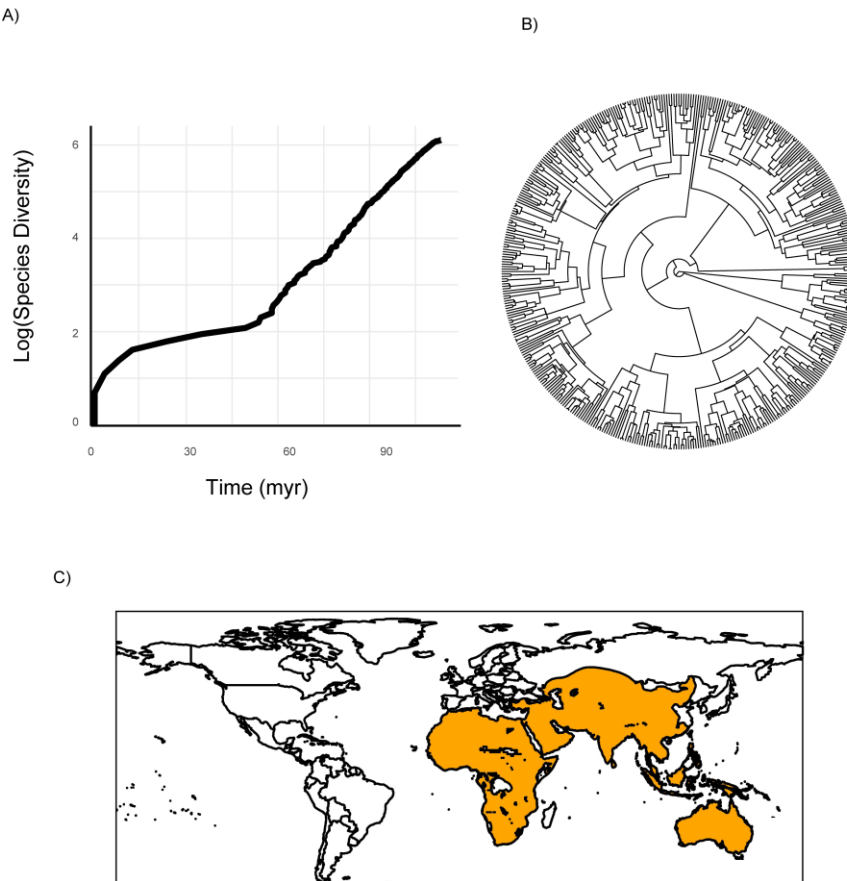


**Figure 3.1.** Lineages-through-time plot (A), time-calibrated phylogeny (Tonini et al. 2016) (B), and distribution (Roll et al. 2017) (C) of agamid dragons (family Agamidae).

A suite of ancestral range estimation (ARE) methods are available to infer when in history lineages have occupied different regions based on models of geographic range evolution (Ronquist 1997; Ree and Smith 2008; Landis et al. 2013; Matzke 2013a). These methods model range dynamics by taking geographic range information, as measured by the present-day occupancy of species in discrete regions (often coded broadly at the scale of ecoregions, biomes, or biogeographic realms), as well as a time-calibrated phylogeny, and fitting models of geographic range evolution to these data. Different implementations of AREs model range shifts via dispersal between regions, speciation amongst or between regions, or extirpation from a region. ARE models can be constrained to account for the effect of geographic or

environmental distance on dispersal (Van Dam and Matzke 2016), trait-based dispersal capacity of species (Klaus and Matzke 2020), historical information on geographic ranges from the fossil record (Matzke 2013a), or can be time-stratified to account for the ontogeny of different regions, such as the formation of islands or rise of mountains (Matzke 2014).

Given this flexibility and suitability of ARE models to a range of diverse systems, the application of ARE methods is prolific in the field of biogeography and many different models, including variants of the dispersal-extinction-cladogenesis model (DEC; Ree and Smith 2008), dispersal-vicariance-analysis (DIVA; Ronquist 1997), and BayArea model (Landis et al. 2013), are commonly implemented in the R package BioGeoBEARS (Matzke 2013b, 2014). However, despite the advancement of these analytical methods for ARE, methods to visualise the temporal dynamics of range evolution and diversification tends to be limited to painting the branches of a phylogeny based on the inferred ancestral condition according to a model of range evolution (e.g., Figure 2 in Matzke 2014). This limitation generally makes it difficult to extract the temporal information contained in the output of these models. In this paper, I present a method for post-hoc data extraction and visualisation of temporal species diversity information contained in the output of a BioGeoBEARS analysis. These lineage-through-space-and-time (LTST) plots form a bridge between clade-level LTTs and infra-clade regional diversity dynamics.

## Methods

### Data collection and ancestral range estimation background

The method for generating a LTST is presented in the R package `ltstR` ([github.com/alexskeels/ltstR](https://github.com/alexskeels/ltstR)) and described below using a global radiation of agamid dragons (family Agamidae) as an example. The agamid dragons are a large clade of over 400 species which are broadly distributed through much of the Australasian, Indomalayan, Afrotropical, and Palearctic biogeographical realms (Figure 3.1C). This radiation is over 90 million years old, and appears to be showing a slowdown in diversification towards the present (Figure 3.1A), which is confirmed by estimating the  $\gamma$  statistic on this group ( $\gamma = -2.624$ ; Pybus and Harvey 2000). The following analysis was performed on a randomly selected phylogeny from the post-burn-in posterior distribution of phylogenies from Tonini et al. (2016; Figure 3.1B), and spatial information obtained from Roll et al. (2017; Figure 3.1C).

The first step towards generating a LTST is to perform an ARE analysis using BioGeoBEARS. BioGeoBEARS implements user-specified ARE models from which the probability that each node and internal branch in a phylogeny occupies a given state (geographic range) can be estimated. Biogeographic stochastic mapping (Dupin et al. 2016) uses stochastic simulations based on the phylogeny and the specified ARE model and parameters to assign a state to internal branches and nodes. Because they are probabilistic, stochastic maps will tend to differ from one another and account for alternative biogeographic histories based on the ARE model and parameters. As such LTSTs require at least a single stochastic map and, to account for biogeographic uncertainty LTSTs, can be produced using a distribution of stochastic maps. Phylogenetic uncertainty is another source of variation for LTSTs, as ARE is typically performed on a representative phylogeny such as a maximum clade credibility phylogeny from

a Bayesian posterior. Phylogenetic uncertainty can be accounted for by replicating ARE estimation across, for example, alternative phylogenetic trees from a Bayesian posterior. However, replicating AREs is likely to be computationally prohibitive for many large data sets. Therefore, it is advised that users acknowledge this source of uncertainty when interpreting LTSTs.

For the agamid dragons, I scored the biogeography of species by categorising them as present or absent from the major biogeographical realms of the world. The agamids were present in four of these, the Afrotropical, Indomalayan, Australasian, and Palearctic realms, which we used to fit a DEC model to illustrate the application of LTST. From the maximum likelihood estimates of the DEC model parameters, we obtained 50 biogeographic stochastic maps from which we generated LTST plots (Figure 3.2).

LTSTs are generated with the R package `ltstR` ([github.com/alexskeels/ltstR](https://github.com/alexskeels/ltstR)) or with R scripts found in the appendix and requires four objects: 1) a time-calibrated phylogeny, 2) a BioGeoBEARS geography file, and two objects from the output of biogeographic stochastic mapping under an ARE model with BioGeoBEARS; the 3) anagenetic events data table, and 4) cladogenetic events data table. The first two objects are required input for a BioGeoBEARS analysis, and the last two are the standard output from biogeographic stochastic mapping with BioGeoBEARS. Users having performed biogeographic stochastic mapping with BioGeoBEARS will have all the necessary components.

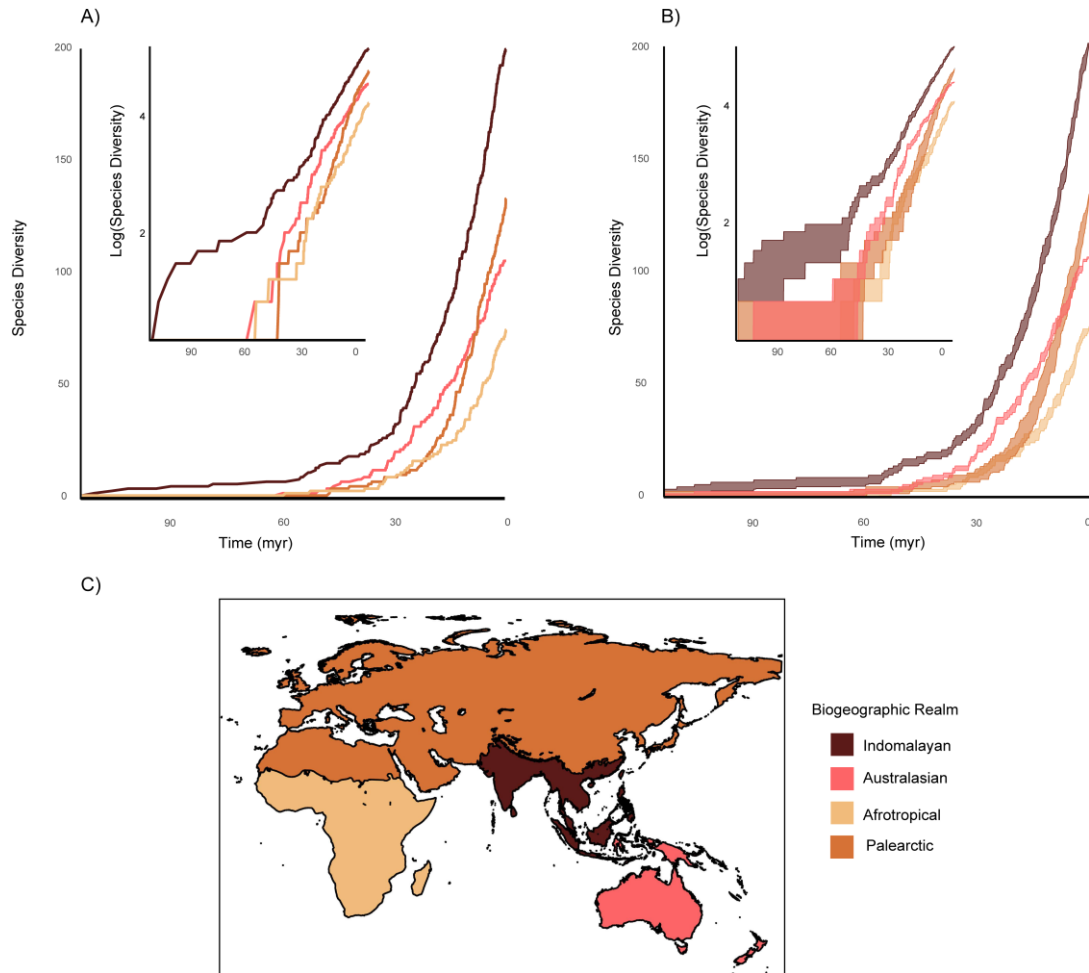


Figure 3.2. Lineages through space and time plots (LTSTs) for agamid dragons. This figure shows a LTST from a single stochastic map (A), a LTST displaying the distribution of diversity through time from 50 stochastic maps by showing the 95% quantile diversity recorded at each time step (B), and a colour-matched map of the biogeographical realms used in the biogeographical analysis (C).

### Step-by-step guide to producing LTSTs

The following outlines a step-by-step guide to producing LTST plots. A vignette and associated data to replicate this analysis for the agamid as well as further details on the R code can be found within the appendix or on GitHub ([github.com/alexskeels/lsttR](https://github.com/alexskeels/lsttR)).

- 1) The method works by first going through the cladogenetic and anagenetic event tables and extracting all the times in which a state change occurs on the phylogeny for a given stochastic

map (*getEventTiming* function). The output from this function is the events timing table, a data frame which gives the time of each event, the node at which the event is located on the phylogeny, whether the event was cladogenetic (occurring at a speciation event, at a node) or anagenetic (occurring in between speciation events, along a branch), the number of species extant at that time, and a running total of the number of species present in each unique state combination. From the events timing table we can infer whether the diversity of a region increases through immigration or speciation, or decreases through emigration or extirpation, to keep a record of diversity changes through time.

2) Lineages can occupy multiple states (be present in multiple regions simultaneously) and BioGeoBEARS gives each state combination a unique identifier. For example, in the agamid lizards, a lineage that occupies Australasia is given state 2, while a lineage that occupies Australasia and Indomalaya simultaneously is given state 8. An intermediate step is required which matches the state combination identifier to the actual geographic ranges. The function *getRangeStates* generates a lookup table (Table 3.1) to perform this matching.

**Table 3.1.** Lookup table for geographic ranges from state combination identifiers for agamid dragons. Agamid species are found in ten different combinations of the four geographic regions; W = Australasia, I = Indomalaya, P = Palearctic, and A = Afrotropics.

Geographic Ranges	State Combination Identifier
W	2
I	5
WI	8
PI	11
P	4
AP	9
A	3
AI	10
WPI	14
API	15

3) Next, to obtain the LTST data for each geographic region separately we employ the functions *getLTSTDataTable*, for a single stochastic map, or *getLTSTFromStochasticMaps*, for multiple stochastic maps. These functions take the events timing table from *getEventTiming* and the lookup table from *getRangeStates* to produce the LTST data table, a data frame (or list of data frames for multiple stochastic maps) which contain the number of species present in each geographic range at each event time (Table 3.2). At this stage the LTST data table for a single stochastic map can be plotted (see vignette in the appendix or on GitHub; Figure 3.2A). However, comparing LTSTs across multiple stochastic maps requires further processing because the timing and number of events will be different between iterations of the stochastic mapping and therefore not align perfectly.

**Table 3.2.** First four rows of the LTST data table for agamid dragons showing the number of species present in the four geographic regions at each time point. W = Australasia, I = Indomalaya, P = Palearctic, and A = Afrotropics.

Time	W	I	P	A
113.3	0	1	0	1
110.1	0	2	0	1
105.3	0	3	0	1
101.0	0	4	0	1

4) To account for the discrepancy in event timing between stochastic maps, the function *slidingWindowForStochasticMaps* performs a sliding window analysis to get the number of species present in each region within regular time intervals based on the window size. The default is 0.1 time units, but users should select values that make sense for their particular datasets. For example, if the phylogeny is measured in units of million years, then 0.1 represents 100,000 years. If the depth of the phylogeny is, for example, 30 million years then this may be a fine enough resolution to assess meaningful patterns, but if the depth of the phylogeny is only

1 million years then it may make sense to narrow the window size (e.g., 0.01). The output is a time-standardised LTST data table.

5) To visualise the LTSTs from multiple stochastic maps we then summarise the variability of species diversity values for each region at each time point in the list of time-standardised LTST data tables. The function *timeRangeAcrossStochasticMaps* finds the upper (97.5%) and lower (2.5%) quantiles for each region at each time step and returns this in the LTST quantile data table which can be used to plot the distribution of diversity values for a given LTST (see vignette in the appendix or on GitHub; Figure 3.2B).

Importantly, not only does this method provide a tool for plotting this biogeographic, temporal-diversification information, but it also returns it in a format that is user friendly, making quantitative analysis of these data more accessible to many users. For example, logistic growth models can be fit to the temporal diversity data contained within the LTST data tables to estimate the diversity asymptote, which might be interpreted as the regional diversity carrying capacities (Skeels and Cardillo 2019a).

## Benefits of a biogeographical approach to temporal lineage diversification dynamics

LTSTs and a biogeographical approach to investigating the temporal dynamics of diversification are important to understand the evolution of biodiversity. Diversity is not evenly distributed, with some regions being more diverse than others, for example the Indomalayan realm contains a greater amount of agamid diversity (Figure 3.2). This uneven distribution of diversity may be because clades have been, 1) diversifying more rapidly, 2) diversifying for

longer, or 3) a have greater carrying capacity, in particular regions. LTSTs allow us to more easily visualise these kinds of spatiotemporal dynamics of diversification within clades. In the agamids we can see that diversification appears to have been occurring much earlier in the Indomalayan region, followed by the Australasian, Afrotropical, and Palearctic regions. We can also see that diversity began to build in the Palearctic, Afrotropics and Australasian regions at a fairly similar time but different temporal dynamics have led to stark differences in diversity between these regions. Notably, we can see that the accumulation of diversity was more rapid in Australasia during the period of between roughly 60-15myr, before slowing towards the present. Palearctic diversity, on the other hand has been increasing more steadily in the past 20myr and at some point around 10myr overtook Australasia in species diversity. Comparatively, the Afrotropics have had a lower rate of species accumulation.

Investigating regional patterns in diversification may also help clarify processes that are lost when looking at clade-level temporal diversification dynamics. For example, in the Agamidae as a whole we see a diversification slowdown towards the present (Figure 3.1A). This pattern appears to be repeated in differing degrees within the different biogeographic realms. In the Palearctic, however, we can see that diversification appears to be still increasing steadily, or only showing the earliest beginnings of a slowdown (Figure 3.2B), suggesting ongoing steady diversification from a relatively late-start in this region. This interesting aspect of agamid diversification is overlooked without an explicitly biogeographical approach.

## Conclusion

Lineage-through-space-and-time plots contain information that is useful for interpreting how diversity has arisen in different biogeographic regions. Clade-level temporal diversification

dynamics such as understood using the classic lineages through time plot may miss key dynamics that occur within and between different regions. Differences in the tempo of lineage accumulation in different regions is particularly obvious in the case of agamid lizards but is likely to be true in many systems across different spatial and phylogenetic scales. LTSTs offer a visualisation tool for post-hoc exploration of these dynamics, and the method presented here also allows users to extract this temporal diversity data which can be used for novel applications (e.g., Skeels and Cardillo 2019).

## Chapter 4: Alternative pathways to diversity across ecologically distinct lizard radiations



Photo © Damien Esquerré

**Skeels, A., Esquerré, D. & Cardillo, M.** Alternative pathways to diversity across ecologically distinct lizard radiations. *Global Ecology and Biogeography*. 29 (3), 454:469.

## Abstract

Lizard assemblages vary greatly in taxonomic, ecological and phenotypic diversity, yet the mechanisms that generate and maintain these patterns at a macroecological scale are not well understood. We aimed to characterize the ecological and environmental drivers of species richness patterns in the context of macroecological theory for ten independent lizard radiations. We analyzed patterns of species and ecological trait diversity in ten ecologically distinct and widely distributed clades encompassing nearly all known lizard species. Using recently published spatial, phylogenetic, and ecological trait datasets, we built spatially explicit structural equation models to ask whether species diversity was directly or indirectly related to functional divergence or convergence within communities, and with features of the environment, including measures of productivity, complexity, and harshness. Our results show that high species diversity is achieved via different pathways in different lizard clades, with both functionally divergent and convergent assemblages harboring high diversity in different clades. More generally, we also find common, positive effects of temperature, productivity, and topography on species richness within lizard clades. Thermal constraints, topographic complexity, and spatial structuring of functional diversity help explain the presence of highly diverse lizard assemblages, suggesting the importance of environmental filters in shaping present-day diversity and assemblage structure. Our results show how different pathways to high richness in different clades have contributed to the overall global pattern of species richness in reptiles.

## Introduction

Species richness in lizards is unequally distributed around the world, and in many cases, lizards show discordant diversity patterns compared to other major clades of terrestrial vertebrates. Some of the greatest diversity in lizards is present in the hot and dry deserts of Southern Africa, the Arabian Peninsula, and Western Australia (Pianka 1973; Roll et al. 2017), biomes relatively low in diversity of other vertebrates. On the other hand, other lizard diversity hotspots, including tropical America and Southeast Asia, are also hotspots for many other groups of vertebrates (Jetz et al. 2012; Oliveira et al. 2016; Roll et al. 2017). This variation in species richness patterns has made diagnosing the drivers of lizard diversity difficult, and suggests that a range of potential drivers of diversity in lizards exists, some of which may be unique among terrestrial vertebrates (Powney et al. 2010; Tallowin et al. 2017). Investigating the structure and correlates of diversity of global lizard assemblages across major taxonomic divisions may help to infer the processes that have shaped the range of patterns within lizards, one of the most conspicuous, abundant, and ecologically important groups of terrestrial vertebrates (Pianka and Vitt 2003).

Species pools from which communities are assembled tend to be comprised of closely related species (Jordan 1905; Warren et al. 2014). Given that allopatric subdivision is the most likely mode of speciation in many vertebrate clades (Mayr 1963; Skeels and Cardillo 2019*b*), sympatry between species is often the result of secondary dispersal after speciation. Therefore, to understand how diversity has arisen, we require an understanding of how closely related species can coexist in the same geographic space. If close relatives are the strongest potential competitors for resources (Darwin 1859; Elton 1946), then secondary sympatry must be driven by differences in the ecological niche that limit competition (MacArthur and Levins 1967).

Alternatively, some regions may support ecologically similar species because a shared resource is abundant enough for multiple species to maintain a minimum viable population size (the more individuals hypothesis; Srivastava & Lawton, 1998; Storch *et al.*, 2018). In such cases, sympatry might be unrelated to niche divergence.

These alternative scenarios relate to expectations about the strength of competitive interactions as filters in the formation of assemblages, and we might expect the strength of different assembly mechanisms to vary across environments. For example, the more-individuals hypothesis argues that greater similarity of species' ecological niches in high diversity assemblages is possible in ecosystems (such as tropical rainforests) with high environmental productivity and resource availability (Srivastava and Lawton 1998; Storch et al. 2018). Other hypotheses, however, may make different predictions based on the same variables. For example, biotic interactions, including mutualisms, competition, parasitism, and predation, are often considered to be more important in high-productivity ecosystems such as tropical rainforests (Dobzhansky 1950; Schemske et al. 2009), which might lead to species-rich assemblages consisting of ecologically divergent species due to ecological specialization and coevolution.

It is unlikely that a single theoretical model that describes the relationships between species richness, ecological divergence, and environmental features can account for the variety of species richness patterns seen in diverse vertebrate radiations such as lizards. This is because different mechanisms may be responsible for generating high diversity in different regions, different clades, or both. One way to approach testing this idea is by categorizing environmental predictors into broad classes that relate to the key aspects of each hypothesis. For example, several core macroecological hypotheses make predictions related to some measure of either

environmental productivity, complexity, or harshness (e.g., Laliberte *et al.*, 2014; Fine, 2015) and these three axes of environmental variation can form the basis of a pluralistic explanatory framework for lizard diversity.

Productivity is associated with environmental energy and resource quantities and at large spatial scales is expected to be positively correlated with species richness (Waide *et al.* 1999). Productivity may promote ecological similarity by increasing the number of individuals that can use similar resources (Srivastava & Lawton, 1998; Hypothesis 1, Table 4.1), or drive ecological divergence by promoting biotic interactions (Brown, 2014; H2). Harshness is a measure of environmental extremes such as freezing temperatures or aridity. Harshness may act as an environmental filter, placing constraints on functional or species diversity by restricting the number and kind of species that can tolerate extreme conditions (Webb *et al.*, 2002; Kraft *et al.*, 2015; H3), or may promote ecological divergence due to increased competition for scarce resources, or selection for novel ecological strategies (Botero *et al.*, 2014; H4). Complexity is a measure of environmental heterogeneity or structure such as topographic ruggedness, which is expected to be positively correlated with species richness. Complexity may promote ecological divergence by increasing the number of environmental niches available in a given area (Badgley *et al.*, 2017; H5), or may increase the opportunity for allopatric speciation without necessarily increasing ecological or phenotypic diversity (Badgley *et al.*, 2017; H6). These six hypotheses are not mutually exclusive and different environmental variables may span different categories (for example temperature might be a measure of both productivity and harshness). However, this simplified scheme allows us to present a hypothesis testing framework to investigate alternative possible drivers of species richness simultaneously (Table 4.1).

**Table 4.1.** Six hypotheses that link ecological divergence, species richness, and three major environmental factors, harshness, productivity, and complexity, and their predictions for the relationships between variables. Env = environment; SR = species richness; ED = ecological divergence. – negative correlation; + positive correlation; ~ no correlation.

		Predictions		
	Hypothesis	SR ~ Env	ED ~ Env	SR ~ ED
H1	Productivity: more individuals	+	- / ~	-
H2	Productivity: biotic interactions	+	+	+
H3	Harshness: environmental filtering	-	+	+
H4	Harshness: competition	- / ~	+	-
H5	Complexity: niche diversity	+	+	+
H6	Complexity: allopatric speciation	+	- / ~	-

Recent publication of several large databases (Tonini *et al.* 2016; Roll *et al.* 2017; Meiri 2018) has now made it possible to begin to explore how the environment and ecological and phenotypic trait diversity interact to shape spatial diversity patterns in lizards on a global scale (e.g., Vidan *et al.*, 2019). Different lizard taxa also show varied spatial diversity patterns (e.g., Powney *et al.*, 2010), and this makes them excellent independent case studies to further explore the mechanisms that drive diversity. We therefore predict that different mechanisms may be responsible for the origin of different regional diversity patterns in different taxa. For example, patterns of species and functional diversity in teiid and gymnophthalmid lizards, which reach their highest levels in high-productivity tropical regions may be best explained by the more-individuals hypothesis (H1) or the productivity / biotic interactions hypothesis (Schemske *et al.*, 2009; H2). Harshness mechanisms (H4) may best explain arid-zone hotspots for groups such as agamid dragons and scincoids, which reach maximum diversity in the western Australian deserts, due to competition-driven niche divergence (Pianka, 1973). Diversity in groups such as liolaemids, with maximum diversity in the Andes, might be best explained by environmental heterogeneity associated with topographic complexity (H5), or allopatric species pumps (Esquerre *et al.*, 2019; H6). This study aims to estimate patterns of ecological and

phenotypic divergence (hereafter functional divergence) within different taxonomically and ecologically defined lizard taxa, and then to compare the support for six models described above by testing the relationships between species richness, ecological divergence, and major environment features, within each taxon.

## Methods

### Clade Selection

Estimating patterns of ecological divergence to understand the drivers of species richness requires comparisons between ecologically similar units that share an evolutionary history. We selected lizards to include all squamate reptiles excluding snakes, amphisbaenians, and dibamids, which are vastly different in their ecomorphology. In addition, we divided lizards into ecologically cohesive sub-clades to investigate diversity patterns, as the hypotheses we were testing assume that interactions such as competition for shared resources are most likely to take place between closely related species with similar ecologies. While there is value in looking at patterns of diversity at a very broad taxonomic scale (e.g., all lizards), interpretation of ecological divergence becomes more difficult. For example, the addition of any very distantly related species to an assemblage might disproportionately and misleadingly influence the measure of ecological divergence, such as the presence of one apex-predator monitor lizard (Varanidae) in an assemblage largely consisting of small leaf-litter scincoids (Scincidae). We selected 10 clades: anguids (Anguidae, Anniellidae, and Diploglossidae), varanids (Varanidae), agamids (Agamidae), scincoids and allies (Scincoidea), pleurodonta and allies (Pleurodonta), teiids (Teiidae), gymnophthalmids (Gymnophthalmidae), chameleons (Chamaeleonidae), lacertids (Lacertidae), and geckoes (Gekkota). These groups not only represent independent

monophyletic clades, but vary substantially in their ecology, diversity and geographic distributions (Figure 4.1), making them suitable independent case studies to test our hypotheses.

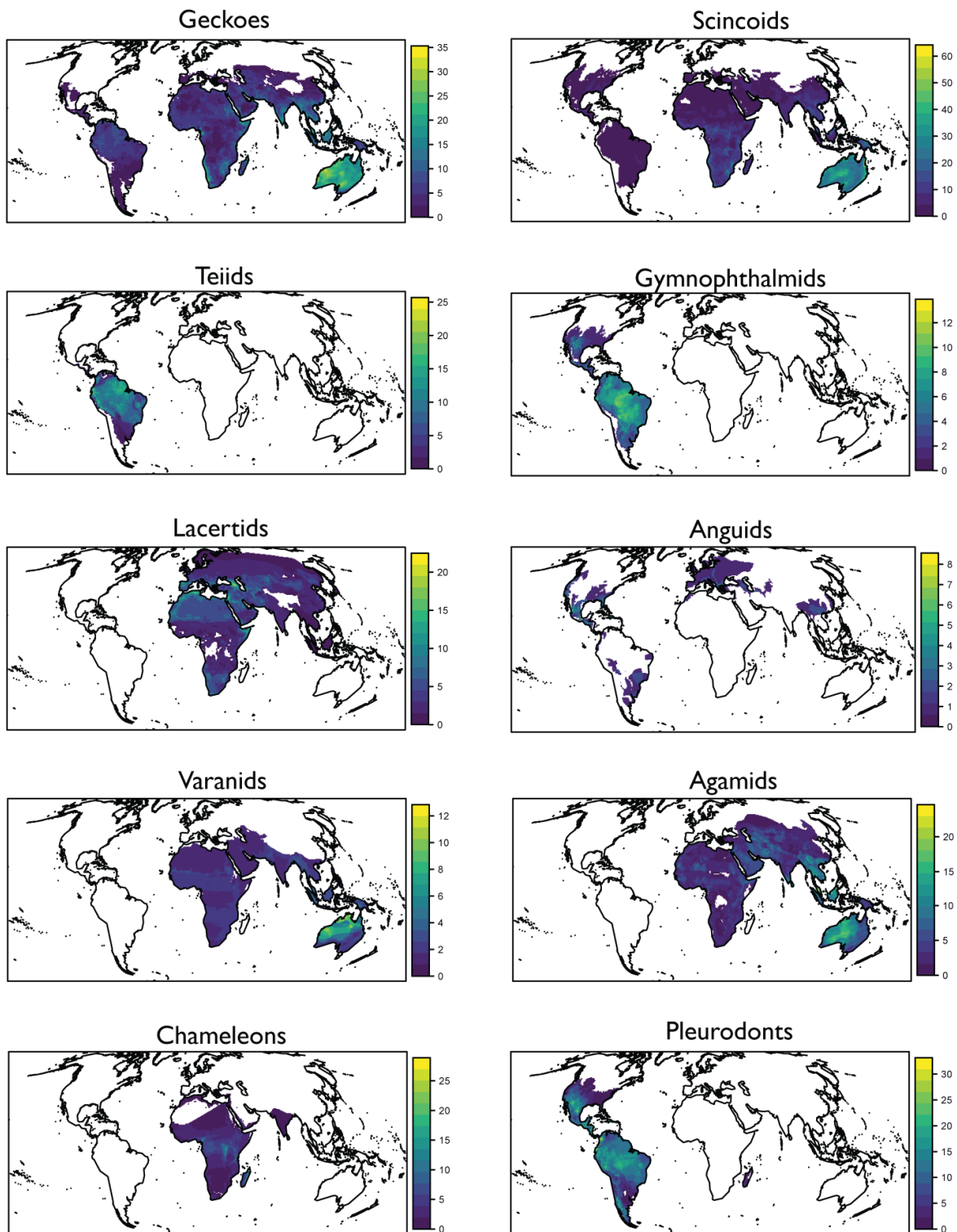


**Figure 4.1.** Geographic patterns of species richness in ten lizard clades. Species richness was estimated within 50x50km equal-area grid cells using species range maps from Roll *et al.* (2018).

## Spatial, phylogenetic, and trait data

We used the most recent estimates of lizard species geographic distributions and phylogenetic relationships. The phylogeny we used was the consensus super-tree of squamate reptiles from Tonini et al. (2016), a revision of a phylogeny first presented by Pyron et al. (2013). This phylogeny is based on molecular data for roughly 55% of taxa, with the remaining taxa placed using taxonomic inferences (PASTIS; Thomas *et al.*, 2013). Spatial data are from Roll et al. (2018) and contains polygonal maps for almost all squamate reptiles based on expert assessment and occurrence records. Trait data are from Meiri (2018). This comprehensive database contains ecological and phenotypic data for nearly all species of lizards, compiled from the lizard biology literature.

Many of the traits in the database are incompletely sampled across lizard species. To account for this we imputed missing data using random forest machine learning in R ('missForest' v1.4; Stekhoven & Bühlmann, 2012). We used random forest data imputation because there is a tendency for missing data to be biased with respect to species ecology (particularly species rarity and geographic range location) and multiple imputation has been shown to reduce bias by maintaining the relationships between traits (Penone et al. 2014). Random forest machine learning has been shown to outperform several other imputation methods (e.g., KNN; Troyanskaya *et al.*, 2001) by allowing for complex non-linear relationships between mixed variable types. Phylogenetic imputation (e.g., PhyloPars; Bruggeman *et al.*, 2009), on the other hand, requires transforming categorical variables into sets of binary variables and as such was not used in this analysis. We used all traits in the Meiri et al. (2018) dataset for data imputation, including taxonomic family included as an additional variable to account for phylogenetic component of variation in trait values. However, we selected only a subset of traits to use in

downstream analysis. Firstly, we selected traits that had > 50% representation across all lizard species. We found nine traits that had > 50% coverage (3000+ species) and most of these had > 80% coverage (4800+ species). These traits were maximum snout-vent-length (SVL), female SVL, activity time, diet, reproductive mode, smallest and largest clutch size, leg development, and microhabitat. We also obtained body mass data based on a conversion of maximum SVL using family specific equations (Meiri 2010, 2018; Feldman et al. 2016).

We used body mass in place of both maximum and female SVL as it is regarded as one of the most important ecological traits in reptiles (Hedges 1985; Meiri 2010) and is also highly correlated with maximum and female SVL. We discarded clutch size (largest and smallest) and reproductive mode as these traits were unlikely to be involved in niche partitioning between species. Microhabitat data were originally grouped into seven categories (fossorial, cryptic, saxicolous, arboreal, terrestrial, marine, semi-aquatic); we extended this to eight categories by including a generalist category for species belonging to more than one habitat class. Diet was classified as whether a species consumes mostly plants (herbivorous), mostly animal matter (carnivorous) or mostly animal matter with significant proportion of plant matter (omnivorous). Leg development was classified as whether species had four limbs, only forelimbs, only hind limbs or was limbless. Activity time was classified as whether species were nocturnal, diurnal, or cathemeral (Meiri 2018). Body mass data were log transformed to normalize the distribution and make differences between species proportional.

We therefore used five traits for our analyses, body mass (which required imputation in <1% of species), and four categorical variables; activity time, diet, microhabitat (which required imputation in <50% of species), and leg development (no missing data). To ascertain an estimate of imputation error, we subsampled the trait data for all species which had complete

observations for the five traits (3066 species). We then simulated missing data by removing 10% of observations randomly. We imputed these missing data then estimated the imputation error rate as the proportion of falsely classified entries.

Each database had some entries that were not found in the other databases due to taxonomic difference (e.g., synonyms or species descriptions post-dating the publication of the data), or spelling incongruencies. We found 198 species mismatched between the spatial and trait data, all of which were synonyms, so we relabelled databases based on the most up-to-date taxonomy in The Reptile Database (Uetz and Hošek 2019). There were a further 309 species with trait and spatial data that were not present in the phylogeny. Of these, 201 of those were synonyms and five were misspellings. The remaining 103 species were described after the time of publication of the phylogeny and were excluded from analyses. This resulted in a dataset containing traits, ranges, and phylogenetic relationships for 6129 species of lizards, or 5959 after excluding the amphisbaenians, dibamids, and species from the ecologically and phenotypically distinct but low diversity Helodermatidae, Lanthanotidae, Shinisauridae and Xenosauridae. The ten clades we selected included 1581 geckoes, 1704 scincoids, 246 teiids, 144 gymnophthalmids, 318 lacertids, 126 anguids, 78 varanids, 453 agamids, 201 chameleons, 1108 pleurodonta.

## Geographic sampling

Ecological processes can lead to patterns that emerge at different spatial scales and extents. Macroecological studies typically study ecological processes at broad spatial extents (continental or global) and coarse spatial resolutions (e.g., 100x100km quadrats; McGill, 2019). However, it is broadly recognised that ecological interactions between species typically occur at finer resolutions (Rahbek 2005). We sampled 50x50km equal area grid cells based on a

Mollweide projection of the spatial data across the distribution of each clade to provide a reasonable balance of the trade-offs between the extent of our study (global), the resolution of our species-level spatial data (broad spatial polygons), the resolution in which the ecological processes we were interested in may manifest as discernible patterns (local-scale species interactions), and the computational constraints of large spatial data sets.

At broad spatial resolutions (e.g., 50x50km) a signature of ecological interactions may be difficult to detect because species may occur in allopatry across topographic and environmental gradients within assemblages of this size. We make a distinction here between assemblages (in which species may interact) from communities (in which species do interact), and we attempt to address this in our approach to selecting appropriate predictor variables for modelling species richness and ecological divergence (see below). By including a variable to represent topographic complexity, we aimed to distinguish between scenarios where species richness is driven by habitat diversity or allopatry (H5 and H6, Table 4.1) within assemblages. We also re-analysed the data at a finer spatial scale (25x25km grid cells), in which ecological interactions may be more likely to structure assemblages (though the same issue is present at this spatial resolution). However, it is noted that at this finer spatial scale we can be less certain of the accuracy of species compositions, because 25x25km is a finer scale than that at which the spatial data were collected. Results at both spatial scales are qualitatively similar and discussed in the Supplementary Information (Appendix S1). For the remainder of the main text we discuss analyses done at the 50x50km scale.

We stratified the sampling of sites across ecoregions to make sure we sampled a representative amount of the total ecological and species diversity for each clade. Ecoregions represent ecologically and geographically distinct units that typically share a common fauna (Smith et al. 2018). We converted spatial polygons for each species into a site x species presence absence

matrix using the lets.presab function in ‘letsR’ package in R (Vilela and Villalobos 2015). We then sampled sites in each ecoregion in proportion to the area occupied by the clade within them, sampling a minimum of one grid cell from each occupied ecoregion. We sampled the number of sites ( $n$ ) for each clade ( $i$ ) according to the function  $n = S * (A_i / A_{\max})$ ; that is, the proportion of the area occupied by each clade ( $A_i$ ) compared to the maximum area occupied by any clade ( $A_{\max}$ ) for a maximum of roughly 2,500 sites ( $S$ ). This ensured each clade was sampled at an equal density across their distribution.

## Functional divergence

Different metrics exist to capture ecological diversity (hereafter functional diversity as we use functional traits as proxies for species ecological niches) within assemblages. Different measures of functional diversity capture different aspects of the distribution of traits within an assemblage (Mason et al. 2005). To determine if lizard species were divergent or convergent within functional trait space across assemblages, we estimated functional divergence (FD) using Rao’s quadratic entropy (Rao’s Q). Rao’s Q is the sum of pairwise distances between species as measured by Gower distances (Podani 1999) between trait values, scaled between 0 (species are functionally equivalent) and 1 (species are maximally functionally divergent; Botta-Dukát, 2005). We estimated FD based on Gower distance of all five traits together ( $FD_{\text{multi}}$ ), as well as for body mass alone ( $FD_{\text{mass}}$ ), at each site for each clade, using the rao.diversity function in the R package ‘SYNCSA’ (v1.3.3; Debastiani & Pillar, 2012). We selected body mass for separate analysis because it is the single trait most likely to reflect broad differences in ecology and life history between species (Hedges 1985), and we used both  $FD_{\text{multi}}$  and  $FD_{\text{mass}}$  to see if the multivariate and univariate measures of divergence give similar results.

Rao's Q is not completely independent of species richness. This makes the raw values unsuitable independent predictors of diversity. To understand how the behavior of FD changes across assemblages and relates to species richness we compared their values to null expectations given a biogeographically constrained null model of community assembly; the dispersal null model (DNM; Miller *et al.*, 2017). The DNM simulates assemblages by sampling species from nearby sites with a probability inversely proportional to their distance to the focal site, while approximately maintaining species frequency and site diversity. We calculated site by site distances using great-circle distances with the function rdist.earth from the 'fields' package in R (v9.6; Nychka *et al.*, 2017). Under the DNM, species from local species pools, which are less likely to be biogeographically constrained from dispersing into a site, will be preferentially sampled. For each clade separately, we estimated FD across each site in each simulated assemblage, for 1000 simulations of the DNM.

From the distribution of values of FD from each site in the simulated datasets we calculated the standardized effect size (SES) of FD:

$$\frac{FD_{observed} - \text{mean}(FD_{simulated})}{SD(FD_{simulated})}$$

Positive SES values represent assemblages that contain species with more divergent traits than expected under the null model and negative values indicate species are more convergent than expected. Values greater than 1.96 or less than -1.96 are considered significantly more or less divergent (respectively) than null expectations, given an alpha of 0.05.

## Modeling species richness

To test our hypotheses about the influence of abiotic factors on species richness directly, or indirectly through their influence on FD, we extracted values for four environmental predictors across sites for each clade. We selected mean temperature of coldest quarter ( $^{\circ}\text{C}$ ) from the CliMond database (temperature; Kriticos *et al.*, 2014) and Thornwaite's aridity index from the ENVIREM database (aridity; Title & Bemmels, 2018) to represent measures of environmental harshness. "Harsh" values of these variables are at different ends of their scales, for example harsh conditions of aridity are measured at high values of the aridity index, but harsh values of the temperature variable (for lizards) are expected at low values of temperatures (cold winter temperatures). This means that a positive effect of harshness may be measured as a positive correlation with aridity but a negative correlation with temperature. We selected topographic ruggedness index from the ENVIREM database (topography; Title & Bemmels, 2018) as a measure of environmental complexity, and net primary productivity as a measure of environmental productivity (productivity; Imhoff *et al.*, 2004b,a). All variables were resampled at the same resolution as our sampled sites (50x50km grid cells) using the raster package in R (Hijmans 2016) and a single value was extracted for each site.

We were interested in the direct effects of different environmental factors and FD on species richness (species richness  $\sim$  FD + environment), as well as the indirect effects of the environment on species richness via direct effects on FD (FD  $\sim$  environment). To account for this hierarchy of direct and indirect effects we used piecewise structural equation models (pSEM) to investigate the relationships between multiple response and predictor variables. pSEM is a type of pathway analysis that allows users to specify hypothesised causal relationships between multiple response and predictor variables in the same causal network

(Lefcheck 2016). pSEM differs from traditional SEM in that pathways in the model are solved independently, rather than simultaneously finding a global solution (Lefcheck 2016). This allows for a greater flexibility in the kinds of models can be fit in causal network. This is important because spatial data, such as assemblage level estimates of species richness and environmental predictors, can be highly spatially autocorrelated which will violate the assumptions of standard linear regression (Legendre 1993). To account for this, we fit spatial autoregressive error models (SAR) along the pathways of our pSEM.

SARs are a modification of standard linear regression with an added error term which accounts for spatial autocorrelation by weighting the influence of neighbouring sites on the contribution of each site, based on a spatial weights matrix. To determine the appropriate spatial weights matrix, we identified neighbours within seven different distances from each focal site (50km, 100km, 150km, 200km, 250km, 300km, 350km, and the maximum distance in which all sites have at least one neighbour, which varied between groups), and weighted these neighbours using three different schemes; a row standardised, globally standardised, and variance stabilising (Tiefelsdorf et al. 1999). These three coding schemes reflect differences in balancing well connected sites (globally standardised), weakly connected sites (row standardised), or both (variance stabilising). We used model selection based on Akaike information criterion and Nagelkerke pseudo-R<sup>2</sup> values to determine which spatial weights matrix were used to generate the best fitting models separately for each SAR (e.g., species richness ~ FD + environment; FD ~ environment) and for each clade. We then used these weights matrices for SAR models in the pSEM framework. Creating spatial weights matrices was done using the dnearest and nb2listw functions in the package ‘spdep’ (v1.1.2; Bivand *et al.*, 2013; Bivand & Wong, 2018).

We fit a pSEM specifying both species richness and FD as a response and FD and environment as predictor variables. We first fit fully specified models where each pathway was specified in the pSEM. We then removed pathways which did not explain a significant amount of variation in the response and heuristically repeated the analysis using tests of d-separation to include or exclude pathways. Tests of d-separation are used to assess the goodness of fit of a pSEM by asking if relationships between pathways that are not specified in the model are independent after considering the pathways that are specified in the model (Shipley 2000). For each clade we determined the minimum model in which all pathways significantly explained species richness and FD<sub>SES</sub>. SARS were fit using the ‘spdep’ and ‘spatialreg’ packages in R (v1.1.3; Bivand *et al.*, 2013), while pSEM was fit with ‘piecewiseSEM’ package in R (v2.0.2; Lefcheck, 2016). We repeated analyses using the SES of FD<sub>multi</sub> and FD<sub>mass</sub>.

## Functional trait diversity

To assess how the ten different clades varied in trait diversity, we estimated the amount of functional trait space that each clade occupies by estimating the functional richness of each clade, standardised by the total functional trait space occupied by all ten clades, using the R package ‘FD’ (v1.0.12; Laliberte & Legendre, 2010; Laliberte *et al.*, 2014b). The functional richness metric is measured as a proportion of the total convex hull of multi-dimensional functional trait space of all lizards occupied by the convex hull of each separate clade, and is scaled between 0 and 1. We asked whether functional richness was a linear function of species diversity in each clade using a phylogenetic generalised least squares (Freckleton *et al.* 2002) test on a phylogeny reduced to a single tip for each clade, using the pgls function in the “caper” package (Orme *et al.* 2018).

## Phylogenetic signal of traits

To understand the distribution of functional diversity across assemblages considering the evolutionary history of each trait, we estimated phylogenetic signal of each of the five traits separately using Pagel's  $\lambda$ . For quantitative traits we estimated  $\lambda$  using `phylosig` function in 'phytools' (v0.6.60; Revell, 2012) and for categorical traits we estimated  $\lambda$  using continuous-time markov models of character evolution, independently estimating the transition rate between character states (all-rates-different model), with the `fitDiscrete` function in 'geiger' (v2.0.6.1; Harmon *et al.*, 2008).  $\lambda$  is a branch-length transformation parameter, and its maximum likelihood estimate is widely used as a measure of phylogenetic signal (where a value of zero indicates no phylogenetic signal and a value of one indicates evolution under a Brownian motion model). To assess whether traits showed significant phylogenetic signal we used likelihood ratio tests to compare estimates of  $\lambda$  for each trait along the phylogeny to those estimated when the phylogeny was transformed with  $\lambda = 0$ .

## Results

### Data imputation

The data imputation error rate, as measured by the proportion of falsely classified traits in the subset data used for cross validation, for the three categorical variables was low (7.6%). Missing data were unevenly distributed across the clades used in this study. Varanids had the highest proportion of complete observations for the three categorical traits with missing data (5% for diet, 3% for microhabitat and 6% for activity), while teiids had the highest proportion of missing data (67% missing for diet, 26% for microhabitat, and 43% for activity time). Results from

piecewise structural equation models (see below) were very similar when using a single trait, body mass (a trait which required imputation for only 23 species, or less than 1% of species) and multiple traits (with imputed data).

## Geographic patterns of functional divergence

Measuring functional divergence (FD) in communities using a multi-trait ( $FD_{multi}$ ) approach as well as for a single trait (body mass;  $FD_{mass}$ ), we found that FD within assemblages was spatially structured and different between lizard taxa (Figure 4.2). In all clades, for both  $FD_{mass}$  and  $FD_{multi}$ , very few assemblages were significantly divergent, showing values greater than expected based on the dispersal null model ( $FD_{SES} > 1.96$ ), with significantly divergent assemblages accounting for less than 1% of assemblages. On the other hand, for  $FD_{multi}$ , several clades (geckoes, scincoids, anguids, agamids, and pleurodons) showed regions in which assemblages were significantly convergent, with greater than expected functional similarity ( $FD_{SES} < -1.96$ ) compared to the dispersal null model. In these clades, convergent assemblages accounted for between one and five percent of all assemblages. These were typically concentrated in small areas such as Borneo in agamids or Patagonia in pleurodons (Figure 4.2). For  $FD_{mass}$ , convergent assemblages accounted for less than two percent in pleurodons and scincoids, and less than one percent in all other clades.

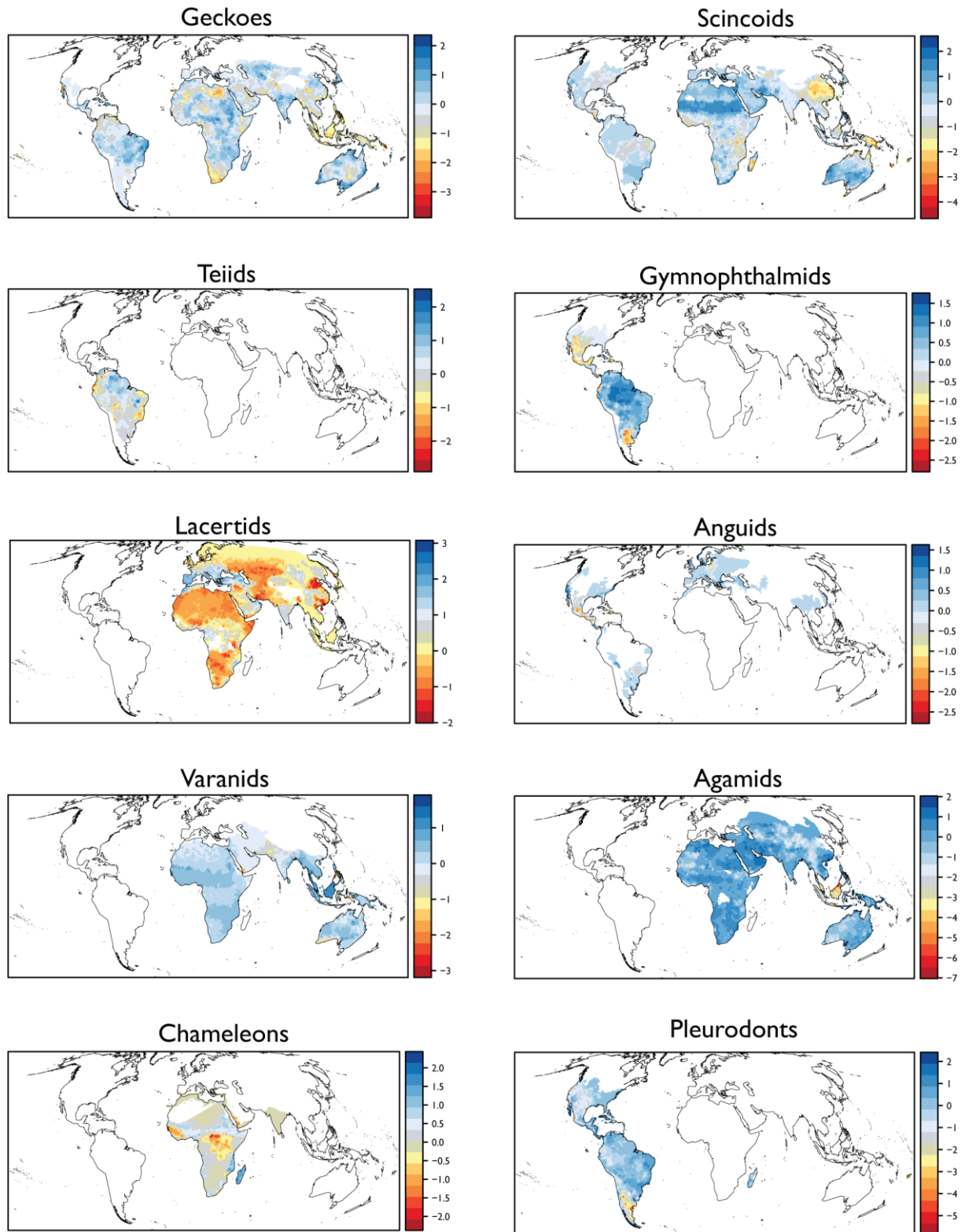


**Figure 4.2.** Geographic patterns of functional divergence ( $FD_{multi}$ ) of five different phenotypic and ecological traits. Values are the standardized effect size (SES) of Rao's Q measured using Gower distances of traits compared to values simulated under a dispersal null model measured in 50x50km grid cells. Positive values (blue) indicate

functional divergence and negative values (red) indicate functional convergence compared to the null model. Significant SES values are greater or less than 1.96 and -1.96 respectively.

## Drivers of species richness and functional divergence

Using spatial autoregressive models (SAR) in a piecewise structural equation model framework, we found that spatial autocorrelation present in the residuals of ordinary least squares models was well accounted for. We also found that using a measure of FD<sub>SES</sub> based on multiple traits (FD<sub>multi</sub>) or a single trait (FD<sub>mass</sub>) give largely similar results and we found a positive correlation between standardized coefficients for significant pathways shared between models (Pearson's  $r = 0.6$ ). Here we will present the results based on FD<sub>multi</sub> and describe where FD<sub>mass</sub> differs in the appendix (Figure A4.1, A4.2).

Species richness was significantly related to several different environmental features in each clade, and while no relationships were shared amongst every clade, there were several common relationships, repeatedly appearing in more than five different clades. We found that minimum temperature of the coldest quarter, a measure of environmental harshness, was significantly, positively related to species richness in six different clades (geckoes, scincoids, teiids, varanids, anguids, and agamids) meaning richness is lower in cold-climate assemblages (Figure 4.3). In most cases, temperature was the strongest predictor of richness (Figure 4.3). Chameleons were the only group to show an opposite pattern where richness was strongly negatively related to temperature.

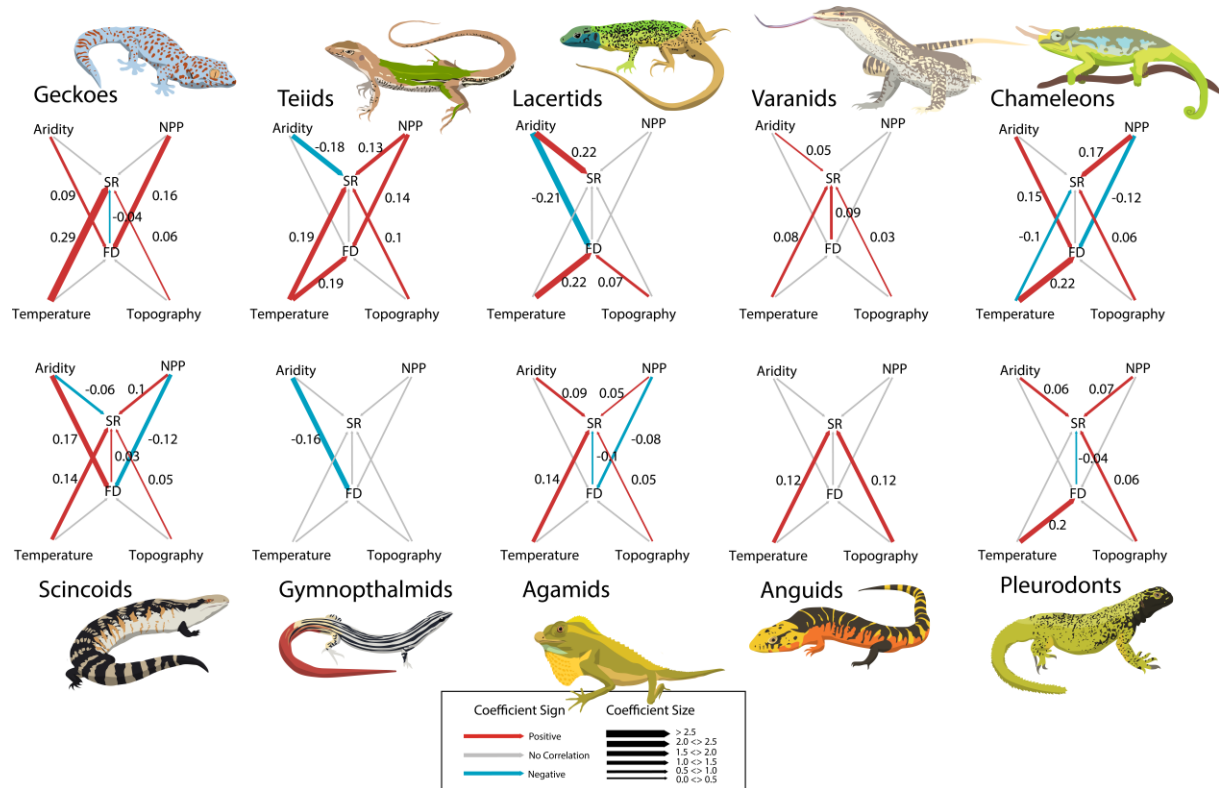


**Figure 4.3.** Pathways in piecewise structural equations models of species richness and ecological divergence (the standardized effect size of Rao's Q for five different ecological traits). Arrows show all pathways in the full model. Coloured paths indicate significant pathways in the final model which were chosen using tests of d-separation and comparing goodness of model fit, while grey pathways indicate excluded pathways from the final model. Red pathways indicate positive standardized coefficient estimates for the pathway and blue pathways are negative coefficients. Line width reflects the size of the standardized coefficient, indicated next to each significant path, with strong effect sizes in bolder lines. Illustrations are by Damien Esquerré and show a representative species from each clade: *Gekko gekko* (geckoes), *Ameiva ameiva* (teiids), *Lacerta schreiberi* (lacertids), *Varanus gouldii* (varanids), *Trioceros jacksonii* (chameleons), *Tiliqua scincoids* (scincoids), *Vanzosaura rubricauda* (gymnophthalmids), *Diploglossus monotropis* (anguids), *Lyriocephalus scutatus* (agamids), *Phymaturus maulense* (iguanids).

Topographic ruggedness, a measure of environmental complexity, was positively related to species richness in eight clades (geckoes, teiids, anguids, chameleons, agamids, varanids, pleurodonta, and scincoids). Aridity, a measure of environmental harshness, was positively related to richness in four clades (agamids, varanids, pleurodonta, and lacertids) and negatively in two clades (scincoids and teiids). Net primary productivity, a measure of environmental

energy and resource quantity, was correlated with richness in five clades (teiids, scincoids, agamids, pleurodons, and chameleons).

Species richness was also correlated with functional divergence within assemblages, with FD<sub>SES</sub> significantly related to species richness in five of ten lizard clades (Figure 4.3). In two clades the relationship was positive (varanids and scincoids), while it was negative in three clades (geckoes, pleurodons and agamids). FD<sub>SES</sub> itself was explained by different environmental predictors, suggesting environmental drivers of ecological assemblage structure, and in some cases together with a significant relationship between species richness and FD<sub>SES</sub>, suggests a further, indirect, effect of the environment on species richness. Temperature was positively related to FD in four clades (teiids, lacertids, pleurodons, and chameleons), and in each case was the strongest relationship in the pathway analysis. Aridity showed a positive effect in three clades (scincoids, chameleons, and geckoes) and a negative in two clades (gymnophthalmids and lacertids). Productivity was positively related to FD in two clades (geckoes and teiids), and negatively in three clades (chameleons, agamids, and scincoids). Topography was only related to FD in lacertids.

## Functional Trait Space

Based on estimates of functional richness of ecological traits within clades, standardized as a proportion of the total functional richness across all clades, we found that clades differed in the total amount of ecological trait space they occupied. This was positively related to clade richness after accounting for phylogeny using PGLS ( $R^2 = 0.77$ ,  $p < 0.001$ ). Scincoids and geckoes, the two most species-diverse clades, occupied a large proportion of the overall trait space (functional richness = 0.91 and 0.87 respectively). The remaining clades occupied smaller

proportions of this space (functional richness = 0.4 for anguids, 0.36 for pleurodents, 0.29 for chameleons, 0.28 for teiids, 0.25 for agamids, 0.10 for lacertids, 0.08 for varanids, and 0.05 for gymnophthalmids).

## Phylogenetic signal

We estimated phylogenetic signal as Pagel's  $\lambda$  for five different traits in each of the ten clades. There were eight instances where a clade showed zero variance for a trait (all species had the same trait value) and 37 of the 42 remaining trait-clade combinations showed significant phylogenetic signal, suggesting that trait distances tend to reflect the divergence times between taxa (Table A4.1). The exceptions to this, where traits did not show significant phylogenetic signal, were for diet in teiids and anguids, activity time in varanids, agamids, and chameleons. However, values of  $\lambda$  for these traits was still very high ( $>0.9$ ), and it is likely that it is because these traits tended to show near zero variation (e.g., are highly conserved), phylogenetic signal appears not significant. For example, activity time is mostly diurnal with only a handful of nocturnal or cathemeral species in varanids, agamids, and chameleons. Similarly, diet shows very little variation in teiids and anguids, with only a handful of species that are not carnivorous.

## Discussion

Lizards are an incredibly diverse group that occupy a wide variety of ecological niches and display an array of phenotypes that is hard to match amongst terrestrial vertebrates, ranging from tiny fossorial skinks with reduced limbs (*Lerista*), to large apex predators like monitor lizards (*Varanus*); from marine foraging iguanas (*Amblyrhynchus*) to gliding canopy dwelling

dragons (*Draco*). This ecological diversity has allowed lizards to occupy almost every terrestrial habitat on earth, except for the coldest places at high altitudes and latitudes, owing to one of their most important shared ecological traits: ectothermy, the dependence on environmental temperatures to regulate their own body temperature. Despite these observations, it has long been unclear whether the ecological and phenotypic diversity present in lizards promotes species diversity in lizard assemblages. It has been argued that this is because different lizard lineages in different regions likely respond to different abiotic and biotic factors (Pianka 1973).

Using a global, macroecological approach, our results support this idea and suggest that there are alternate ecological pathways to diversity amongst lizard clades, with support for three of the six hypotheses for diversity presented in Table 4.1 (H1, H3 and H6). Given differences in morphology, ecology, and biogeography between the major taxonomic divisions of lizards, it is perhaps unsurprising that we do not see a general pattern among clades. In some cases (geckoes, agamids, and pleurodonts), we see high species richness associated with low functional divergence (FD) between cooccurring species, while in other cases, high species richness is associated with greater FD (scincoids and varanids), or shows no association (lacertids, chameleons, gymnophthalmids, anguids, and teiids). However, despite largely idiosyncratic patterns among clades, there are some common trends. One widespread trend, shared by six of ten clades, is a negative association between species richness and environmental harshness, and particularly cold winter temperatures (Figure 4.3). We also see a positive effect of environmental productivity (net primary productivity) in five clades, and a relatively weaker positive effect of environmental complexity (topographic ruggedness) on species richness in eight of the clades.

## Functional convergence and divergence

Both functional divergence and convergence have been demonstrated to explain diversity in different taxa. For example, species-rich assemblages have been associated with functional convergence in particular groups of plants (Freschet et al. 2011; Ordonez and Svenning 2018), birds (Pigot et al. 2016; Cooke et al. 2019), mammals (Cooke et al. 2019), and corals (McWilliam et al. 2018), and functional divergence in carnivoran mammals (Davies et al. 2007), fish (Mason et al. 2008), and plants (Kraft et al. 2008; Skeels and Cardillo 2019*a*). Yet, we still do not have a good understanding of why diversity is associated with either of these alternative patterns. In lizard assemblages these patterns seem to be independent of fundamental differences between clades, including the geographic distribution of clades (because clades that show similar distribution patterns, for example varanids and agamids, show opposite trends; Figure 4.1); the number of species in a clade (both small and large clades show similar trends); the ecological trait diversity of a clade (clades that are widely and narrowly distributed in functional trait space can show similar trends).

Alternative mechanisms likely underlie functional convergence and divergence in high diversity assemblages of different clades (Table 4.1), and the range of FD<sub>SES</sub> values suggests an explanation for the effect of FD on species richness. For most clades, we see very few assemblages that have greater functional divergence than expected under our null model, however many clades show values of FD<sub>SES</sub> skewed towards functional convergence. For clades that show a positive FD-richness relationship, this means that functional traits in high richness assemblages do not tend to be more divergent than null expectations, but low richness assemblages do tend to be more similar than expected. A negative FD-richness relationship means that high richness assemblages tend to be more functionally convergent than expected.

Hypotheses which predict that species richness is driven by the evolution of niche diversity, either related to biotic interactions and the limiting similarity principle (H2 and H4, Table 4.1) or functional divergence in heterogenous environments (H5), are therefore not well supported, at least along the broad niche axes used in this study (e.g., diet, microhabitat, activity times). This is because we rarely see any assemblages which are structured by strong functional divergence at all. Instead, ecological convergence in both high and low richness assemblages, as well as supporting evidence from a number of significant environmental correlations, suggests a stronger role for environmental filtering effects (H3).

## Environmental filtering

One factor that may drive functional convergence at low species richness across assemblages is environmental filtering (H3, Table 4.1): when environmental constraints prevent species with (or without) particular traits from persisting. Environmental filtering might reduce phenotypic and functional diversity if more extreme environments select for particular traits and adaptations, as well as reduce species richness if fewer species have evolved adaptations to persist in extreme environments (Dobzhansky 1950; Currie et al. 2004). Under this hypothesis we expect environmental features that may place the strongest physiological constraints on lizard clades, such as low water availability in arid regions (Neilson 2002; Pastro et al. 2013; Cox and Cox 2015), or cold winter temperatures (Aragón et al. 2010; Pie et al. 2017), to have the greatest effect suppressing species richness or FD. Across the ten lizard clades used in this study, this hypothesis receives the greatest support, with a strong effect of temperature in six clades, and relatively weaker effect of aridity in two clades.

Temperature clearly plays an important role in limiting the abundance and distribution of lizard species, since cold temperatures place physiological constraints on metabolic rates of ectotherms (Buckley et al. 2008, 2012). Low diversity of lizard assemblages may follow from this in several ways. 1) Relatively few lizard species have evolved adaptations to these thermal extremes due to evolutionary conservatism of thermal tolerances (Pie et al. 2017). Phylogenetic signal present in many ecological traits suggests that ecological strategies such as reproductive mode, clutch size, and body size, which are all related to temperature in lizards (Shine 1985, 2004; Adolph and Porter 1993; Pincheira-Donoso et al. 2008), are not highly labile. 2) Low diversity of cold regions may be the result of competitive exclusion by endothermic clades that have a greater physiological capacity to maintain activity in cold climates (Buckley et al. 2012). The temperature-diversity correlation may also have a historical basis if, 3) cold regions have more recently been colonized from warmer regions leading to a time-for-speciation effect in warm regions (Wiens and Graham 2005), or 4) the rate of extinction is greater in colder regions due to greater fluctuations of climate throughout the evolutionary history of lizards (Dynesius and Jansson 2000; Pyron 2014).

A measure of harshness on a different environmental axis, aridity, was also associated with species richness in several clades, although the effect was smaller than that of temperature. Two clades showed a negative richness-aridity relationship (scincoids and teiids), and two clades showed a negative FD-aridity relationship (gymnophthalmids and lacertids). Many lizard lineages thrive in arid environments due to adaptations to resist desiccation (Bradshaw 1988; James and Shine 2000; Zatsepina et al. 2000). However, the distribution of some clades appears limited by aridity. Teiids, for example, are widespread in the Neotropics but tend to occur at relatively low densities in the drier Cerrado, Chaco, and Caatinga biomes, compared with tropical rainforests. Scincoids are exceptionally diverse in the Australian western deserts, but

this diversity pattern is not repeated to the same degree in arid biomes on other continents, which may explain a more general negative aridity-diversity relationship in this clade after accounting for spatial autocorrelation.

Although aridity appears to dampen diversity in some clades, others show increased species diversity or FD with increased aridity. Lacertids, pleurodons, agamids, and varanids showed a positive richness-aridity relationship and cooccur at high densities in relatively arid regions across their distributions, such as in Southern Africa for lacertids (e.g., *Meroles*, Harris *et al.*, 1998), the southwest deserts of North America in pleurodons (e.g., Phrynosomatidae, Wiens *et al.*, 2013), and the Australian deserts and savannahs in agamids and varanids. Scincoids, chameleons, and geckoes all show a positive FD-aridity relationship which seems to be driven by very low FD in less arid regions such as archipelagic Southeast Asia, compared to more arid savannahs (e.g., Cerrado geckoes), and deserts (e.g., Saharan scincoids and Madagascan Chameleons). The high number of sympatric species in deserts, such as phrynosomatid lizards in North America or *Ctenotus* skinks in Australia, has been attributed to the vast and homogeneous nature of deserts that allow species with a similar climatic niche to have wider distributions and hence tend to overlap (James and Shine 2000; Wiens *et al.* 2013; Vidan *et al.* 2019). Therefore, an FD-aridity relationship might also be a product of overlapping widespread species with diverging ecological traits.

## Productivity and Topography

One long-standing hypothesis is whether environmental energy may promote species richness by increasing resources to support larger minimum population sizes therefore allowing more species sharing ecological traits to use the same resource base (H1, Table 4.1). Under the more-

individuals hypothesis it is expected that high richness assemblages contain ecologically redundant species and therefore a negative richness-FD relationship, as well as an effect of productivity directly or indirectly (if productivity is negatively correlated with FD) on diversity. We found that net primary productivity, a measure of environmental energy, was a significant positive predictor of species richness in five clades (teiids, agamids, chameleons, scincoids, and pleurodents), and a negative predictor of FD in three clades (chameleons, agamids, and scincoids). This suggests that in some cases high productivity is associated with high species richness and functional convergence of species. However, in only one example, the agamids, do we see high richness associated with functional convergence, via this pathway. Previous studies of lizards did not find a relationship between species richness and productivity (Buckley and Jetz 2010), and overall the support for the more individuals hypothesis is equivocal (Currie et al. 2004; Adler et al. 2011; Storch et al. 2018). Instead, it has been suggested that the macroecological consequences of ectothermy are that temperature rather than productivity is a better predictor of species distributions and diversity patterns (Buckley et al. 2012). Our results suggest productivity does play an important role in promoting species richness in lizards, but it does not have a widespread effect of promoting greater niche overlap in lizards. More work to understand the mechanism that drives this relationship is needed.

Topographical complexity is a global driver of species diversity in different clades, reflecting the ecological and evolutionary influences of geological processes (Grenyer et al. 2006; Badgley 2010). Topographical complexity may increase diversity through two main mechanisms. Firstly climatic and habitat heterogeneity across elevations, aspects, and slopes might present ecological opportunity for diversification along different niche axes (H5, Table 4.1), or by increasing landscape barriers, acting as an allopatric species pump (H6; Badgley *et al.*, 2017). We found that eight clades showed a positive topography richness relationship

(geckoes, teiids, agamids, anguids, chameleons, pleurodonta, varanids, and scincoids). If complexity increases species richness through niche divergence across habitats, functional divergence is expected to be greater in topographically complex assemblages than in topographically homogenous ones. We observe this pattern only in the lacertids, however a lack of a richness - topography relationship suggests that this relationship does not act to drive assemblage level diversity in lacertids. Instead, if complexity increases diversity through opportunities for allopatric speciation, we expect functional divergence in topographically complex regions to be less than or equal to topographically homogenous regions, which is the case in the eight clades with a positive richness-topography relationship. The relatively weak but consistent positive effect of topography on diversity supports a role for topographically complex areas acting as “species pumps” to increase diversity in higher taxonomic levels at global scales. This supports a pattern found at lower taxonomic levels in clades such as *Liolaemus* whose radiation is linked to the orogeny of the Andes mountains (Esquerre et al. 2019), but differ from other studies which have found less of a role of topography at regional scales (Guisan and Hofer 2003; Buckley and Roughgarden 2006; Tallowin et al. 2017).

## Conclusion

This study investigated the ecological and environmental drivers of species richness in one of the largest and most ecologically diverse vertebrate radiations. Our results show that there can be alternative pathways to high diversity (functional trait convergence and divergence) as well as more general mechanisms resulting from conserved physiological constraints that are common to all lizards (ectothermy), or structural properties of the environment that allow species to partition geographic space (topographic complexity). One assumption that is implicit in the approach we have used in this study is that species richness is at or near ecological

equilibrium, that is, that present-day patterns of species richness and trait diversity are reflective of environmental limits on diversity (MacArthur 1965; Rabosky and Hurlbert 2015b). A historical and evolutionary approach may complement our understanding of the idiosyncratic diversity patterns in lizards if assemblages are not saturated with diversity (non-equilibrium dynamics), and factors such as evolutionary time (e.g., Skeels & Cardillo, 2017; Miller *et al.*, 2018), or diversification dynamics (e.g., Machac & Graham, 2017) are important in structuring present-day diversity patterns (Fischer 1960; Rohde 2006), or trait-diversity patterns (e.g., Oliveira *et al.*, 2016). A promising approach to more completely understand present-day diversity patterns could be to combine equilibrium and non-equilibrium dynamics into a common model framework (Skeels and Cardillo 2019a), although this would require more complete knowledge of ecological traits that are important in mediating competitive interactions in lizards. Understanding how the differences between lineages contribute to present-day biodiversity is critical to understanding the origin and maintenance of diversity. This study highlights that within large groups, such as lizards, there are both general and idiosyncratic drivers of diversity.

## Appendix

### Results for different measures of functional divergence

We measured functional divergence (FD) in two ways, firstly as Rao's Q of body mass ( $FD_{mass}$ ) and secondly as Rao's Q of body mass, diet, microhabitat, activity time, and leg development ( $FD_{multi}$ ). Results were very similar using both approaches. More than 50% of significant pathways were shared between  $FD_{mass}$  and  $FD_{multi}$  models at 50x50km resolution and more than 60% at 25x25km resolution. The relative importance of significant pathways was also high between models was high (Pearson's r of 0.6 between standardized pathway coefficients). Typically, the environmental predictors of FD maintained their relationships and relative importance (as measured by the standardized pathway coefficients) regardless of which measure of FD was used (Figure A4.1).

There are some exceptions to this, for example in the gymnophthalmids, net primary productivity (NPP) is the only significant (positive) predictor of  $FD_{mass}$  but aridity is the only significant (negative) predictor of  $FD_{multi}$ . These differences are qualitatively similar, because, while not interchangeable, regions with high NPP are typically not arid and non-arid places are often highly productive. In other cases, we see changes in whether environmental variables directly or indirectly effect species richness. Temperature is a positive predictor of species richness in anguids, when the model is fit with  $FD_{mass}$ . When we fit the model with  $FD_{multi}$ , temperature is indirectly related to species richness through its direct relationship with  $FD_{multi}$ . In both cases, temperature is an important predictor of species richness, but how we interpret its effect changes with the different measure of FD. Only in one case do we sign a difference in sign between  $FD_{mass}$  and  $FD_{multi}$ . This is for the relationship between FD and species richness

in geckoes which is positive in when measured using  $FD_{mass}$  and negative when measured using  $FD_{multi}$ . However, in both cases the relationship is between FD and species richness is relatively weak compared to other pathways in the model.

## Results at different spatial resolutions

We also found that results were consistent when variables were measured at 25x25km resolution and 50x50km resolution. Roughly 50% of all significant pathways were shared between models at different spatial resolutions and the standardized pathway coefficients showed a positive correlation (Pearson's  $r = 0.75$  for  $FD_{multi}$  and  $r = 0.67$  for  $FD_{mass}$ ). Typically, the strongest environmental predictors of species richness were the same between spatial resolutions, whereas pathways with weak effect sizes (standardized pathway coefficients close to zero) were more variable between spatial resolutions. For example, the importance of temperature as the strongest predictor of species richness is the same at both spatial scales. This suggests that identifying the strongest predictors of species richness were robust to spatial resolution, however the ordering of variables with weaker relationships to species richness is sensitive to spatial resolution. The major differences between spatial scales were the relative importance of functional divergence (FD). At finer resolution (25x25km) FD is a predictor of species richness in nine clades for  $FD_{multi}$  and eight clades for  $FD_{mass}$  (Figure A4.2), compared to five clades each at 50x50km resolution. There could be several reasons for this. Firstly, we expect the role of ecological interactions to be stronger at finer spatial scales and we also might expect species richness patterns to be more closely tied to patterns of functional diversity. Alternatively, it could be an artifact of the data, because if the spatial data (measured as broad spatial polygons) is less precise at finer spatial scales we might overestimate the number of co-occurring species which could inflate the degree of divergence we estimate in an assemblage.

More work still needs to be done to estimate how spatial precision affects our estimates of community assembly and functional diversity metrics.

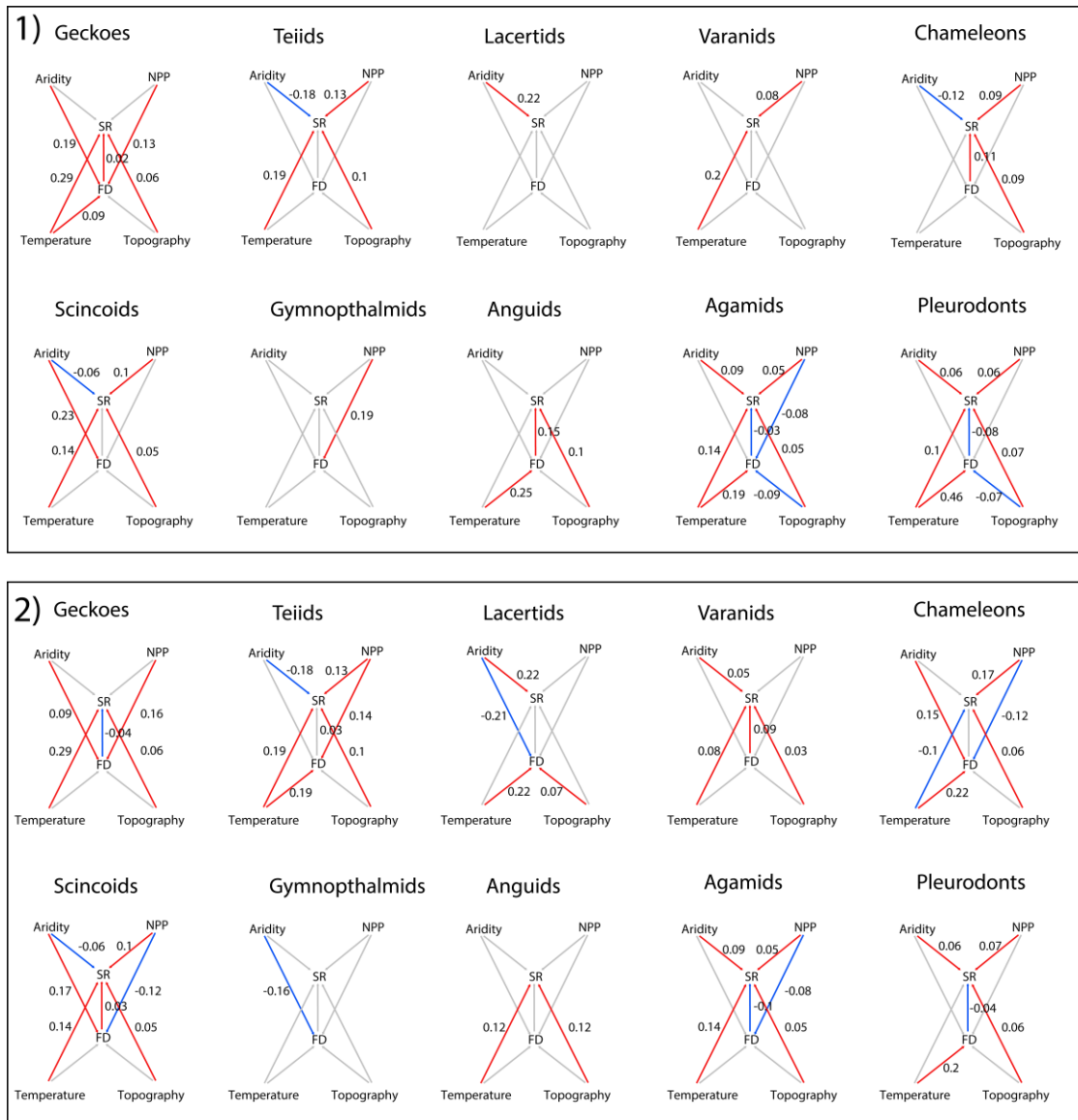


**Figure A4. 1.** Pathways in piecewise structural equations models of species richness (SR) and functional divergence (FD). All variables were extracted and calculated at a spatial resolution of 50x50km. Panel 1 shows the models for when FD is calculated as the standardized effect size of Rao's Q for a single trait, body mass, whereas panel 2 shows for when FD is calculated as the standardized effect size of Rao's Q for five traits together, body mass, diet, activity time, leg development, and microhabitat. Colored paths indicate significant pathways in the final model which were chosen using tests of d-separation and comparing goodness of model fit, while grey pathways indicate excluded pathways from the final model. Red pathways indicate positive standardized coefficient estimates for the pathway and blue pathways are negative coefficients, with coefficient values next to the paths.

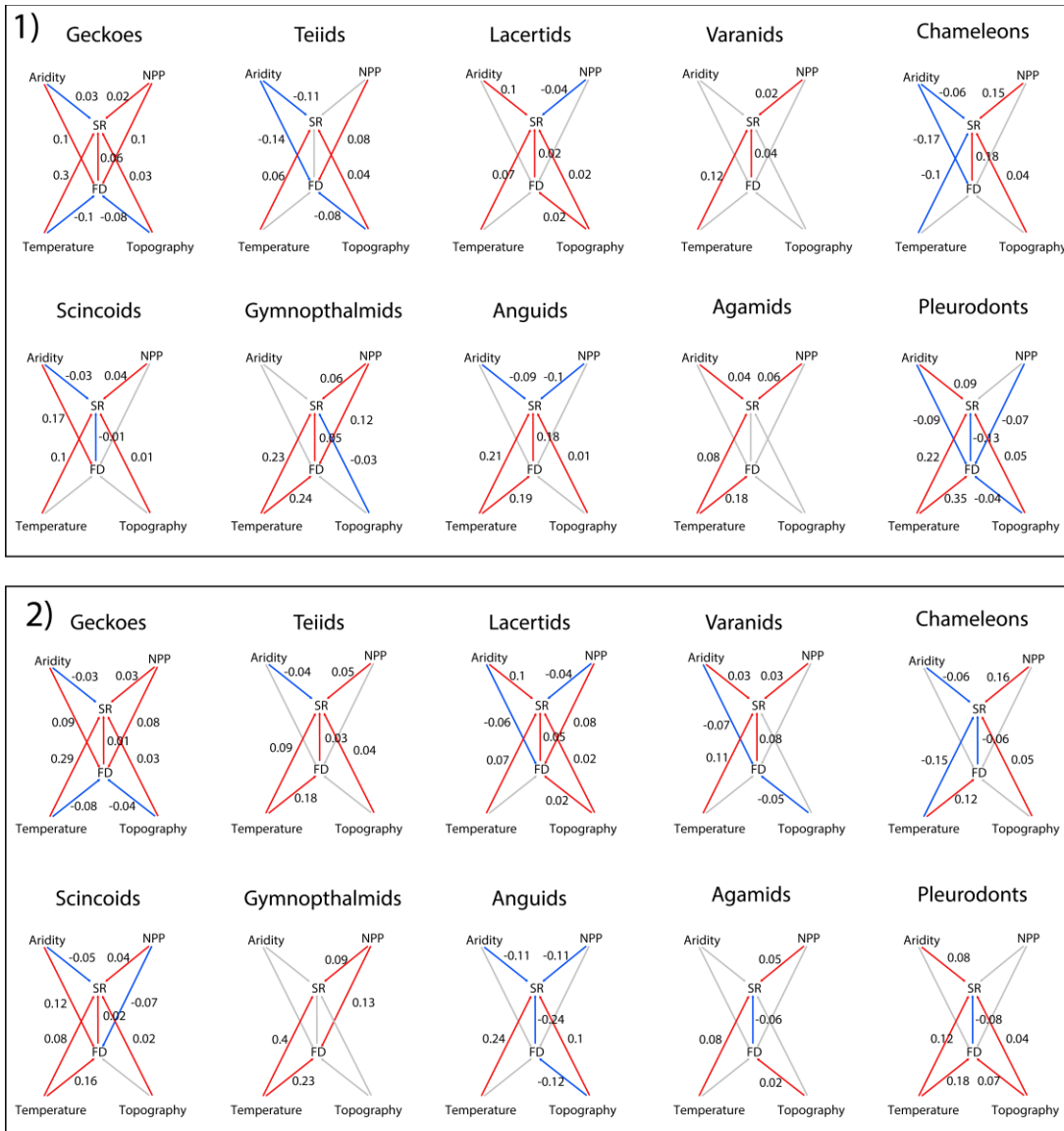


**Figure A4. 2.** Pathways in piecewise structural equations models of species richness (SR) and functional divergence (FD). All variables were extracted and calculated at a spatial resolution of 25x25km. Panel 1 shows the models for when FD is calculated as the standardized effect size of Rao's Q for a single trait, body mass, whereas panel 2 shows for when FD is calculated as the standardized effect size of Rao's Q for five traits together, body mass, diet, activity time, leg development, and microhabitat. Arrows show all pathways in the full model. Colored paths indicate significant pathways in the final model which were chosen using tests of d-separation and comparing goodness of model fit, while grey pathways indicate excluded pathways from the final model. Red pathways indicate positive standardized coefficient estimates for the pathway and blue pathways are negative coefficients, with coefficient values next to the paths.

**Table A4.1.** Phylogenetic signal, as measured using Pagel's  $\lambda$ , for five traits in ten lizard clades. Eight traits were not variable within clades (-), 37 out of 42 traits showed significant phylogenetic signal (\*  $p < 0.05$ ), and eight traits did not show significant phylogenetic signal, though many of these contained a very small proportion of species exhibiting different character states (nearly zero variation).

Clade	Body	Activity	Micro	Diet	Leg
	Mass	Time	Habitat	Development	
Geckoes	0.89*	0.72*	0.78*	0.11*	1*
Scincoids	0.95*	0.89*	0.85*	0.88*	0.98*
Teiids	0.85*	0.88*	0.84*	1	1*
Gymnophthalmids	0.84*	-	0.83*	0.88*	-
Lacertids	0.83*	-	0.74*	0.71*	-
Anguids	0.81*	0.44*	0.75*	1	1*
Varanids	0.91*	1	0.93*	1*	-
Agamids	0.93*	0.9	0.92*	0.83*	-
Chameleons	0.94*	1	0.6*	0.73*	-
Pleurodonta	0.91*	0.42*	0.68*	0.76*	-

# Chapter 5: Equilibrium and non-equilibrium phases in the radiation of *Hakea* and the drivers of diversity in Mediterranean-Type Ecosystems



Skeels, A. & Cardillo, M. 2019. Equilibrium and non-equilibrium phases in the radiation of hakea and the drivers of diversity in Mediterranean-type ecosystems. *Evolution*. 73 (7) 1392-1410.

## Abstract

Mediterranean-Type ecosystems (MTEs) contain exceptional plant diversity. Explanations for this diversity are usually classed as either “equilibrium”, with elevated MTE diversity resulting from greater ecological carrying capacities, or “non-equilibrium”, with MTEs having a greater accumulation of diversity over time than other types of ecosystems. These models have typically been considered as mutually exclusive. Here we present a trait-based explanatory framework that incorporates both equilibrium and non-equilibrium dynamics. Using a large continental Australian plant radiation (*Hakea*) as a case study, we identify traits associated with niche partitioning in co-occurring species ( $\alpha$ -traits) and with environmental filtering ( $\beta$ -traits), and reconstruct the mode and relative timing of diversification of these traits. Our results point to a radiation with an early non-equilibrium phase marked by divergence of  $\beta$ -traits as *Hakea* diversified exponentially and expanded from the southwest Australian MTE into biomes across the Australian continent. This was followed from 7Mya by an equilibrium phase, marked by diversification of  $\alpha$ -traits and a slowdown in lineage diversification as MTE-niches became saturated. These results suggest that processes consistent with both equilibrium and non-equilibrium models have been important during different stages of the radiation of *Hakea*, and together they provide a richer explanation of present-day diversity patterns.

## Introduction

The world's Mediterranean-type ecosystems (MTEs) are temperate regions defined by a seasonal climate, with cool wet winters and hot dry summers, typical of the Mediterranean Basin. Another feature typical of MTEs is an exceptional diversity and endemism of plant species, yet how this diversity is generated and maintained in these comparatively low-productivity environments is still incompletely understood. A substantial portion of MTE plant diversity is contributed by clades that are continentally (or globally) widespread but show a peak of diversity within MTE regions. For example, three of Australia's most widespread and species-rich plant families (Myrtaceae, Fabaceae, and Proteaceae) have at least twice the number of species in the MTE of southwest Australia than in structurally similar ecosystems of eastern Australia (Thiele and Prober 2014). Previous studies have highlighted some possible drivers of high MTE diversity in these clades, including greater diversification rates triggered by the evolution of key traits (Sauquet et al. 2009; Reyes et al. 2015; Onstein et al. 2016), or a longer period of occupation (Valente et al. 2009; Cardillo and Pratt 2013; Cook et al. 2015; Linder and Bouchenak-Khelladi 2015; Skeels and Cardillo 2017). Hypotheses of this kind come under the broad class of non-equilibrium explanations (Fischer 1960; MacArthur 1972; Rohde 2006), which view differences in present-day diversity as the outcome of historical patterns of diversity accumulation through time. Alternatively, equilibrium explanations argue that differences in diversity between regions is determined by different environmental carrying capacities and available opportunities for niche partitioning in ecological space (MacArthur 1965). Despite traditionally being considered alternative diversification paradigms, it is increasingly recognised that these distinctions are blurred. For example, diversification can be decoupled from equilibrium dynamics if changes in the landscape of ecological opportunity mean that ecological limits to diversity are a moving target (Marshall and Quental 2016), due

to factors such as a changing environment or key adaptation. This means that the major processes determining diversification might shift between what are traditionally considered equilibrium or non-equilibrium factors. As such, consideration of both types of dynamics simultaneously might help to explain the origination of biodiversity hotspots, yet rarely have the relative contribution of equilibrium and non-equilibrium processes been investigated in MTE regions.

The way diversity accumulates in different regions must be shaped at least partly by the tempo and mode of trait evolution. One way of investigating the relative contribution of equilibrium and non-equilibrium processes to present-day diversity patterns, therefore, is by reconstructing the evolutionary history of ecological traits within large clades. By focusing on patterns within clades (as opposed to geographically-delimited assemblages), hypotheses can be tested in the context of diversification and trait-evolution models. Within a clade, shared ancestry means closely related species may share traits that shape their environmental niche, and as a result may be more likely to co-occur in similar environments. However, the ecological similarity of close relatives may also lead them to compete for resources more strongly than with more distant relatives (Darwin 1859; Elton 1946). Hence, accumulation of diversity within a clade may be shaped by the balance between trait similarity (for common adaptations to the same broad environmental conditions) and trait differences that allow differentiation of ecological niches to reduce competition and permit coexistence. Traits involved with adaptation to broad environmental conditions, and traits involved in mediating competitive interactions, correspond, respectively, to species'  $\beta$ - and  $\alpha$ -niches (*sensu* Silvertown et al. 1999; Silvertown 2006).  $\beta$ -traits, related to the environmental niche, may determine the turnover of species between environments and the geographic partitioning of space. On the other hand,  $\alpha$ -traits,

involved in niche partitioning, influence local-scale co-occurrence and thus the accumulation of species with sympatric distributions.

The relative timing of diversification of  $\beta$ - and  $\alpha$ -traits may provide clues that allow us to explore if and when equilibrium dynamics begin to emerge from non-equilibrium lineage diversification. Under classic adaptive radiation models in regions of restricted ecological space (such as island systems), both trait and lineage diversification are expected to be rapid in early stages of the radiation, in response to ecological opportunity (Schluter 2000; Rundell and Price 2009; Stroud and Losos 2016). Much of this early diversification may be in traits associated with  $\alpha$ -niche axes, driven by intense competition among populations with largely sympatric distributions (Simões et al. 2016). In a continental setting, diversification may instead be driven by 1) geographic opportunity to expand into new regions along climatic gradients, or 2) geographical isolation resulting from allopatric speciation across geomorphic or climatic barriers (Rundell and Price 2009; Simões et al. 2016; Maestri et al. 2017). In this case, we would expect trait diversification along  $\beta$ -niche axes earlier in the radiation than along  $\alpha$ -niche axes (the “ $\beta$ -first” or “habitat-first”, model of radiation: Diamond et al. 1986). This may be followed by constrained evolution around distinct optima for different environmental regions (such as biomes) due to fitness requirements imposed by the environment.

Equilibrium and non-equilibrium models of species diversification make distinct predictions for stages of a radiation following early geographic expansion. Equilibrium models propose that geographic variation in diversity results from variation in regional carrying capacities, based on the available resources, niche availability, or trait diversity of the species present in each region (MacArthur 1965). Equilibrium dynamics also predict that increased competition between species will drive the rapid evolution of  $\alpha$ -traits in sympatric lineages, so that as

diversity increases co-occurring species should repel each other in phenotypic space (Brown and Wilson 1956; Mahler et al. 2010). Hence we should see greater diversity of  $\alpha$ -traits (relative to species numbers) in regions of high species richness (such as MTE regions). On the other hand, under non-equilibrium explanations for the differences in diversity between regions, we expect that regions occupied for longer or containing more rapidly diversifying lineages have accumulated more diversity (Ricklefs and Schlüter 1993; Figure 5.1). Diversification is expected to be driven largely by greater opportunity for allopatric speciation across large geographic areas, so instead of sequential bursts of diversification of  $\beta$ - and  $\alpha$ -traits, we might expect constant rates of trait diversification (Figure 5.1). We also predict no significant differences in  $\alpha$ -trait diversity between regions differing in species richness, although regions that have been occupied for longer or undergoing more rapid speciation may have greater diversity in  $\beta$ -traits due to adaptation to local environmental conditions in isolation.

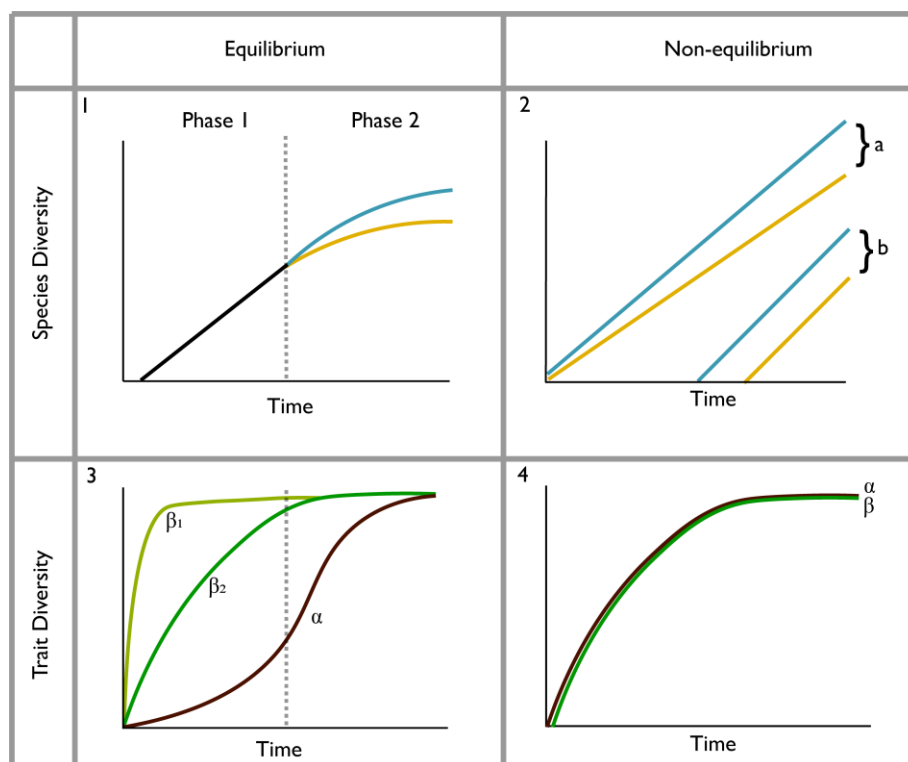


**Figure 5.1.** Predictions of equilibrium and non-equilibrium lineage diversification and trait diversification dynamics. Equilibrium models predict differences in carrying capacities between high richness MTE regions (blue line) and low richness non-MTE regions (yellow line; Panel 1). These dynamics are expected to be coupled with “ $\beta$ -first” dynamics of trait diversification in two phases. Phase 1: species diversity increases as species fill a range of environments and/or speciate geographically. At this stage  $\beta$ -traits diversify rapidly ( $\beta_1$ ) or steadily ( $\beta_2$ ) depending on these processes. Phase 2: saturation of species diversity, and diversity increases in  $\alpha$ -traits in response to competition between species (Panel 3). Non-equilibrium dynamics predict either differences in diversification rates (Panel 2a) or differences in occupation time (Panel 2b) between MTE and non-MTE regions (blue and yellow). Non-equilibrium models do not necessarily predict sequential phases of trait diversification (Panel 4) or lineage diversification.

In this study, we use a large Australian endemic plant radiation, *Hakea*, as a case study to develop an explanatory framework for MTE diversity that integrates equilibrium and non-equilibrium dynamics, lineage diversification, and trait diversification. *Hakea* is a large genus in the family Proteaceae with nearly ubiquitous distribution across the Australian continent, but with exceptionally high diversity in the MTE of southwest Australia (Figure 5.2). Reconstruction of the biogeographic history of the clade suggests repeated expansion from the MTE into other biomes over the past 30Myr (Cardillo et al 2017). The genus exhibits a diversity of phenotypic traits including growth forms, foliar, and reproductive morphologies. High numbers of co-occurring species at a local scale make *Hakea* a suitable case study to test hypotheses for the associations between inter-specific interactions with close relatives and modes of evolution of different traits. We use a variety of data types (community-survey, phenotype, climate, soil, and biogeographic data) to compare the roles of the environment and biotic interactions on the evolution of traits to understand how macroevolutionary history of a clade can shape contemporary trait patterns and the accumulation of diversity in MTEs. We identify  $\alpha$ - and  $\beta$ -traits using methods from community ecology, and then apply recently developed phylogenetic comparative methods for the study of trait and lineage evolution to test the conceptual framework presented above. We then test the relative importance of measures

of trait diversity compared to environmental and phylogenetic factors to understand the drivers of spatial diversity patterns.

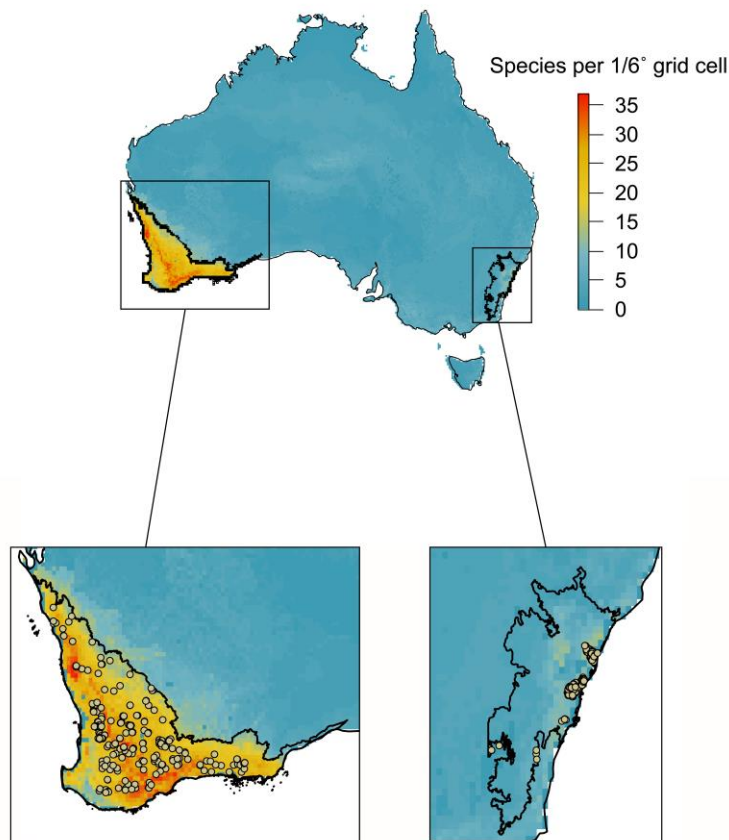


**Figure 5.2.** Map of *Hakea* species richness across Australia and geolocations of community survey plots used in this study from the southwest Australia (lower left panel) and the Sydney Basin and Southern Highland ecoregions of southeast Australia (lower right panel).

## Methods

### Data Collection

The phylogeny we use in this study is a species tree constructed from phylogenomic data using ASTRAL-II, with branch lengths and calibrated divergence times estimated using PAML

(Cardillo et al. 2017). We used two versions of the phylogeny for analyses, one containing 135 taxa at the full species level (out of 152 currently recognized *Hakea* species), and one that also includes 11 of approximately 30 recognized subspecies (n=146).

We obtained presence-absence data for *Hakea* species in 621 survey plots across Southwest Australia and the greater Sydney Basin region in south-eastern Australia (Figure 5.2). Plots in south-eastern Australia were from multiple flora surveys compiled into a single data repository ([bionet.nsw.gov.au](http://bionet.nsw.gov.au)) and those from southwest Australia were from a single flora survey (Gibson et al. 2004). Both employed a comparable sampling strategy (complete floristic data collected in 400m<sup>2</sup> quadrats). The Sydney Basin and Southwest Australia are the two most diverse regions in Australia for *Hakea*, and contain many sites where multiple species of *Hakea* coexist locally.

Phenotypic trait data on a number of reproductive, growth form, and leaf structural traits were collated from the Flora of Australia (Barker et al. 1999), TRY databases (Kattge et al. 2011), and Kew Gardens Seed Information Database (Royal Botanical Gardens Kew 2018). We collated data for 16 traits, selected based on the availability of data values across the genus and reduced this to 13 traits with the highest taxonomic coverage (greater than 80% of species; Table A5.1). For eight traits, maximum and minimum values were available (not species means) and we used the maximum value for all analyses: plant height, leaf length, leaf width, fruit length, pistil length, seed length, flower number, flowering duration. Three traits were scored as binary: flower colour was classed by the presence of anthocyanin (pink, red, or purple colour) vs. absence (yellows, creams, whites) based on description of flower colour (Barker et al. 1999). We compared this information with flower colour information from a previous study of 51 *Hakea* species (Hanley et al. 2009) and found complete congruence with the Flora of

Australia entries. Fire response was classified as regeneration mode after fires, an important life history feature of MTE flora (resprouting from lignotubers and other structures, vs. regenerating from seed). Leaf shape was classified as terete (needle-like) vs. broad. To impute missing data we used a random forest (RF) machine learning technique (MissForest; Stekhoven and Bühlmann 2012).

### Identifying $\alpha$ - and $\beta$ -traits

Given we do not have a good understanding of which traits might be related to different niche axes in *Hakea*, we classified traits into  $\alpha$ - and  $\beta$ -traits objectively, based on methods from community ecology (Cavender-Bares et al. 2006; Silvertown et al. 2006). Traits related to the  $\alpha$ -niche should be involved in mediating negative species interactions of locally co-occurring species, so we predicted that these traits would be more dissimilar among co-occurring species than would be expected under neutral assembly dynamics (Cavender-Bares et al. 2006). Traits related to the  $\beta$ -niche, on the other hand, should be more similar in co-occurring species, because they reflect common adaptations to the same environmental conditions. Using community survey data, we performed a mantel test of species trait distance (Gower distances: Podani 1999) against species co-occurrences (Schoener's index of co-occurrence: Hardy 2008), for each of the 13 traits separately. However, non-random patterns in trait distributions in communities may still arise under a purely neutral assembly model, in two ways (Warren et al. 2014). First, species may show low co-occurrence with their closest relatives due to a history of allopatric speciation. Alternatively, species may be more likely to co-occur with closely related species due to *in situ* radiation within a broadly defined region. To avoid misinterpreting the role of historical biogeography as ecological sorting processes structuring present-day assemblages (Warren et al. 2014), we simulated community data matrices (CDM) using a

dispersal null model (DNM; Miller et al. 2017). Under the DNM, assemblage species richness and individual species occurrence frequencies are approximately maintained, and species are selected to occupy null communities with a probability proportional to the reciprocal of their distance from the community. This method improves on many previous null models of community assembly which assume all species are equally likely to disperse into any particular community, ignoring biogeographic limitations (but see also Pigot and Etienne 2015). We performed the same mantel test of co-occurrence and trait distance for each of 1000 simulated CDMs with the DNM. For comparison, we also simulated 1000 CDMs under the more widely-used independent swap null model (ISN) (Gotelli 2000), which maintains empirical species frequencies and plot richness, but does not place a biogeographic dispersal constraint on community assembly.

We selected  $\alpha$ -traits as those for which the Gower distance in the community survey data was greater than expected compared to the DNM, by testing whether the observed coefficient of the mantel test was greater than 95% of the coefficients from the simulated CDMs. On the other hand,  $\beta$ -traits should be more similar in species that co-occur within regions compared to species in different regions. This makes the DNM unsuitable to test if co-occurring species have more similar traits than expected because the DNM will, by definition, preferentially create assemblages from species in closer geographic proximity (a problem similar to the narcissus effect: Colwell and Winkler 1984). We therefore used the ISN (Gotelli 2000) to test if species traits are more similar than expected compared to null assemblages (mantel coefficients  $< 95\%$  of those under the ISN null). As an additional test to identify  $\beta$ -traits, we tested spatial correlations between traits and environmental features.

We obtained spatial data for 19 WorldClim climate variables relating to temperature and precipitation at a resolution of 30 arc seconds (Hijmans et al. 2005), as well as 22 soil variables (10 variables taken at two different depths; 0-0.5cm and 0.5-1.5cm as well as soil depth and regolith) from the Soil and Landscape Grid of Australia (CSIRO; [clw.csiro.au/aclep/soilandlandscapegrid](http://clw.csiro.au/aclep/soilandlandscapegrid)) at 3 arc seconds. We summarized values for these variables across all 135 species which are present in the phylogeny by extracting the mean value across each species' geographic range (Skeels and Cardillo 2017). To reduce the high number of intercorrelated variables into a smaller subset that explained a high amount of variance in the distribution of species, we used phylogenetic principal components analysis (pPCA; Revell 2009), which accounts for variation attributable to shared ancestry. Similarly, because species may have similar traits due to shared ancestry, confounding the relationship between traits and environment, we used phylogenetic generalised least squares (pGLS) to fit models of species trait values ~ the first four principal components (PC), separately for each trait/PC combination. For binary traits (fire response, flower colour, leaf shape) we performed phylogenetic logistic regression (pLR).  $\beta$ -traits were identified as those that were (1) significantly clustered under the independent swap algorithm of community assembly, or (2) showed a significant correlation with an environmental PC. Some traits may be both environmentally filtered and involved in mediating interactions in local communities (i.e., be both related to both the  $\alpha$  and  $\beta$ -niche) as they may show strong associations with environmental features at a broad scale, however at a local scale may strongly repel each other (high within-region and between-region variance).

Having first identified a set of phenotypic traits corresponding to the  $\alpha$  and  $\beta$ -niche, we used a suite of recently developed phylogenetic comparative methods (PCMs) to understand how the timing and mode of lineage diversification and trait diversification have led to contemporary patterns of *Hakea* species diversity across the Australian continent. Currently available PCMs

are capable of testing a plethora of different evolutionary hypotheses relating to the tempo and mode of lineage diversification and trait diversification, however no PCMs currently exist that integrate trait evolution, geographic range evolution, and lineage diversification in a way that can be used to address all our hypotheses in a single framework. Instead, we apply separate methods to address different questions, accepting that this leads to a lack of coherence in the analysis overall, a point to which we return in the discussion. Table 5.1 presents a summary of the methods we use, the kind of data they require, and how they were used to address our specific study questions.

**Table 5.1.** Summary of phylogenetic comparative methods applied in this study to investigate the tempo and mode of lineage diversification and trait diversification for  $\alpha$ - and  $\beta$ -traits in *Hakea*.

Section	Phy	Trait	Spatial	Questions Addressed	Analyses
Temporal patterns of lineage diversification	X	-	-	Has diversification remained constant through time?	DDD model selection
Spatial patterns of lineage diversification	X	-	X	Are rates of diversification or patterns of density-dependence similar between regions?	bLTT GeoHiSSE
Temporal patterns of trait evolution	X	X	-	What is the relative timing of trait diversification for $\alpha$ - and $\beta$ -traits?	Trait-space saturation
Drivers of trait evolution	X	X	X	Do the environment or species interactions influence the evolution of $\alpha$ - and $\beta$ -traits?	Trait evolution models
Drivers of species richness	X	X	X	Is species richness predicted by the diversity of $\alpha$ - or $\beta$ -traits, features of the environment, or phylogeny	OLS and phylo-spatial GLS regressions

phy = phylogeny, DDD = diversity dependent diversification, bLTT= biogeographic lineage through time, GeoHiSSE = geographic hidden state speciation and extinction, OLS= ordinary least squares, GLS = generalized least squares.

## Temporal diversification analysis

The tempo of lineage diversification can give information about equilibrium and non-equilibrium dynamics. Equilibrium hypotheses predict that diversification should slow down as diversity increases, because if diversity is limited by the existing occupancy of niche space, then as niche availability decreases through time so should the rate of speciation. However, the observation of a diversification slowdown could also be an artefact of a protracted speciation process, in which incomplete speciation causes the number of independent lineages near the tips of a phylogeny to be underestimated (Etienne and Rosindell 2012). We explored the tempo and mode of *Hakea* diversification by comparing a constant-rates birth-death model of diversification to five different models of diversity-dependent diversification (linear decrease in speciation, exponential decrease in speciation, linear increase in extinction, exponential increase in extinction, and a speciation + extinction model), and a protracted speciation model of diversification. To fit diversification models we used the DDD and PBD packages in R (Etienne and Rosindell 2012; Etienne et al. 2016) and compared the fit of the seven models using Akaike weights. We repeated these model tests on the full-species and sub-species phylogenies. The phylogeny containing sub-species contains proxy information about the protracted speciation process, as sub-species are often considered as intermediate stages in the speciation process.

## Spatial diversification analysis

To explore whether the accumulation of lineages in different biomes reflects different carrying capacities, we estimated the tempo of species accumulation in the six major biomes which *Hakea* is present in (arid, Mediterranean, temperate grassland, temperate forest, tropical

savanna, and tropical forest) across Australia using biogeographic lineages through time (bLTT) analysis (Skeels *unpublished*). We obtained estimates of the number of lineages present in each biome through time across 50 stochastic maps simulated under the parameters of the best-fitting biogeographic model (BAYAREALIKE+J; Landis et al. 2013; Matzke 2013) from a previous study of range evolution in *Hakea* (Cardillo et al. 2017). From these 50 diversity-through-time curves, we estimated species-level carrying capacity (K) of each biome by fitting parametric non-linear growth models to these curves in the R package “growthrates”. This method uses an L-BFGS-B optimization algorithm to search for estimates of three parameters (intercept, growth rate, and K) that minimise the sum of squares in an ordinary least squares regression (OLS). To visualise the accumulation of lineages in each biome through time, we plot the bLTT as estimated from a single stochastic map pulled randomly from the distribution of 50. This approach is a variant of the traditional lineages through time plot (LTT) that presents the number of lineages in different regions reconstructed under a biogeographic model, accounting for anagenetic and cladogenetic range shifting and extirpation among regions (Skeels, *unpublished*).

To test whether there are diversification rate differences between the MTE region of southwest Australia and other regions we fit 10 alternative models of range evolution and diversification using the GeoHiSSE framework (Goldberg et al. 2011; Caetano et al. 2018). The GeoHiSSE method accounts for recognised problems with state-dependent speciation and extinction models, by modelling the influence on diversification rates of “hidden” states (such as unmeasured traits or external influences) that are independent of geographic range. Due to small sample sizes of species in different states, we simplified species geography into those that fall within the MTE biodiversity hotspot of southwest Australia, vs. non-hotspot regions. We tested a number of different models that held diversification constant between hotspot and non-hotspot

regions (area-independent diversification; AID) and allowed diversification rate to differ between regions (area-dependent diversification; ADD). We tested three ADD models and three AID models, allowing for 0, 1, or 2 hidden states each ( $\text{ADD}_0$ ,  $\text{ADD}_1$ ,  $\text{ADD}_2$ ,  $\text{AID}_0$ ,  $\text{AID}_1$ ,  $\text{AID}_2$ ). We also tested four null models in which diversification rates were dependent on the hidden state rather than the observed state ( $\text{ADD}_1\text{Null}$ ,  $\text{ADD}_2\text{Null}$ ,  $\text{AID}_1\text{Null}$ ,  $\text{AID}_2\text{Null}$ ), reducing the number of free parameters to be estimated. We determined relative model support using Akaike weights.

## Tempo of trait evolution

To test whether  $\beta$ -traits diverged before  $\alpha$ -traits we analysed patterns of trait-space saturation (Rolshausen et al. 2018). Early diverging traits should show high levels of trait saturation when phylogenetic distances between species are low (i.e., during the early phase of a radiation), while late-radiating traits should reach saturation at larger phylogenetic distances. We employed a method by Rolshausen et al (2018) to estimate the point of trait saturation in each  $\alpha$  and  $\beta$  trait. We compared the values of  $\theta_{50}$ , which represents the minimum phylogenetic distance where 50% of the diversity in traits has evolved, between traits. We used a jackknife procedure that iteratively calculates trait saturation curves by removing 10 percent of the species randomly (Rolshausen et al. 2018). This provides confidence intervals for the trait saturation curves from which we compared overlap between each individual trait against the trait-space saturation expected under Brownian motion (BM), Ornstein-Uhlenbeck (OU), and early-burst (EB) models of trait evolution. Early diverging traits should show significant overlap with traits simulated under an EB model, while late diverging traits should display low overlap with all three models. Traits that do not show early or late divergence should be consistent with either a BM or OU model of trait, but not an EB model.

## Mode of trait evolution

To test whether  $\alpha$  and  $\beta$ -traits were characterised by different evolutionary histories we tested four different trait evolution models in a model selection framework. We performed evolutionary trait analyses only on continuous trait values identified as being candidates for  $\alpha$  or  $\beta$ -traits. Our hypotheses were that traits might 1) converge in sympatry if there is strong environmental selection, 2) diverge in sympatry if competitive interactions drive character displacement, 3) drift neutrally, independent of the ecology and geography of the lineages, 4) drift neutrally but at different rates in different regions if occupation of different regions drives independent trait-diversification rates. Specifically we expect  $\beta$ -traits to fit the first scenario and  $\alpha$ -traits to fit the second. These scenarios are specified by four different evolutionary models. 1) a multiple-optima OU model (OUM; Beaulieu et al. 2012) where lineages present in different biogeographic regions are under different selective regimes towards different environmental optima, 2) a matching competition model (MC; Drury et al. 2016) where species in sympatry repel each other in phenotypic space, 3) a Brownian motion model (BM1), reflecting random drift in trait values through time, and 4) a multiple-rate Brownian motion model (BMM) where rates of trait evolution can vary between lineages in different biogeographic regions. BMM and OUM models require estimates of ancestral states to be specified at nodes within the phylogeny. We randomly selected one of 50 stochastic maps from the best-fitting model of range evolution (BAYAREALIKE+J; Cardillo et al. 2017) and used this stochastic map to label internal nodes according to the estimation of ancestral biome occupancy. We also used this best-fitting model as input to fit the MC model. We compared model fit using Akaike weights from the sample-size corrected Akaike Information Criteria (AICc).

## Drivers of spatial patterns of species richness

Finally, we tested whether geographic variation in species richness is better predicted by phenotypic diversity of  $\alpha$  and  $\beta$ -traits, amount of evolutionary history (phylogenetic diversity), or features of the environment. We hypothesised that under an equilibrium model of diversification, species richness should be associated with  $\alpha$ -trait diversity, whereas strong associations of species richness with  $\beta$ -trait diversity, the environment, and phylogenetic diversity would provide more support for a non-equilibrium model of diversification. There are many spatially explicit measures of trait diversity. We calculated the functional dispersion (FDis) of traits as this metric is multivariate, estimates the distance of each individual species to the centroid of all species in the community, and is independent of species richness (Laliberte and Legendre 2010). The spatial unit for these tests was the IBRA7 classification of Australian ecoregions, which define 89 geographically distinct regions that each enclose areas of similar climate, geology, landforms, and vegetation. Ecoregions are an appropriate scale to measure diversity as they represent distinct biogeographic and ecological entities (Smith et al. 2018), they have a reasonable sample size, and they contain highly variable numbers of species. For each ecoregion, we estimated the mean value across grid cells for each climatic and edaphic variable, as well as net primary productivity (NPP). We then used principal component analysis to reduce these environmental variables into a set of uncorrelated PCs. We used the first three PCs, which explained roughly 80% of the variation in the environmental variables, as predictor variables.

To quantify phylogenetic diversity, we calculated mean pairwise phylogenetic distance (MPD) between all species in each ecoregion (Webb et al. 2002). We compared observed values of MPD in each ecoregion to a null distribution of MPD values generated by applying the DNM

across ecoregions. Using the null distribution of MPD we calculated the standardised effect size as  $(\text{observed mpd} - \text{mean(null mpd)}) / \text{sd(null mpd)}$ .

We applied a generalised least squares (GLS) model to fit a regression between  $\log(\text{species richness})$  and seven predictor variables (MPD,  $FDis_\alpha$ ,  $FDis_\beta$ , PC1, PC2, PC3, area). Because ecoregions share species with adjacent ecoregions, spatial autocorrelation in species richness makes spatial units non-independent data points, and can inflate the influence of widespread species on analyses. To account for this we used a method that accounts for both phylogenetic and spatial autocorrelation in the data (Hua et al. 2019), which is similar to a model described by Freckleton & Jetz (2008). This method works by constraining the residual correlation in the response ( $\log(\text{species richness})$ ) between ecoregions to be a linear function of spatial and phylogenetic proximity, measured as the pairwise geographic distance between the centroid of each ecoregion, and phylogenetic variance-covariances. To compare the relative effect of environmental, phylogenetic, and phenotypic predictors on richness we compared a set of nested models using likelihood ratio tests.

## Results

### Identifying $\alpha$ - and $\beta$ -traits

We identified five candidate  $\alpha$ -traits (seed mass; fruit length, seed length, pistil length, and leaf shape) that had mantel coefficients greater than 95% of those generated under the DNM null model (Figure A5.1). This indicates that these five traits are more dissimilar among co-occurring species than expected. We also identified two traits (height and leaf length) that had

estimated mantel coefficients lower than 95% of those generated under the ISN null model.

This indicates that these traits are more similar among co-occurring species than expected.

The first four axes of the pPCA explained ~80% of the variation in environmental features between species. Using pGLS for quantitative traits and pLR for binary traits we found that after accounting for phylogenetic relatedness, flower colour and fire response were associated with an aridity axis (PC1; Table A5.2), leaf shape, pistil length, and fruit length were associated with temperature seasonality axis (PC2); plant height was associated with a precipitation seasonality axis (PC3); and height, pistil length, and flowering time were associated with soil water availability and salinity (PC4). Based on these tests and those described above, we classified seed mass and seed length as  $\alpha$ -traits, and height, leaf length, flowering time, flower colour, and fire strategy as  $\beta$ -traits. Three traits (fruit length, pistil length, leaf shape) met the criteria for  $\alpha$ -traits under the co-occurrence analysis, and the criteria for  $\beta$ -traits under the pGLS/pLR analysis. We classified these traits as both  $\alpha$ - and  $\beta$ -traits. The remaining traits did not appear to show patterns consistent with either the  $\alpha$ - or  $\beta$ -niche.

## Temporal diversification analysis

Support for diversity dependent and protracted speciation models of diversification was much stronger than for the time-constant birth death model (Table A5.3), suggesting that *Hakea* diversification has undergone significant slowdown. We found strongest support for the protracted speciation model on the full-species tree which suggests that the observed slowdown might be due to lag times between beginning and completion of speciation, although relatively strong support for two diversity-dependent models suggests that it is difficult to discern the drivers of the observed slowdown. To tease apart the role of protracted speciation and diversity

dependence, we applied the same model selection procedure to the sub-species phylogeny. This phylogeny still provided evidence for diversification slow down, but there was reduced support for the protracted model, and Akaike weight was divided between two diversity-dependent models (Table A5.3). The distribution of the  $\gamma$  statistic through time also supports a scenario of density-dependent rather than protracted-speciation driving the diversification slowdown and shows that diversification began progressively slowing approximately 7Mya (Figure A5.2), which is observable in the bLTT plot (below).

## Spatial Diversification analyses

We found evidence of biome-specific carrying capacities (K) by fitting density dependent growth models to biome-specific species accumulation curves reconstructed from a biogeographic model (bLTT). The Mediterranean biome had the greatest estimated K, followed by temperate forests, arid zone, tropical savanna, temperate grasslands, and tropical rainforest (Figure 5.3). Using GeoHiSSE, we found that two models were given 98% of the Akaike weight according to AIC (Table A5.4); AID<sub>1</sub>Null (48%) and AID<sub>2</sub>Null (50%). Under these models, diversification rate is independent of geographic area (MTE vs non-MTE), and instead better explained by either one (AID<sub>1</sub>Null) or two (AID<sub>2</sub>Null) unmeasured “hidden” variables (Table A5.4).

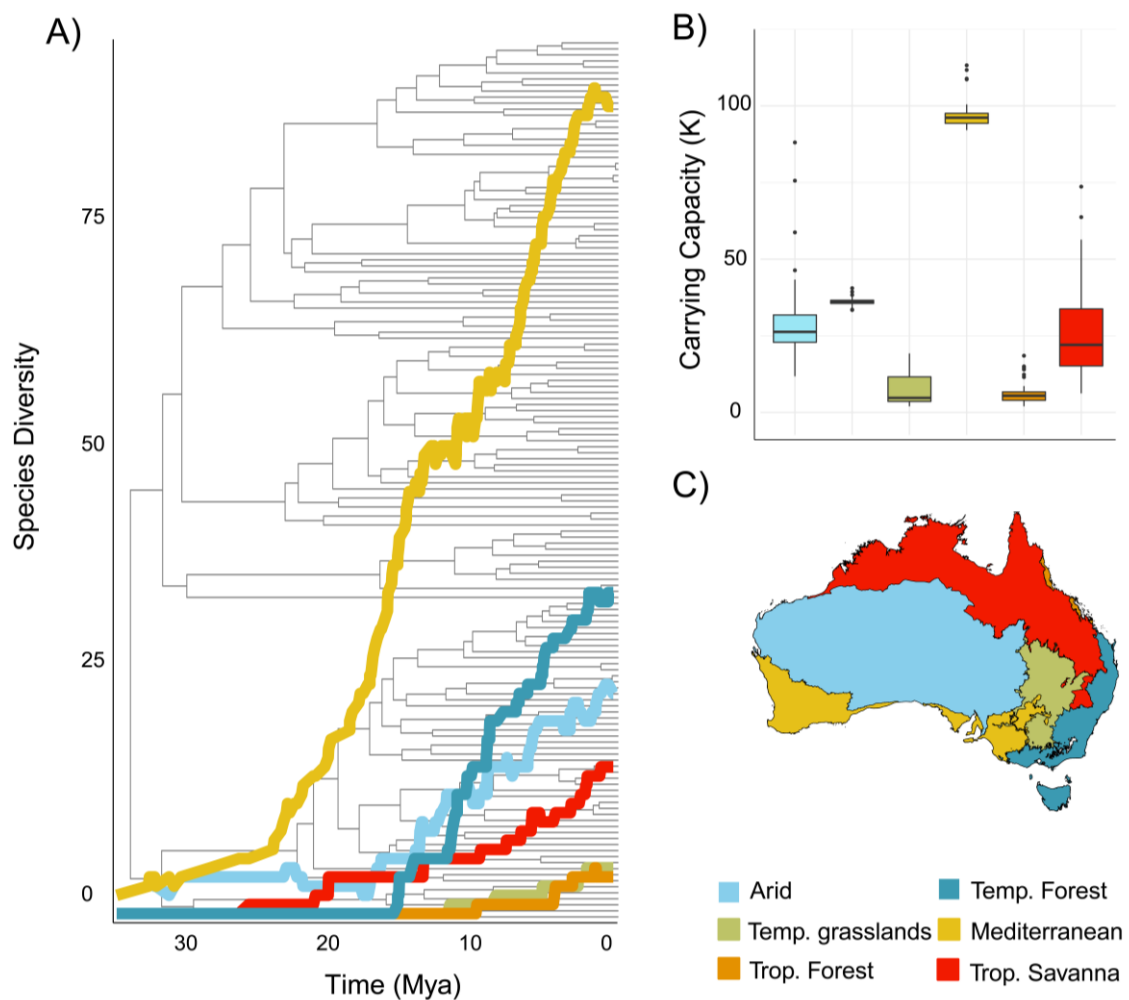


**Figure 5.3.** A) Biogeographic accumulation of lineages through time (bLTT) from a randomly sampled stochastic map based on a biogeographic model of range evolution, superimposed onto the *Hakea* phylogeny. B) Estimated carrying capacity (K) across biomes from logistic growth models across 50 stochastic maps from a biogeographic model of range evolution. C) Map of the six biogeographic regions (biomes) used in this study.

### Tempo of trait evolution

The evolution of height, flowering duration, seed length, fruit length, pistil length, and leaf length were all inconsistent with an early burst model, but did not differ from a BM or OU model. These traits showed values of  $\theta_{50}$ , an estimate of the minimum standardised phylogenetic distance at which 50% of diversity in each trait had evolved, between 0.065 and

0.18. These values are related to the relative timing of the evolution of trait diversity, with low values of  $\theta_{50}$  suggesting diversity evolved earlier in the radiation than traits with larger values of  $\theta_{50}$  (Rolshausen et al. 2018). The evolution of seed mass was inconsistent with all three models and this trait had a far higher  $\theta_{50}$  of 0.48. The earliest diverging traits, height and flowering time, were both identified as  $\beta$ -traits, while the later diverging trait, seed mass, was identified as an  $\alpha$ -trait (Figure 5.4).

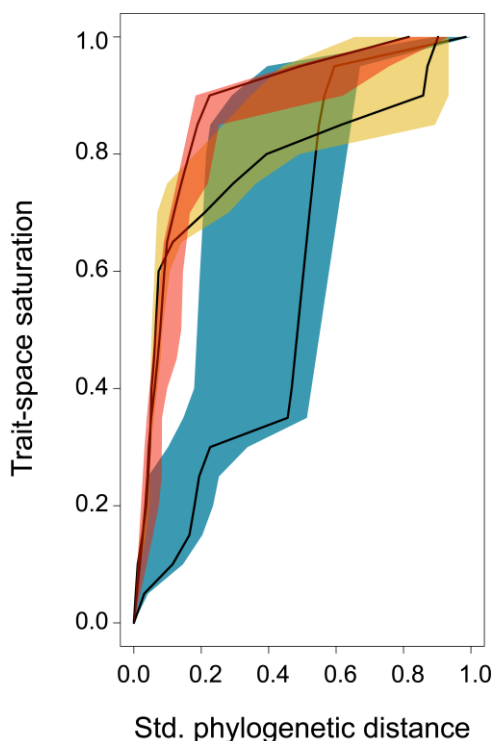


**Figure 5.4.** Trait-space saturation of two traits which showed the earliest trait diversification, height (yellow), and flowering duration (red), and the single trait which showed the latest relative diversification, seed mass (blue). This figure shows the minimum estimated phylogenetic distance between taxa (x axis) at which a given proportion of present-day diversity (y axis) has evolved, and as such gives an estimate of the relative timing of the diversification of each trait.

## Mode of trait evolution

We compared the fit of four distinct phenotypic evolution models on quantitative (not binary) candidate  $\alpha$ - and  $\beta$ -traits. We determined the best fitting model using Akaike weights derived

from AICc (Figure A5.3). We found that two hypothesised  $\beta$ -traits (flowering duration, height) showed strongest support for an OUM model with biome-specific trait optima, and one (leaf length) for a BMM model where different biomes had different rates of trait evolution. For the  $\alpha$ -traits, seed mass showed strong support for a matching competition model, in which trait evolution is best predicted by the number of sympatric lineages in each biome, while seed length showed support for an OUM. Fruit and pistil length, showing distributions consistent with both  $\alpha$ - and  $\beta$ -traits, showed strongest support for BMM models, in which there are different rates of trait evolution in different biomes, which are not constrained around biome-specific optima (as in the OUM model).

## Drivers of spatial patterns of species richness

The first three axes of a PCA on environmental predictors captured roughly 80% of the variation in environmental variables between ecoregions. Using OLS we found that features of the environment (PC axes), phylogeny ( $MPD_{ses}$ ), and dispersion of  $\alpha$  phenotypic traits ( $FDis_\alpha$ ) are strongly associated with present-day species diversity among ecoregions (Table 5.2). However, after accounting for spatial and phylogenetic autocorrelation using the phylo-spatial GLS method, only phylogenetic relatedness ( $MPD_{ses}$ ) and  $FDis_\alpha$  were associated significantly with richness above their covariation with other predictor variables (Table 5.2). The difference between  $R^2$  values of the OLS (0.67) and GLS (0.32) models indicates that approximately 35% of the variation in species richness explained by the predictors is due to phylogenetic and spatial autocorrelation in the data (Hua et al. 2019). The distribution of predictor and response variables across ecoregions can be seen in Figure 5.5.

**Table 5.2.** Coefficient values of predictors in regressions on log(species richness) for *Hakea* assemblages across 89 Australian ecoregions. We present results for an OLS regression and a GLS model that accounts for spatial and phylogenetic autocorrelation.\*p<0.05, \*\*p<0.01, \*\*\*p<0.001

Variable	OLS	PhyloSpatial GLS
FDis <sub>a</sub>	0.434***	0.354***
FDis <sub>b</sub>	0.054	0.057
MPD <sub>ses</sub>	-0.238**	-0.258***
PC1	-0.294**	-0.036
PC2	0.197*	0.095
PC3	-0.620***	-0.125
Area	0.075	0.033

## Discussion

Our approach to understanding the exceptional diversity of Mediterranean-Type Ecosystems (MTEs) has been to investigate the roles of both equilibrium and non-equilibrium dynamics in the diversification of a large, monophyletic MTE radiation. Overall, the *Hakea* radiation shows a strong pattern of diversification slowdown, with different estimated carrying capacities within different biomes, patterns often interpreted as signatures of density-dependent diversification and equilibrium diversity dynamics (Moen and Morlon 2014). This would lead to the expectation that current geographic differences in diversity (including elevated diversity of MTE regions) are associated with present-day environments and ecological limits (Moen and Morlon 2014; Rabosky and Hurlbert 2015a). On the other hand, geographic diversity patterns in *Hakea* (and several other Australian plant groups) also show signatures of non-equilibrium

dynamics, with the deeper evolutionary origins of MTE lineages a major contributor to their elevated diversity (Cardillo and Pratt 2013; Cook et al. 2015; Skeels and Cardillo 2017).

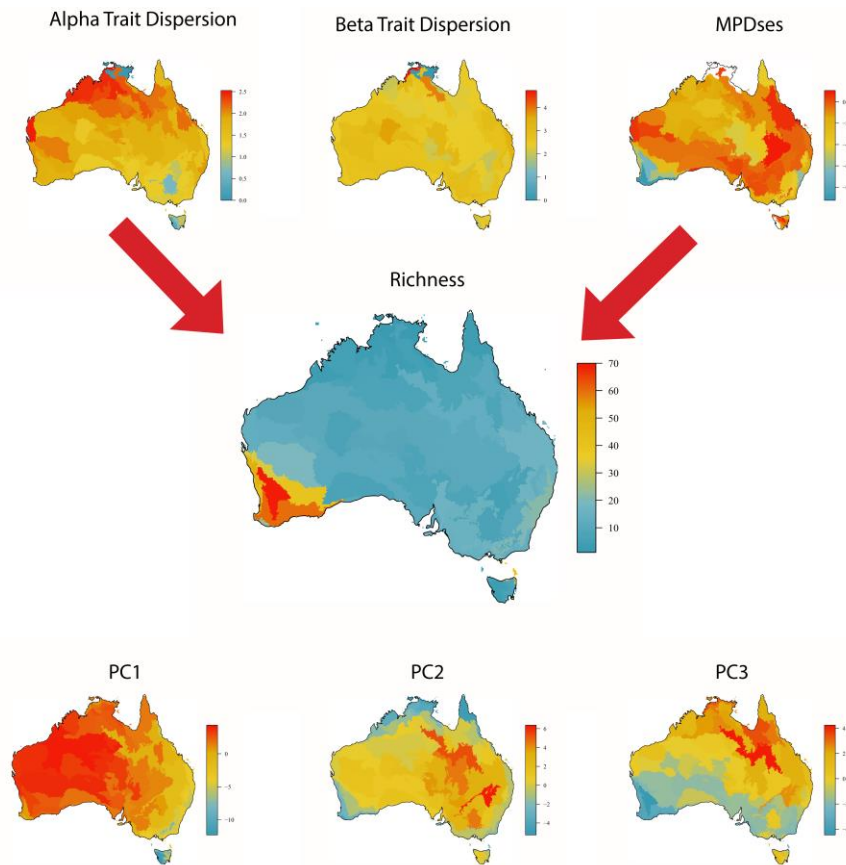


**Figure 5.5.** Present-day species richness, functional dispersion of  $\alpha$ -traits,  $\beta$ -traits, MPD<sub>ses</sub>, and the first three axes of a PCA of climate and soil values across ecoregions. Arrows indicate significant predictors ( $\alpha$  trait dispersion, and MPD<sub>ses</sub>) of species richness after accounting for covariation with the other predictor variables as well as phylogenetic and spatial autocorrelation.

Our reconstruction of the evolution of phenotypic traits suggests that both equilibrium and non-equilibrium processes have been involved in the radiation of *Hakea*, and have made contributions to the present-day patterns of diversity. Phenotypic traits associated with adaptation to broad environmental conditions ( $\beta$ -traits; e.g., plant height and flowering duration) diversified steadily in the radiation, apparently driven by evolution towards different

climatic optima across biomes. Traits associated with partitioning of ecological space ( $\alpha$ -traits; e.g., seed mass) diversified later in the *Hakea* radiation with the development of phenotypic repulsion among close relatives in sympatry (although it is important to note not all  $\alpha$ - and  $\beta$ -traits fit this pattern; Figure A5.3). Present-day species richness of ecoregions is best explained by the dispersion of  $\alpha$ -traits relative to species richness, and by phylogenetic clustering of lineages. This supports a growing body of literature that links diversification slowdowns with high geographic range overlap amongst closely related species (Kennedy et al. 2018; Machac et al. 2018). Taken together, our results paint a picture of a “ $\beta$ -first” radiation with two distinct phases. An initial, non-equilibrium phase (from approximately 30Mya-7Mya) was characterized by geographic expansion from the southwest Australian MTE across the Australian continent, with lineages diversifying into a wide range of environments. This was followed, beginning around 7Mya, by an equilibrium phase in which diversification rates slowed progressively, and species richness within regions was consolidated and maintained by the increasing diversity of  $\alpha$ -traits.

## Non-equilibrium drivers: time-for-speciation

Non-equilibrium explanations for MTE diversity typically involve one or more of three scenarios: 1) there has been a greater time for lineages to accumulate diversity in MTEs because these regions are older than other temperate biomes (“time for speciation”); 2) MTEs have had reduced extinction rates (Hopper 2009; Hopper et al. 2016); or 3) MTE lineages or environments have features that have promoted increased speciation rates (Hopper and Gioia 2004; Linder 2005; Sauquet et al. 2009; Schnitzler et al. 2011; Reyes et al. 2015). After rainforests, the Mediterranean biome may be the oldest of Australia’s biomes, with recent estimates suggesting the development of a Mediterranean type climate from 30Mya (Lamont

and He 2017), whereas temperate forests probably did not become widespread until 25-15Mya (Byrne et al. 2011), and modern woodland, grassland, savannah, and arid ecosystems until 8-3Mya (Hill 2004; Beerling and Osborne 2006; Byrne et al. 2008; Bowman et al. 2010; Andrae et al. 2018). Of an increasing number of MTE clades investigated, many (including *Hakea*) appear to have started their radiation within an MTE, supporting the “time for speciation” model (Valente et al. 2009; Cardillo and Pratt 2013; Cook et al. 2015; Cardillo et al. 2017; Skeels and Cardillo 2017). Several studies have found evidence for elevated diversification rates in MTE regions and clades (Onstein et al. 2014, 2016; Cowling et al. 2015; Reyes et al. 2015; Pirie et al. 2016), and there is fossil evidence for a diverse but now extinct Pleistocene flora in Eastern Australia (Sniderman et al. 2013), suggesting elevated extinction outside the southwest MTE. However, we did not find evidence of diversification rate differences between MTE and non-MTE regions in *Hakea*. However, this could be because extinction is notoriously difficult to detect from molecular phylogenies (Marshall 2017). Instead, the major source of diversification rate variation in *Hakea* might be attributable to the same factors that drive diversification slowdown across the clade, rather than differences between regions. Given that (1) one of the main predictors of high *Hakea* species richness within ecoregions was greater phylogenetic clustering (shorter mean branch length between species), (2) the ancestor of present-day species appears to have occupied the southwest MTE region, and (3) that there is no evidence to support substantial diversification rate differences between the MTE and non-MTE regions, it appears likely that the non-equilibrium scenario of *in-situ* diversification over a long period of time (time-for-speciation effect) contributes substantially to the present-day high diversity of the southwest MTE.

## Equilibrium drivers: diversity dependent diversification and $\alpha$ -niche traits

Over the past ca. 7Myr, a consistent slowdown in *Hakea* diversification (Figure A5.2, Figure 5.3) marks a shift from the earlier, geographic expansion phase to an equilibrium phase, in which biotic interactions and partitioning of ecological space seem to have become more prominent. Under equilibrium dynamics, differences in species richness among regions result from differences in ecological carrying capacity, which in turn is the result of one or more of (1) the total energy available (resource volume), (2) the partitioning of resources among species (niche breadth), or (3) the overlap in resource use among species (MacArthur 1972; Ordonez and Svenning 2018). While resource volume has been proposed to explain some large-scale biodiversity patterns (such as the latitudinal diversity gradient), this is unlikely to be the explanation for high diversity of MTE regions, because primary productivity is often lower than adjacent temperate forest and woodland biomes (Jetz and Fine 2012). Although different biomes had different estimated carrying capacities based on the accumulation curves of species in these regions (Figure 5.3), environmental PC axes, which included measures of environmental energy as net primary productivity, were unable to explain a significant amount of variance in species richness among ecoregions, after accounting for spatial and phylogenetic autocorrelation (Table 5.2). Instead, the functional dispersion of  $\alpha$ -traits and phylogenetic clustering of lineages explained a significant amount of variance in species richness between ecoregions. This suggests that diversity in the equilibrium phase of the *Hakea* radiation is associated not with resource volume, but with the partitioning of ecological niche space among closely-related species within regions.

We identified five candidate  $\alpha$ -traits that appear to be more differentiated in co-occurring species than one would expect based on a biogeographically informed null model of co-

occurrence. Four of these traits relate to reproductive structures (fruit, seed, and pistil length, and seed mass), while another trait reflected the vegetative structure of leaves (leaf shape). One trait in particular, seed mass, appears to be associated with ecological partitioning in the later stages of the *Hakea* radiation. Furthermore, the evolution and diversification of seed mass best fits a model of interspecific competition in sympatry (Figure A5.3). These results are consistent with differences in seed mass among species evolving as species richness within regions approached saturation levels and inter-specific interactions intensified.

Four of the five candidate  $\alpha$ -traits were reproductive traits, suggesting that the apparent niche-partitioning in diversity-saturated regions involves differentiating reproductive strategies. . Reproductive traits have previously been highlighted as strong candidates for mediating negative interactions between species (Weber and Strauss 2016), and may mediate several distinct types of interactions between close relatives that permit their coexistence. Firstly, different reproductive traits might reflect different strategies relating to seedling establishment. Seed mass is positively associated with seedling mortality in *Hakea* (Lamont and Groom 1998), as well as more generally (Coomes and Grubb 2003), and also negatively associated with the number of seeds produced (Coomes and Grubb 2003). Species that produce fewer, larger seeds invest more energy per seed, and produce seedlings that are better equipped to deal with drought than species with smaller seeds (Lamont and Groom 1998; Coomes and Grubb 2003). It has been shown that although very little regional variation in average seed size exists, coexisting species often show large variation in seed size (Westoby et al. 1996). In highly seasonal, drought-prone, or fire-prone environments, different reproductive strategies may favour the temporal staggering of seedling establishment as a form of bet-hedging (Pake and Venable 1996; Coomes and Grubb 2003), so that variation in seed size of sympatric species may have evolved as an evolutionarily stable strategy in response to strong competition (Westoby et al.

1996; Rees and Westoby 1997). Secondly, different reproductive traits may be selected for in co-occurring species due to reproductive interference, the reduction in fitness caused by wasted resources during hetero-specific mating attempts (Weber and Strauss 2016). Species with similar floral morphology may be visited by the same pollinators and in some cases set inviable seeds with hetero-specific pollen. In these cases there would be strong selection for reproductive differentiation among co-occurring species, if species with similar morphology have reduced fitness when they co-occur compared to when they do not co-occur. Identifying which mechanisms explain the diversity of  $\alpha$ -traits will be key to understanding how  $\alpha$ -trait diversity influences species diversity.

So why do we see greater partitioning of  $\alpha$ -traits in MTE regions compared to non-MTE regions? If the southwest MTE is where the ancestors of extant *Hakea* began diversifying (Cardillo et al 2017), then the radiation of MTE lineages is more mature, and we may simply be observing in the present a snapshot of the late stages of a radiation which is still running its course in other regions. In the MTE, greater  $\alpha$  trait diversity is related to greater species density and competition between species, while in other regions major axes of phenotypic and ecological differentiation may be along  $\beta$  rather than  $\alpha$ -niche axes. An alternative interpretation is that there may be features of MTE regions that promote  $\alpha$ -niche differentiation. Differentiation along  $\alpha$ -niche axes may occur following speciation as species repel each other in trait space (reinforcement); alternatively, strong competition within species may drive ecological speciation in sympatry. Evidence for sympatric speciation in MTE hotspot clades is mixed, with support for allopatric speciation in several South African cape clades (Schnitzler et al. 2011), and budding speciation (sympatric or parapatric) in the Californian floristic Province (Anacker and Strauss 2014). A recent survey of speciation modes of clades which included *Hakea* as well as other MTE genera of Proteaceae (*Banksia* and *Protea*), found strong

support for a prevailing sympatric mode of speciation (Skeels and Cardillo 2019b). Southwest Australia lacks major geological barriers associated with allopatric speciation between plant groups, which instead may have differentiated largely along edaphic niche axes (Hopper and Gioia 2004). Soil oligotrophy (the depletion of nutrients in soil) might drive fine scale partitioning of the edaphic niche as species either specialise on acquiring different plant-available nutrients (e.g. forms of P and N), or specialise in their utilisation of these nutrients (e.g., investment in leaves for photosynthesis, Hopper and Gioia 2004; Laliberte et al. 2013; Thiele and Prober 2014). Our results point to a possible sympatric speciation mechanism in MTE regions, the differentiation of reproductive strategies, where strong competition between species for limited soil nutrients drives differentiation of investment strategies for fruit and seed morphology. We suggest that a further avenue of research into MTE diversity would be to compare speciation modes and mechanisms between MTE and non-MTE clades to test whether unique processes operate in MTE regions to drive high diversity.

## Conclusions

Our analyses of the diversification and radiation of *Hakea* support a  $\beta$ -first model that can help to explain the exceptional diversity of the southwest Australian MTE. Early diversification appears to be geographic, as species colonise new environments and diverge along  $\beta$ -niche axes associated with environmental gradients. As diversity accumulates within regions, diversity dependent processes emerge. Species diverge along  $\alpha$ -niche axes that mediate inter-specific interactions, and diversification slows through a damped speciation rate resulting from a reduction in ecological opportunities to speciate. Our results suggest that time, ecological carrying capacities, and biome-specific diversification dynamics combine to shape present-day patterns of diversity. This challenges the notion that equilibrium and non-equilibrium dynamics

are mutually exclusive determinants of present-day diversity of large clades, a conclusion that has also been supported recently with *in-silico* experiments (Pontarp and Wiens 2017). Instead, these dynamics operate at different stages of a radiation and we can use phenotypic, phylogenetic, and geographic data to infer their relative timing and driving processes. We suggest that this integrated equilibrium/non-equilibrium approach captures more of the complexity of historical and ecological processes involved in the evolution of diversity, compared to models based on equilibrium or non-equilibrium dynamics only.

Together, the set of results from our analyses paint a compelling picture of the evolutionary dynamics leading to high MTE diversity in *Hakea*. Like many contemporary macroevolution studies, however, this study applies a suite of disparate analytical methods to test different questions regarding the tempo and mode of diversification, methods that have been developed independently for different purposes. As such, the various methods and models we use are not well integrated into an overarching modelling framework, and rely on assumptions that are not always well supported by the data (Cooper et al. 2016). For example, models of trait evolution often assume that trait evolution is independent of lineage diversification, however as we have suggested above, ecological speciation may drive diversification of lineages that is coupled with  $\alpha$ -trait diversification in sympatric lineages. This is not well accounted for with current methods. Despite this, the active development of macroevolutionary methods has come a long way in attempting to minimize misinterpretation of statistical signal (e.g., HiSSE methods; Beaulieu and O'Meara 2016), and we find it encouraging that independent tests seem to support the same general conclusions about evolutionary dynamics in *Hakea*.

## Appendix

**Table A5.1.** Data on phenotypic traits collated for *Hakea*, the number of species with missing data, and data source (1 = Flora of Australia, 2= TRY database).

Trait	Missing data (number of species)	Data source
Height	0	1
Flower number	1	1
Pistil length	0	1
Fruit length	0	1
Seed length	2	1
Flowering duration	0	1
Leaf length	0	1
Leaf width	0	1
Leaf length: leaf width	0	1
Leaf nitrogen: phosphorous	58	2
Seed mass	23	2
Leaf dry mass	57	2
Specific leaf Area	52	2
Flower colour	0	1
Fire response	20	1
Leaf shape	0	1

**Table A5.2.** Coefficients of standardised trait/environment relationships in *Hakea* species after accounting for phylogenetic relatedness using phylogenetic generalised least squares for quantitative traits and phylogenetic logistic regression for binary traits (fire response, leaf shape, flower colour).

Trait	PC1	PC2	PC3	PC4
Height	-0.0123	-0.0142	-0.0335	0.0396
Flower number	0.0035	-0.0084	-0.0032	-0.0017
Pistil length	0.0049	-0.0239	-0.003	0.0308
Fruit length	0.0097	-0.0319	0.0026	0.0045
Seed length	0.0057	-0.0175	0.0001	0.0035
Flowering duration	0.0065	-0.0189	0.0114	0.0449
Leaf length	-0.0069	-0.011	0.0067	0.0058
Leaf width	-0.0013	-0.0032	0.0091	0.0000
Leaf length: leaf width	-0.0079	-0.0062	0.0055	-0.0073
Seed mass	0.0046	-0.0108	-0.0011	-0.0095
Fire response	-0.0347	0.0159	0.0245	0.02
Leaf shape	-0.0027	0.04	-0.0271	0.0000
Fire response	0.041	0.0105	0.0137	-0.0507

**Table A5.3.** Akaike weights for temporal diversification model selection in *Hakea*. Seven models were compared for two phylogenetic hypotheses, one with only recognised full species, and one with 11 sub-species sampled. Akaike weights sum to one, and quantify the relative support for each model.

Model	Full species (n=135)	Sub-species
		(n=146)
Birth-death	0	0
Diversity dependent speciation (linear)	0.35	0.72
Diversity dependent speciation (exponential)	0	0.01
Diversity dependent extinction (linear)	0	0
Diversity dependent extinction (exponential)	0	0
Diversity dependent speciation + extinction	0.13	0.26
Protracted Speciation	0.52	0

**Table A5.4.** Akaike Information Criteria and Akaike weights of ten alternative GeoHiSSE models for geographic range dependent diversification in *Hakea* related to presence or absence in the southwest Australian Mediterranean-type-ecosystem. The two best fitting models, AID1Null and AID2Null share roughly half the Akaike weight. AID = area independent diversification, ADD = area dependent diversification.

Model	AIC	AICw
AID0	1086.88	0
ADD0	1092.59	0
AID1	1080.91	0.02
ADD1	1102.49	0
AID2	1101.37	0
ADD2	1104.84	0
AID1Null	1074.66	0.48
ADD1Null	1092.28	0
AID2Null	1074.56	0.5
ADD2Null	1097.26	0

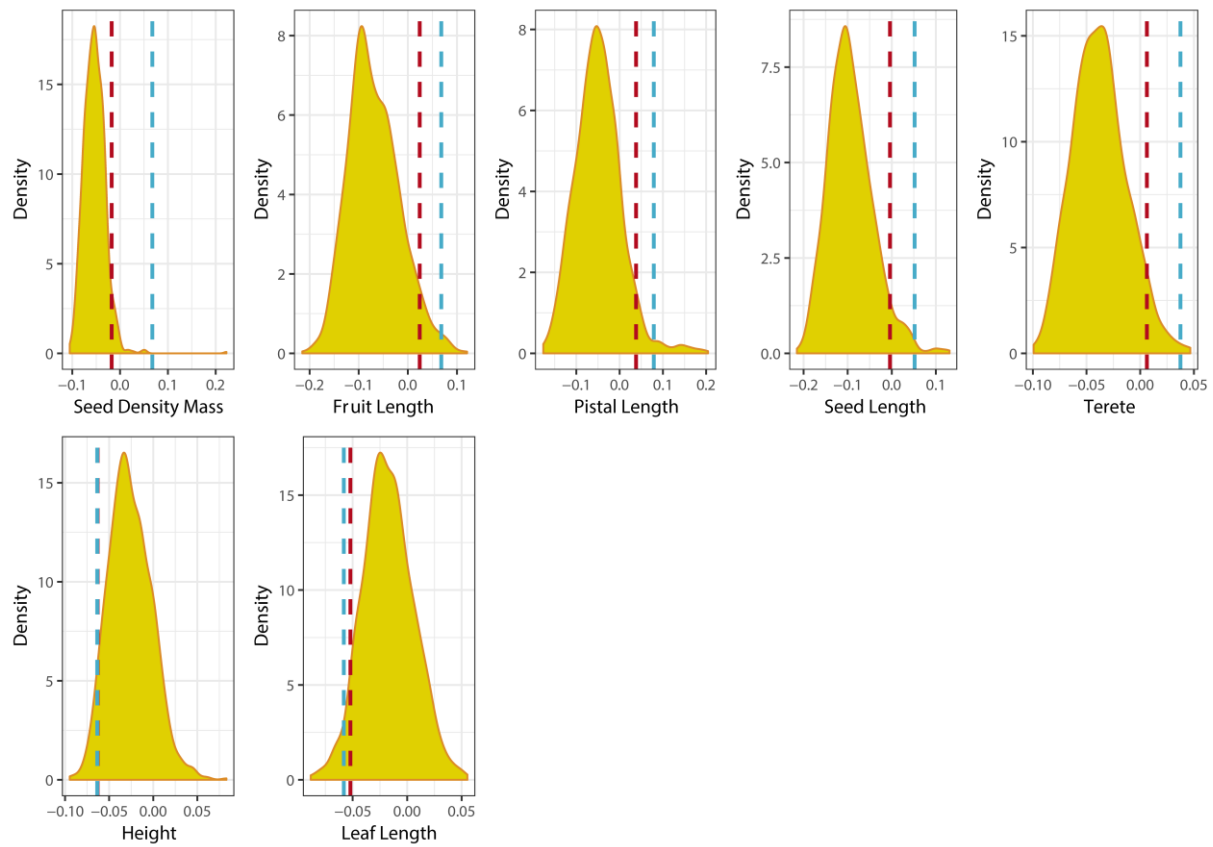


**Figure A5.1.** Observed vs null distributions of  $r$  values from mantel tests between pairwise trait distances (Gower distance) and co-occurrence (Schoener's C) of *Hakea* species recorded in communities across southwest and southeast Australia. On the top row are traits which showed an observed  $r$  (blue dashed line) > than 95% of simulated data (red dashed line) under a dispersal null model (candidate  $\alpha$ -traits). On the bottom row are traits that show observed slope < 95% of simulated data (red dashed line) under an independent swap null model (candidate  $\beta$ -traits).

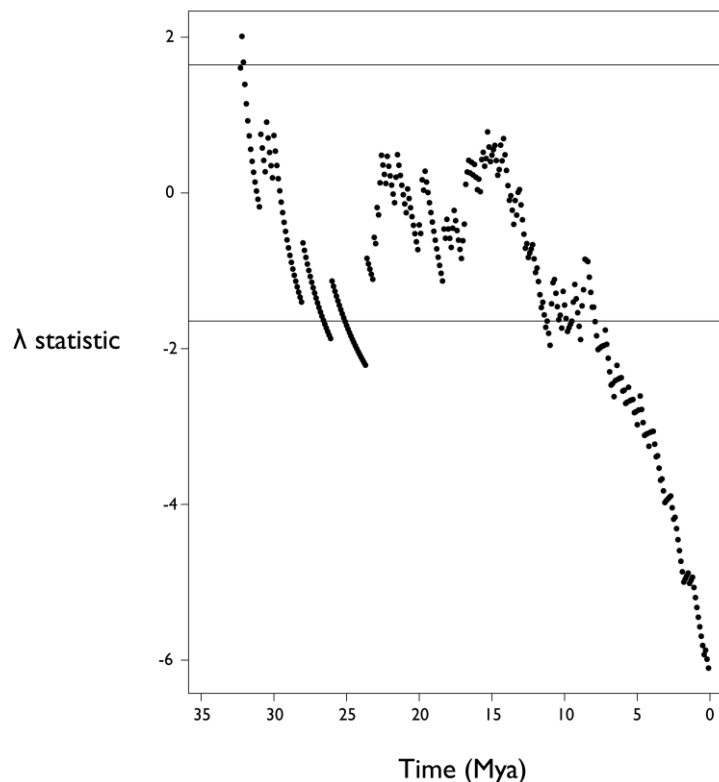


**Figure A5.2.**  $\gamma$  statistic at 100 thousand year intervals across *Hakea* phylogeny.  $\gamma$  is a measure of the distribution of node heights in a phylogeny and values  $< -1.96$  (bottom horizontal line) indicate clustering of nodes towards the root of the phylogeny indicating slowdown, while values  $> 1.96$  (top horizontal line) indicate speed up of diversification as nodes are distributed more towards the tips of the phylogeny. Consistent slowdown is observable across roughly the last 7 million years.

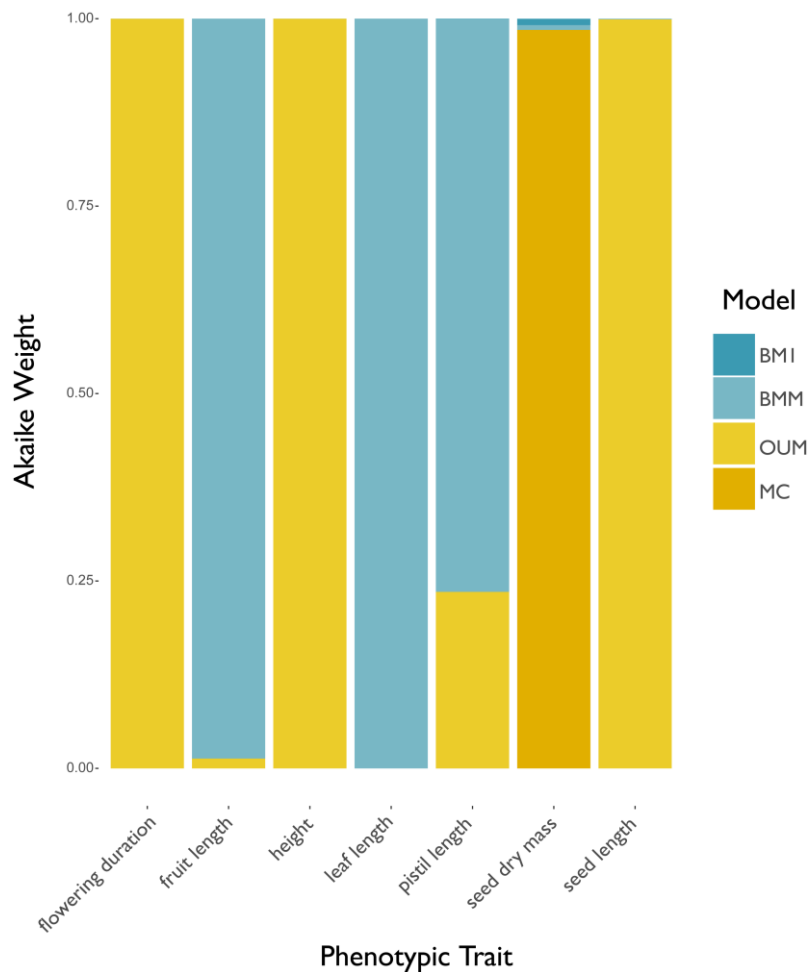


**Figure A5.3.** Akaike weights of four different phenotypic evolution models for seven  $\alpha$ - and  $\beta$ -traits; single rate Brownian Motion (BM1), multiple rate Brownian Motion (BMM), multiple optima Ornstein-Uhlenbeck (OUM), and Matching Competition (MC). Seed mass and seed length were recorded as  $\alpha$ -traits and showed support for MC and OUM models. Height, flowering time, and leaf length were recorded as  $\beta$ -traits and supported OUM and BMM models. Pistil length and fruit length showed characteristics of both  $\alpha$ - and  $\beta$ -traits and supported a BMM model.

# Chapter 6: Ecological interactions shape the evolution of floral traits in communities across a temperate biodiversity hotspot



Skeels, A., Dinnage, R., Medina, I., & Cardillo, M. Ecological interactions shape the evolution of floral traits in communities across a temperate biodiversity hotspot. Submitted.

## Abstract

Understanding the processes driving the diversification of floral traits is integral to understanding the assembly of plant communities, as sympatric species aim to minimize pollinator competition or reproductive interference. Floral divergence may directly drive speciation events (1) or may occur after speciation either by drift or local adaptation in allopatry (2) or by negative interactions between species in sympatry (3). Here, we generated predictions for macroevolutionary, and community assembly patterns expected under these three models and tested these in a diverse hotspot genus, *Hakea* (Proteaceae), from Southwest Australia. Patterns of community assembly suggest that flower colour is more divergent in communities than the expectation from null models and macroevolutionary patterns for flower colour supported the role of diversity-dependent processes driving floral divergence. Together our results highlight how ecological interactions have shaped the evolution of pollination niches and the assembly of phenotypically diverse communities in a biodiversity hotspot.

## Introduction

How do closely related plant species coexist in diverse ecological communities? Closely-related species are most likely to compete for resources with one another (e.g., space, light, nutrients, water) due to shared ecological and life-history characters inherited from a recent common ancestry (Darwin 1859; Elton 1946). Moreover, closely related plant species may also share similar reproductive morphology, phenology, pollinator signals, and pollinator animal vectors. In some cases, this may lead to strong negative biotic interactions (hereafter negative interactions) such as competition for pollinators (Levin and Anderson 1970) or reproductive interference, where species bear a cost from heterospecific pollen flow (Gröning and Hochkirch 2008; Moreira-Hernández and Muchhalá 2019). In other cases, however, similar pollination strategies may actually be advantageous if shared floral resources increases pollinator abundances and visitation rates (Bertness and Callaway 1994; Elzinga et al. 2007; Sargent and Ackerly 2008; Junker et al. 2015). One of the major challenges to coexistence in closely related plant species is managing trade-offs between the potential benefits of floral similarity and the pitfalls of negative interactions. There is growing interest in understanding how plant-pollinator systems evolve over macroevolutionary timescales, and how these processes can shape species distributions and floral traits in present-day communities (Sauquet and Magallón 2018).

To reduce negative interactions within a community, species may diverge along a number of distinct pollination niche axes, including flowering phenology, floral morphology, or pollinator signaling, each operating as a pre-zygotic barrier to reproductive interference to minimize synchronous use of the same pollinator vectors (Schiestl and Schlüter 2009; Baack et al. 2015b). Flowering at different times in the year reduces the potential for pollen sharing between

individuals of different species. However, flowering phenology in seasonal environments is often constrained by the availability of resources including water, pollinators, and the timing of other life history events such as fruiting (Johnson 1993; Forrest and Miller-Rushing 2010), which may promote synchrony in flowering time. If species flower in synchrony, we might expect divergence along at least one of two other pollination niche axes (Armbruster et al. 1994; Eaton et al. 2012). Divergence in floral morphology, such as the size of the flower, alters the mechanics of pollination and determines which animal vectors can receive and deliver pollen, while floral signaling, including scent, colour, or rewards, serve to attract pollinators and can be generalized (e.g., nectar reward; Heywood et al. 1978) or specialized (e.g., sexual deception; Peakall et al. 2010) to service different animal vectors (Grant 1949, 1994). Evidence from floral trait patterns in ecological communities typically support the role of divergence between close relatives along at least one of these three niche axes (Aizen and Vázquez 2006; Eaton et al. 2012; Muchhalá et al. 2014; Gómez et al. 2015; Weber et al. 2018).

Divergence in floral traits is common in angiosperms and may be associated with up to one quarter of lineage divergence events (Niet and Johnson 2009; Van der Niet and Johnson 2012). Floral divergence has been used as evidence that pollinator shifts may have driven the exceptional diversification of flowering plants compared to their non-flowering relatives (Hernández-Hernández and Wiens n.d.; Kay and Sargent 2009; Vamosi and Vamosi 2010; Kiester et al. 2016; Vamosi et al. 2018). However, how the variation in pollination-trait has evolved over time and is related to angiosperm diversification remains an open question (Sauquet and Magallón 2018). This is because it is often difficult to infer from comparative data whether divergence in floral traits is directly related to speciation events (e.g., pollinator shifts leading to reproductive isolation cause or reinforce speciation) or whether divergence in floral traits occurs subsequently to lineage divergence, either the result of drift in allopatric

populations, or character displacement in sympatric lineages (Whalen 1978; Pfennig and Pfennig 2009).

These alternative mechanisms of floral trait evolution are amenable to testing because they predict distinct patterns in reconstructions of their macroevolutionary history (Armbruster and Muchhalal 2009; Roncal et al. 2012; Weber et al. 2018). If floral traits are involved in driving or reinforcing speciation (speciational model; Fig. 6.1), rapid diversification will be coupled with rapid floral divergence, and so we expect to see a positive relationship between the rates of lineage diversification and floral trait diversification (rates correlation, Fig. 6.1). Because speciation is associated with changes in floral traits, trait differences should not be well predicted by phylogenetic relatedness, or in other words, traits should show low phylogenetic signal (phylogenetic signal, Fig. 6.1). Communities on the other hand would be expected to contain close relatives (and show phylogenetic clustering) because the speciation process places florally divergent sister-species in sympatry (community phylogenetics, Fig. 6.1).

Alternatively, if floral traits diverge gradually in allopatric populations due to random drift in phenotypes or adaptation to different environments (allopatric drift model, Fig. 6.1), we do not expect a relationship between lineage diversification and floral trait diversification rates, as we expect trait differences to be a function of time-since-divergence, and therefore support a Brownian Motion model of trait evolution, with phylogenetic signal consistent with this pattern. Under this model, recently diverged sister species will be the most similar in floral traits and communities of florally divergent species should be assembled from more phylogenetically distant lineages. Finally, if floral traits diverge as a result of selection to minimize competition or reproductive interference among sympatric lineages, (negative interactions model, Fig. 6.1) then we expect to see floral trait diversification in proportion to the potential for competition

among species. As the number of lineages increases in a region, so do the number of potential interspecific interactions. This has the two-fold effect of decreasing the rate of diversification, due to reduced opportunity for ecological speciation (Schluter 2000; Phillimore and Price 2008; Harmon et al. 2019), and increasing the rate of floral trait divergence, to minimize negative interactions between interacting species. Therefore, the rate of lineage diversification should be negatively correlated with the rate of floral trait evolution. This model makes no predictions about the phylogenetic structure of communities because negative interactions may occur between closely related or distantly related species.

Model	Model predictions		
	Phylogenetic signal	Rates correlation	Community phylogenetics
Speciational model	No		
Allopatric drift model	Yes		
Negative interactions model	No		

**Figure 6.1.** Predictions for macroevolutionary patterns in floral trait divergence and lineage diversification under three alternative models. Model illustrations show the branching of a lineage into two new species in allopatry (or also in sympatry as shown in the speciational model) and then returning to sympatry. The speciational model predicts phenotypic change to be associated with the divergence of the lineages which could drive speciation in sympatry. The allopatric drift model predicts gradual change over time. The negative interactions model predicts changes to be driven by interspecific interactions in sympatry. These three models have different predictions for the presence of phylogenetic signal in traits values, for the correlation between rates of trait diversification (TDR) and lineage diversification rate (LDR), and the phylogenetic structure of ecological communities (explained in detail in the main text).

In this study we aim to explore how the macroevolutionary history of floral trait diversification has contributed to contemporary structure and diversity of floral traits in ecological communities. Specifically, we want to know 1) do ecological communities exhibit non-random patterns of floral trait diversity (similarity or divergence) along different pollination-niche axes? 2) Do the phylogenetic distribution of floral trait values or the relationships between the rates of floral trait evolution and lineage diversification support either the speciation model, the allopatric drift model, or the negative interactions model of floral trait divergence described above? To investigate the link between present-day patterns of community assembly and the macroevolutionary history of lineage and trait diversification, we use the Australian plant genus *Hakea* Schrad. & J. C.Wendl. (Proteaceae) as a case study.

*Hakea* is a large genus of 152 species with a center of diversity in the Mediterranean-climate-region of Southwest Australia. Southwest Australia is a recognized biodiversity hotspot and one of the world's most diverse temperate ecoregions. Here, closely related species co-occur in high numbers at local spatial scales (Thiele and Prober 2014), providing a good opportunity to look at how biotic interactions shape biodiversity patterns. *Hakea* has a well sampled molecular phylogeny (Cardillo et al. 2017) and phenotypic database (Skeels and Cardillo 2019a). Floral trait diversity in this genus suggests an important role of floral evolution in the clade's history as *Hakea* exhibits a diverse range of pollination strategies and floral characters (Hanley et al. 2009), with repeated shifts inferred between major animal pollination syndromes - insect and avian (Mast et al. 2012; Lamont et al. 2016a).

## Methods

### Data collection

The phylogeny we use in this study is a species-tree constructed from phylogenomic data using ASTRAL-II, with branch lengths and calibrated divergence times estimated using PAML (Cardillo et al. 2017). We placed five missing species at the node of the most recent common ancestor of all species in the same intrageneric species groupings (Barker et al. 1999). For certain analyses we pruned the phylogeny to contain only species in the survey data (hereafter sample-based phylogeny).

Community survey data were obtained from Gibson et al. (2004), who recorded all plant species in 400m<sup>2</sup> plots across a large area of Southwestern Australia. This dataset includes 275 sites which recorded at least a single *Hakea* species (Fig. 6.2), with 52 *Hakea* species recorded in total. We obtained morphological and phenological data (start, finish, and duration of the flowering period in months) from Skeels and Cardillo (2019) and Flora of Australia vol. 17B, for these 52 species together with an additional 39 species of *Hakea* found in Southwestern Australia. We selected the maximum length of the pistil (female reproductive organ including the style, stigma, and pollen presenter; Fig. 6.2) as a single, widely available, morphological trait that best reflects plant-pollinator interactions (Hanley et al. 2009; Lamont et al. 2016b). This is because, in Proteaceae, the pistil determines where pollen is both deposited on the pollinator (the pollen presenter) and delivered to the flower (the stigma). The distance between the nectary, the pollinator reward, and pollen presenter (pistil length) will mechanically determine which animal species are able to pollinate a *Hakea* species. We selected flower

colour as the trait that best reflects pollinator signalling in *Hakea* (Hanley et al. 2009), which we derived from a photographic library.

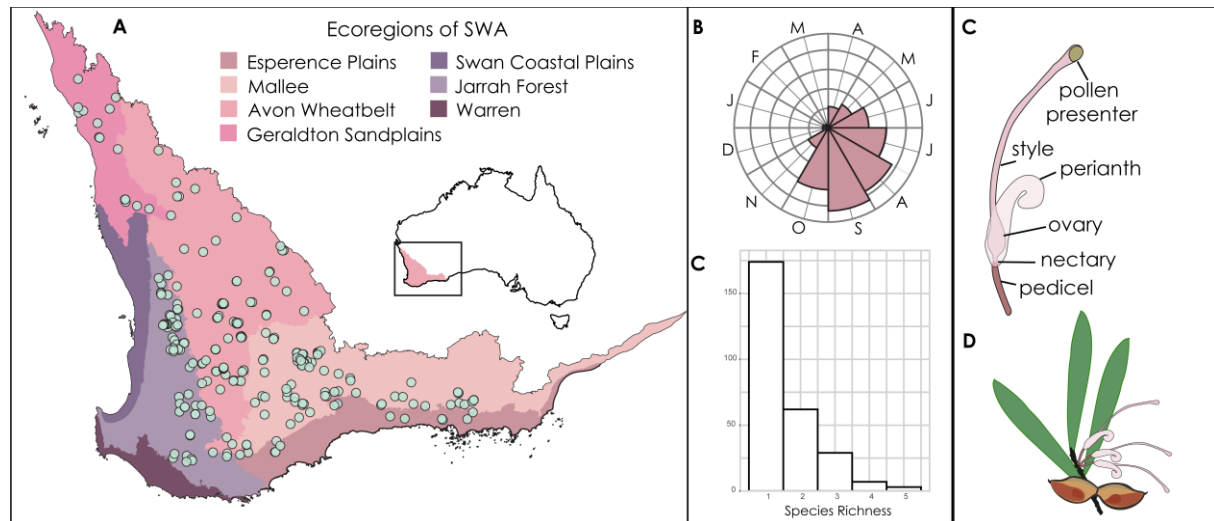


**Figure 6.2** A) Southwestern Australian floristic survey data from Gibson et al. (2004). B) histogram of the species flowering in different calendar months. C) histogram of species richness of *Hakea* species across sites. D) simplified illustration of the floral morphology of a *Hakea* flower, and E) inflorescence on stem (drawn by A. Skeels).

## Photographic library

For each of the 52 species in the community survey data, we collated a digital photographic library of in-bloom inflorescences primarily from the Australian Plant Image Index ([anbg.gov.au/photo](http://anbg.gov.au/photo)), as well as iNaturalist ([inaturalist.org](https://inaturalist.org)) and flickr ([flickr.com](https://flickr.com)). From this photographic library, we selected between one and three photographs (depending on availability) to extract RGB colour data from different organs of the inflorescence (style, pollen presenter, nectary, pedicel, and upper and lower perianth separately when they differed; Fig. 6.2) and recorded the relative proportion of the organ to the total colour signal of an inflorescence (for more details on the collection and validation of colour data see the

Supplementary Information). Flower colour cannot be represented simply by a single trait because each colour is made up of three values (R, G, B), and each flower is made up of several colours in different proportions. To account for this, we obtained pairwise chromatic distances using earth-mover's distances of colour histograms for each species using the colordistance package in R (Weller and Westneat 2019). This method takes into account not only colour differences in a colour space, but also the proportion of the signal occupied by each colour (Weller and Westneat 2019). We did not consider any particular visual system (avian or insect) because we assume that the trait being explored is the colour of the flower produced by the plant, and not the particular perception of it.

## Pollinator classification

*Hakea* species primarily meet an avian or insect pollination syndrome and 36 species in the survey data (and 52 overall) have been assessed for pollination syndrome in previous studies (Hanley et al. 2009; Lamont et al. 2016b). We classified pollination syndrome in the remaining 16 species using a random forest classification technique (Breiman 2001). As predictors of pollination class, we compiled data on traits (from Skeels and Cardillo, 2019) suggested to be strongly related to pollination class (Hanley et al. 2009), including plant height, pistil length, flowers per inflorescence, months in flower, teretedness of leaves, and flower coloration (a binary trait, red/white). To classify pollinator class in the species with unknown pollinators, we ran the model using all fully observed data (52 species) and then used it to predict the probability that each species with unknown pollinator class belongs to either avian or insect pollination modes, based on their measured traits.

## Community assembly patterns

We used pairwise phylogenetic distances, morphological differences (pistil length), and pairwise earthmover's colour distances to ask whether communities are more or less similar in these measures than expected by chance. To do this we estimated functional richness (FRic; Villeger et al. 2008), a commonly used community assembly metric which measures functional diversity as the proportion of the trait-space volume of each community compared to the total volume of all species across communities. FRic has been shown to be among the best functional diversity metrics to distinguish between community assembly processes when communities contain < 10 species (Mouchet et al. 2010). FRic can only be calculated on sites > 2 species (39 sites in our dataset). We also calculated mean phylogenetic distances (MPD; Webb 2000) as a measure of phylogenetic clustering. To test whether our empirical estimates of FRic and MPD differ from the range of values expected by chance, we simulated community data under a null model of community assembly which shuffles the observed species occurrences among sites while maintaining species frequencies and site richness (independent swap null; Gotelli 2000). From 1000 simulated assemblages we estimated FRic based on colour and morphological distances using the FD package in R (Laliberte et al. 2014b), as well as MPD with the picante package (Kembel et al. 2010). We then tested whether the mean values of FRic and MPD across communities fall in the upper or lower tail of the simulated distribution.

## Macroevolutionary patterns

To measure phylogenetic signal we used principal component analysis on the RGB values of the dominant colour in each species' inflorescence, as well as the perianth and pistil colours separately as they generally are the two largest organs in *Hakea* flowers. We calculated

phylogenetic signal using Blomberg's K (Blomberg et al. 2003) and Pagel's  $\lambda$  (Pagel 1999) on the first principal component which accounted for more than 90% of the variation in colour for all three measurements. We also calculated K and  $\lambda$  on the raw values of pistil length. To determine the relative timing of diversification of floral traits in *Hakea*, we reconstructed disparity through time (DTT) of flower colour and pistil length separately. We calculate DTT following Harmon et al. (2003), using the R package dispRity (Guillerme 2018), which measures the mean disparity of each sub-clade measured at each node in the phylogeny (mean squared pairwise distances between species) compared to the total disparity of the whole clade. We decomposed the colour distance matrix into a lower number of dimensions using principal coordinate analysis ( $k=5$ ) to use as input for DTT, while we used the raw measurements of pistil length. We compared the DTT of each floral trait compared to 1000 simulations of traits under Brownian motion along the sample-based phylogeny. To complement the DTT analysis we also constructed lineages through time (LTT) plots (Nee et al. 1992) for both the sample-based phylogeny and full phylogeny of *Hakea*. LTTs show the number of reconstructed lineages present at different time points throughout the clade's history.

To assess the evolution of pollination syndromes (avian or insect) we estimated ancestral states using stochastic character mapping. First, we compared two different continuous-time Markov models of state changes along the phylogeny. The first considered equal rates of transitions between avian and insect pollination syndromes (ER) and the second estimated different rates between avian-insect and insect-avian (ARD). Models were fit using the `rerootingMethod` function in `phytools` (Revell 2012). An ARD model was considered the best fit to the data based on a likelihood ratio test ( $df = 1$ ,  $D=12.86$ ,  $p<0.01$ ) and for visualisation of character evolution on the phylogeny we generated 1000 stochastic maps from this model and mapped the posterior

density of state estimations using the densityMap function in the R package phytools (Revell 2012).

To gain a better understanding of evolutionary rate heterogeneity and the dynamics between the rate of floral trait evolution and the rate of lineage diversification through time, we estimated branch-specific values of these rates along the *Hakea* sample-based phylogeny. We estimated the rate of floral colour and pistil length evolution using phylogenetic ridge regression, as implemented in the R package RRPhylo (Castiglione et al. 2018). For simplicity, we ran the model on a single RGB colour value for each species, chosen as the colour making up the largest proportion of the flower. To estimate branch specific rates of lineage diversification we used the ClaDS2 model, which estimates speciation rates across the phylogeny, assuming a constant turnover rate through time, using a Bayesian approach (Maliet et al. 2019) in the R package RPANDA (Morlon et al. 2016). We ran the model for 5000 MCMC iteration, with a thinning rate of 10, using the proportion of species in the sample relative to all *Hakea* species to adjust the model for taxon sampling. For further analysis, we extracted the maximum *a posteriori* estimates for each branch of the phylogeny. We excluded *Hakea* species that were not in the original molecular phylogeny, to avoid any impact their uncertain placement might have on estimating diversification rates.

We then fit a model of how floral trait evolutionary rate depends on diversification rate across branches of the phylogeny, and how this relationship depends on the inferred pollinator status along each branch (from the ARD model). We fit a standard linear model with gaussian error structure (for flower colour and pistil length separately), using log transformed trait evolution rate (+0.1 to deal with some near zero estimated rates) as the response, and log transformed diversification rate (+0.1), and predicted pollinator status (as a categorical factor) as predictors

in the model. We also included a pollinator status by diversification rate interaction to model whether the relationship between diversification rate and floral trait evolution rate varies by the most likely ancestral pollinator.

## Results

### Community assembly

The mean functional richness (FRic) of flower colour for assemblages across Southwest Australia was greater than the null expectation based on the independent swap model of community assembly (Fig. 6.3). The mean FRic of floral morphology (pistil length), and MPD across communities was no greater than expected according to the null model. This suggests that across Southwest Australia, communities tend to occupy a greater volume of trait space for flower colour than if communities across the region were assembled randomly. On average, the volume of morphological space, as well as the mean phylogenetic relatedness of species falls in the null distribution.

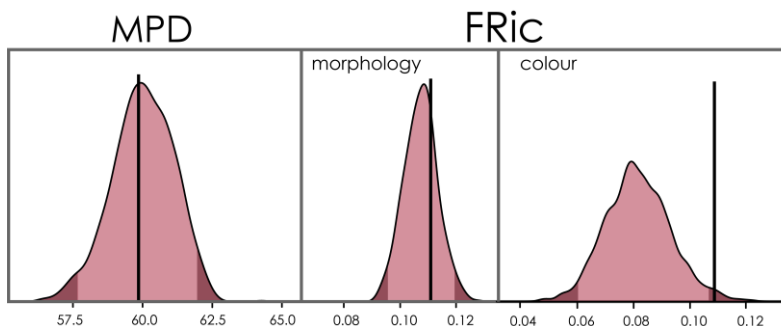


**Figure 6.3.** Observed and null distributions of mean phylogenetic distance (MPD) and functional richness (FRic) measured for two floral traits, maximum pistil length and flower colour, averaged across communities in Southwest Australia. Upper and lower 2.5% quantiles are shaded in dark red, and the observed average metric is given by the vertical black lines.

## Pollination syndromes

We built a random forest classification model to classify pollinator class in 16 species based on observed data from 52 species. The major contributing variables were the maximum and minimum pistil lengths followed by the number of flowers per inflorescence. All species received predicted pollinator class probabilities  $> 75\%$  and most  $> 90\%$ . We therefore assigned pollinator classes to species based on which class received the majority support.

Ancestral state reconstruction of pollinator class (avian or insect) using a continuous-time Markov model identified avian pollination syndrome as the most probable ancestral state, although there is high uncertainty (56% support for avian and 44% for insect). An all-rates-different (ARD) model was a better fit to the data than an equal-rates (ER) model, and the avian to insect transition rate was higher ( $0.06 \pm 0.02$ ) than the insect to avian rate ( $0.02 \pm 0.01$ ). The model highlights two main clades showing different pollination syndromes. One avian clade shows repeated transitions between avian and insect pollination modes, while another insect clade shows far fewer transitions (Fig. 6.4A).

## Evolution of floral traits

There is strong phylogenetic signal in pistil colour ( $K=0.69$ ,  $p=0.006$ ;  $\lambda=0.54$ ,  $p<0.0001$ ), but not in the dominant colour ( $K=0.45$ ,  $p=0.59$ ;  $\lambda<0.0001$ ,  $p<0.0001$ ), perianth colour ( $K=0.54$ ,  $p=0.15$ ;  $\lambda=0.41$ ,  $p=0.24$ ), or pistil length ( $K=0.60$ ,  $p=0.053$ ,  $\lambda=0.19$ ,  $p=0.24$ ). PC1 of the dominant colour was correlated with PC1 of perianth colour (Pearson's  $r = -0.8$ ) but not with pistil colour ( $r = 0.4$ ) and the perianth typically contributed the most to the dominant colour of the inflorescence.

Disparity through time (DTT) analysis showed that sub-clade disparity was mostly consistent with that expected under Brownian motion for both floral morphology (pistil length, Fig. S6.1). Flower colour, on the other hand, shows sub-clade disparity consistent with that expected under Brownian motion for much of this early history (Fig 6.4D), followed by an extended period, from roughly 15 to 5 million years ago, characterised by significant deviation away from this null expectation. Lineages that originated during this later period explain a significant proportion of the total colour variation in the whole group. This suggests that similar colour morphs evolved repeatedly during this period, and the rate of divergence is greater than expected under a Brownian motion model (Fig 6.4D). We also see relatively high pairwise colour distances at low phylogenetic distances (Fig. S6.2), which is inconsistent with Brownian Motion (Cadotte et al. 2017). This relatively late period of radiation is also characterised by a slowdown in lineage diversification. These diversification dynamics are seen in both the full and sample-based phylogenies (Fig 6.4C).

The statistical model of evolutionary rates revealed that there was generally a negative relationship between diversification rate and flower colour evolution rate (slope = -0.24,  $t = -2.43$ ,  $p = 0.017$ ; Table S6.1), such that the slower estimated diversification is, the faster estimated colour change tends to be along phylogenetic branches. This effect is much more pronounced in lineages predicted to be bird pollinated, as implied by a negative interaction between bird pollination mode and diversification rate (slope = -0.42,  $t = -2.06$ ,  $p = 0.042$ ; Fig. 6.4E). There was little evidence of an overall difference in colour rate evolution between the two pollination modes (slope = 0.19,  $t = 0.896$ ,  $p = 0.37$ ). In contrast, rates of pistil length evolution did not show any strong patterns with respect to diversification rate (slope = -0.098,  $t = -0.95$ ,  $p = 0.35$ ), though they were marginally higher in bird pollinated lineages overall.

(slope = 0.37,  $t = 1.71$ ,  $p = 0.091$ ). Likewise, the relationship between pistil length evolution rate and diversification rate did not clearly depend on predicted pollinator class (slope = -0.31,  $t = -1.46$ ,  $p = 0.15$ ).

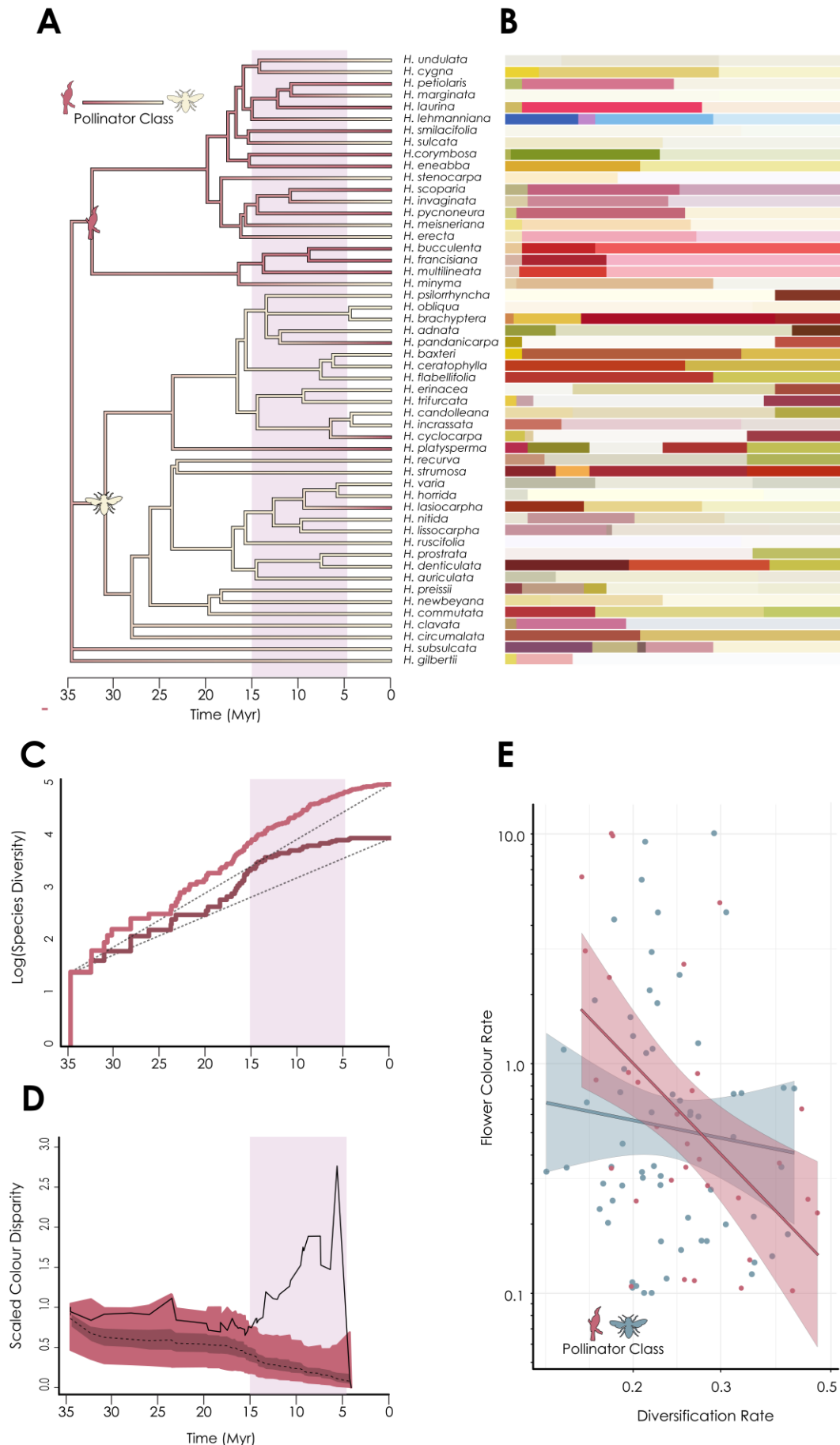


**Figure 6.4.** Evolution of disparity in flower colour. A) phylogeny of 52 species from across Southwest Australia, sampled in the community survey data. Branches are coloured by the inferred probability of belonging to avian (pink) or insect (white) pollinator classes based on a continuous-time Markov chain model of trait evolution. We highlight predominately insect and avian pollinated clades with a corresponding silhouette. B) average colours sampled from each species for five different floral organs, with the size relative to the contributed proportion of the inflorescence colour signal. C) lineages through time plots of log transformed species diversity. The light pink is the LTT of the full phylogeny (135 species), and in dark purple is the sample-based phylogeny (52 species). Dotted lines show the null expectation under a constant rates model of lineage diversification. D) disparity through time plot of flower colour with disparity measured as the mean squared pairwise distances. Red polygons show the expectation under a Brownian Motion model from 1000 simulations, with the dotted line showing the mean disparity from these simulations. The black line shows the estimated disparity for flower colour. E) The relationship between the estimated per branch rates of diversification and flower colour evolution with rates (+ 0.1) plotted on a log scale for both insect (blue) and avian (red) pollination syndromes separately.

## Discussion

Mediterranean-climate shrubland ecosystems are a challenge for ecologists because it is not clear how large numbers of closely related plant species can coexist in such low-productivity environments with very little habitat heterogeneity. Our results for *Hakea*, one of the most diverse plant genera in the Southwest Australian biodiversity hotspot, demonstrate that divergence in reproductive traits is likely to be involved in the assembly of shrubland plant communities. While flowering phenology is reasonably synchronous across species, we find that divergence in floral phenotypes, and in particular, flower colour is associated with non-random community assembly. Together, macroevolutionary patterns of diversification and patterns of ecological sorting across present-day communities suggest that diversity-dependent

processes driven by negative biotic interactions between species play a key role in driving character displacement of flower colour and facilitating the coexistence of species.

## Floral traits in species-rich ecological communities

Floral traits have been shown to be strongly associated with pollinator preferences, and differences in size, colour, pattern, or scent of a floral display act as signals to the behavioural and sensory ecology of animal pollinators (Schiestl and Johnson 2013). Different colours of flowers have repeatedly evolved as a signal to the different optical systems of animal pollinators (Rodríguez-Gironés and Santamaría 2004; Dyer et al. 2012). In some cases, whole communities converge on similar flower colour signals to facilitate the attraction of mutual pollinators (Kantsa et al. 2017). In other cases, species in communities show divergent flower colour signals to reduce competition or reproductive interference with closely related species (McEwen and Vamosi 2010). The average volume of flower colour space across ecological communities in Southwestern Australian *Hakea* supports this latter result; that non-random structure of flower colour in ecological communities is due to diversity, not uniformity, in floral displays.

High functional richness of floral phenotypes in ecological communities of Southwest Australia may promote pollinator diversity while ensuring greater fidelity of pollen flow between individuals of the same species. This is because many pollinator species that rely on floral resources are tuned to pay attention to specific cues from flowers such that they are more likely to visit certain species (Pauw 2013, 2019). In *Hakea* the most immediate distinction between flower colours is that of avian and insect pollinated species. Typical of many plant species, red flowers are commonly associated with an avian pollination mode while insect pollinated species

are more typically yellow, white or cream (Ford et al. 1979; Rodríguez-Gironés and Santamaría 2004). This is generally true in *Hakea* (Hanley et al. 2009), although we found that shifts in pollination syndrome are not always associated with an obvious change between bird-preferred and insect-preferred colours (Fig. 6.4). We also observe a number of colour changes between species within each syndrome. *Hakeas* are known to be pollinated by different orders of insects (e.g., dipterans, lepidopterans, and hymenopterans; Barker et al. 1999), which each have been recorded to show preferences for particular colour morphs in Southwest Australia (Groom and Lamont 2015) and this could explain further colour divergence within the insect pollination syndrome. The specificity of honeyeaters (family Meliphagidae), the primary avian pollinators of *Hakea* (Hopper 1981; Groom and Lamont 2015), are less known, but vertebrate specificity in co-occurring species has been observed in the closely related genus *Banksia* (Collins and Rebelo 1987) and in other bird pollinated plants (e.g., refs in Pauw 2019). Regardless, striking differences in flower colours of co-occurring species is most likely explained by shifting pollinator specificity.

## Floral macroevolution

We tested the predictions of three alternative models of floral evolution (Fig. 6.1) and found that the tempo and mode of flower colour evolution, but not morphology, was consistent with the negative interactions model. We found a negative correlation between the rate of flower colour evolution and the rate of lineage diversification (Fig. 6.4E) and we did not find significant phylogenetic structure of communities or phylogenetic signal in the dominant flower colour. The negative interactions model of floral trait evolution is diversity dependent; as species diversity increases in a region, we expect the number of potential negative interactions to increase, which in turn is expected to increase the rate of diversification of ecological traits

that mediate negative interactions (Skeels and Cardillo 2019a). This is also supported by the general pattern of lineage diversification slowdown, which also supports the role of diversity-dependent processes and increased competition from a higher number of interacting species (Phillimore and Price 2008; Rabosky 2013b). Previous studies have found a relationship between species diversity and floral divergence in sympatric lineages suggesting diversity dependence is important, but so far have been unable to distinguish between the speciation and negative interactions models of floral divergence (Armbruster and Muchhal 2009; Weber et al. 2016). Our result clarifies this in *Hakea*, where we find high species diversity drives floral diversification and is not the result of it. The evidence in support of character displacement goes against the long-standing idea that shifts in floral traits are associated with rapid diversification dynamics in angiosperms. While studies have found positive associations between the presence of floral traits like zygomorphic flowers or nectar spurs with rates of diversification across clades (e.g., O'Meara *et al.* 2016), far fewer studies have investigated the link between rates of floral trait divergence and lineage diversification within clades that share a common flower type. Our study is one of the first to highlight how the diversity in important floral traits has evolved in the later stages of the radiation of *Hakea* when diversity is already high. This was facilitated by the development of new methods to estimate branch specific rates of lineage diversification (Maliet *et al.* 2019) and trait evolution (Castiglione *et al.* 2018).

Flower colour evolution showed increasing rates towards the present-day in both avian and insect pollinated species, however the pattern was much stronger in avian pollinated lineages (Fig. 6.4E). The major group of avian pollinators of *Hakea*, Meliphagid honeyeaters, originated in the late Oligocene (Marki *et al.* 2017) and radiated into a range of ecological niches during the mid-late Miocene (Marki *et al.* 2019). During this period Australia underwent widespread

aridification and open habitats began to dominate temperate ecosystems, spurring the diversification of much of Australia's heavy nectar-producing flora, including many lineages of Proteaceae (Onstein et al. 2016). This period is also concurrent with a period of rapid flower colour evolution in *Hakea*, as illustrated by the observed deviation of flower colour evolution from Brownian Motion during the latter half of the radiation of *Hakea* in the mid to late Miocene (15-5 mya; Fig. 6.4D). Ecologically divergent honeyeaters regularly co-occur in high numbers, utilising different nectar resources in the environment (Miller et al. 2017b; Marki et al. 2019). The radiation of honeyeaters during this period, and the diversity of sympatric honeyeater lineages, may have provided ecological opportunity for pollination niche divergence in *Hakea*. The stronger relationship between rates in avian pollinated species could be because honeyeaters provided a novel resource to reduce negative interactions, rather than insects which had radiated before this period (Condamine et al. 2016). Although we cannot say from our results whether the diversification of flower colour and the Melphagid radiation are causally related or simply coincident in time, investigating pollinator specificity and potential coevolutionary dynamics of these clades together would be of great interest.

## Conclusion

Our combined results from community assembly and macroevolutionary analyses support the idea that negative interactions have shaped the evolution and divergence of floral traits in *Hakea* through character displacement. As diversity increases within a community, species must be more phenotypically and ecologically divergent to sustain stable coexistence (Armbruster and Muchhala 2009; Weber and Strauss 2016). These interactions also play out over much deeper timescales and we see that as diversity increased within Southwest Australia, so too did the rate of phenotypic divergence for an important floral trait – flower colour. By analyzing diversity-

dependent processes at both ecological and macroevolutionary scales in the same framework, our study adds to a growing body of evidence that ecological interactions can shape macroevolutionary patterns, highlighting the importance of considering the ecological context of diversification (Weber et al. 2017; Harmon et al. 2019).

## Appendix

### Flower colour data collection

#### *Photographic library*

A rich source of information on phenotypes are digital photographs and digital photographic libraries are increasingly used in ecological and evolutionary studies (Drury et al. 2019). For each of the 52 species in the community survey data, we collated a digital photographic library of in bloom inflorescences with images primarily from the Australian Plant Image Index (APII); a resource managed by the Australian National Botanical Gardens for the identification of the Australian flora (APII 2019), as well as iNaturalist ([inaturalist.org](https://inaturalist.org)) and flickr ([flickr.com](https://flickr.com)) when the APII did not have suitable photographs. From this photographic library, we selected between one and three photographs (depending on availability) to extract red, green, blue (RGB) colour data from different organs of the inflorescence. Because different floral organs vary in colour and size, the colour signal of an inflorescence cannot be attributed to a single value. To account for this, we estimated RGB values of different floral organs (pistil, pollen presenter, nectary, pedicel, and upper and lower perianth separately when they differed) and recorded the relative proportion of the total colour signal of an inflorescence to which that organ contributes.

Using the image processing software imageJ (Abràmoff et al. 2004), we sampled pixels from each organ and took RGB colour measurements. Where possible, we repeated this across different photographs taken at different times, or with different cameras. Where species did not have multiple photographs, we recorded different flowers within the same photograph. Some

species show intraspecific variation in colour morphs. We aimed to capture the most representative colour morph, rather than capture this variation, and so took RGB measurements that represented the most common morph. This decision was guided by matching colours to those shown in floraBase (FloraBase 2019), which is an authoritative guide to the flora of Western Australia. In total we recorded 444 colour measurements across the 52 species. We averaged colours across different photos for each organ to give us a total of 157 measurements.

#### *Colour standardisation and UV reflectance*

Digital images, while being an abundant and valuable resource, are taken under unstandardized light conditions which may affect the RGB values extracted from each photo. To see what the effect of using digital images from online resources, rather than taken under standardised conditions, we took photographs of the flowers of eleven *Hakea* species under standardised light conditions. We took raw photographs using a Canon 500D digital SLR with a full spectrum fused-silica conversion (Camera Clinic, Melbourne) and a Canon 100 mm macro lens. The lens was fitted with one of two different filters: UVB (320-400 nm) and visible (400-700 nm). For standardised illumination conditions we adjusted manual parameters to allow only light from a flash unit with UV and visible spectral power distribution. We used a constant camera height and all photographs were taken in the same place and a spectralon white balance (LabSphere, NH, USA).

We compared our standardised photographs in the visible range (400 – 700nm) with photographs taken from the same online resources as for our photographic library (namely the APII) sampling colours in the same way as described above. To compare images, we performed a principal component analysis on the RGB values of each organ. We compared PC1, which explained more than 91% of the variation in colour data, for the colour of each floral organ

from our standardised photographic data to the value of PC1 for the same floral organ of the digital photographs from the APII and found a very strong positive correlation (Pearson's  $r = 0.89$ ) suggesting digital images from the APII give very similar colour measurements to those measured under common, standardised conditions.

This study focuses on the visible RGB light spectrum, however many animals including many insect pollinators see ultra-violet light and flowers often attract pollinators using these, rather than visible light wavelengths. To test whether *Hakea* species might be reflecting UV light as a signal to pollinators, we measured UV reflectance measurements of a sample eleven *Hakea* species, including both insect and bird pollinated species. We found that no *Hakea* flowers reflected UV to a significant degree (i.e., detectable under our light conditions), suggesting *Hakea* species might not use UV wavelengths for pollinator attraction.

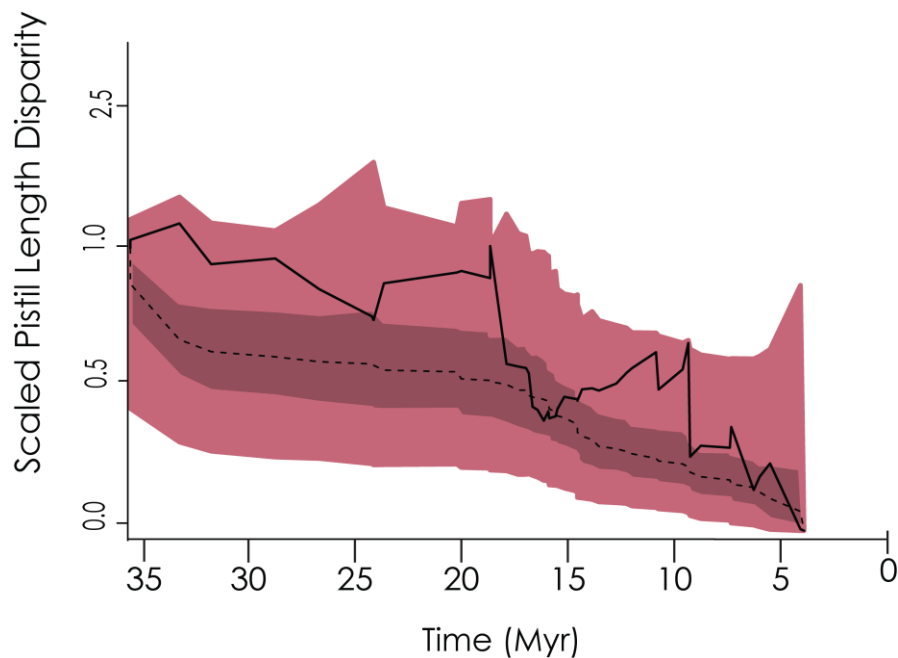


**Figure S6.1** Disparity through time plot for maximum pistil length. Disparity measured as the mean squared pairwise distances. Red polygons show the expectation under Brownian Motion from 1000 simulations, with the dotted line showing the mean disparity from these simulations. The black line shows the estimated disparity for pistil length which falls within the Brownian expectation.

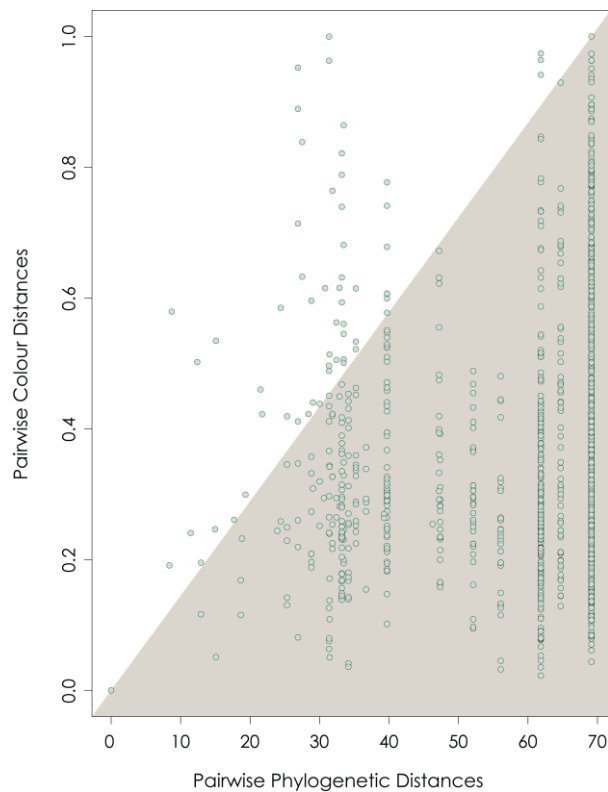


**Figure S6.2** The relationship between species pairwise phylogenetic distance and earth mover's flower colour distance. Under Brownian motion we expect a wedge-shaped pattern (brown triangle).

**Table S6.1** Results of the statistical model estimating the effect of diversification rate and predicted pollinator class on the rate of trait evolution for flower colour, and pistil length. Each cell has the estimated coefficient and the standard error of the estimate (in brackets). Model summary information can be found in the lower panel of the table.

	Colour evolution rate	Pistil length evolution rate
Intercept	0.020 (0.099)	0.013 (0.102)
Diversification rate (DivRate)	-0.243** (0.100)	-0.098 (0.103)
Pollination Syndrome (PollSyn)	0.188 (0.210)	0.370* (0.217)
DivRate ~ PollSyn	-0.418** (0.203)	-0.305 (0.209)
Observations	96	96
R <sup>2</sup>	0.113	0.057
F statistic (df = 3; 92)	3.918**	1.862

Note: \*p < 0.1; \*\*p < 0.05; \*\*\*p < 0.01

# Chapter 7: Conclusion

Linking biodiversity patterns to evolutionary and ecological processes is essential to understanding the extraordinary diversity we see around the world today. However, disentangling the drivers of diversity is a difficult task. Leveraging different kinds of data (phylogenetic, functional-trait, spatial) and methods (process-based models, phylogenetic comparative methods, community ecology, etc.) in a combined framework offers a way forward, by allowing us to test multiple predictions independently, to better understand which evolutionary and ecological processes may have generated the patterns we observe in the present-day. This final chapter discusses the core chapters of my thesis collectively within this broader context, highlighting how different questions, and the methods used to address them, form pieces in the same puzzle and contribute to our understanding of spatial biodiversity patterns.

All diversity inherently originates from speciation, and all spatial patterns of diversity begin with the geographic context in which speciation occurs. Sympatric speciation immediately leads to two species co-occurring in the same space, increasing alpha diversity, and all else being equal secondary sympatry is expected to occur more rapidly in species that have abutting, rather than isolated ranges (parapatric rather than allopatric speciation; Barraclough & Vogler 2000; Anacker & Strauss 2014). It may take millions of years for species isolated by physical barriers to come into secondary contact, especially if their dispersal capacity is low (Pigot and Tobias 2014), leading to greater species turnover (beta diversity) and phylogenetic over-dispersion across a landscape (Graham and Fine 2008; Warren et al. 2014). However, the degree

to which spatial diversity patterns are the result of the geography of speciation or subsequent geographic range movement is contentious (Losos and Glor 2003).

The Dynamic Range Evolution and Diversification (DREaD) model (Skeels and Cardillo 2019*b*), introduced in Chapter Two, was used to show that the geographic mode of speciation leaves a detectable signature in spatial and phylogenetic patterns; from range size frequency distributions, to patterns of range overlap. I leveraged the relationship between these patterns and the geography of speciation to make inferences about the history of speciation, which showed taxonomic patterns consistent with predictions from previous speciation studies (e.g., sympatric speciation appears more common in plants than animals; Rieseberg and Willis 2007). These results highlight how we can use present-day patterns in phylogeny and geography to infer when ecological speciation may be important in the diversification of a clade. This has implications for future studies, as ecological speciation (typically sympatric or parapatric) is typically attributed as the mechanism driving adaptive radiations or diversity-dependent diversification dynamics (Givnish 2015), and contributes to macroevolutionary patterns such as slowdowns in phylogenies. These patterns, however, can be driven by other factors as well (Moen and Morlon 2014; Harmon and Harrison 2015), and some models predict competition between species to accelerate rather than slow diversification (Fischer 1960). Therefore, ecological speciation should be explicitly tested for in comparative studies (e.g., with DREaD), rather than assumed.

DREaD models geographic range evolution and diversification across a continuously varying landscape, however we are often interested in concatenating lineages into regions (such as biomes or ecoregions) to look at dynamics within more discrete units. Lineages through space and time (LTST) plots (Skeels 2019), introduced in Chapter Three, highlight how we can use information on the history of geographic range evolution (Ree and Smith 2008; Matzke 2013*a*)

and lineage diversification (Nee et al. 1992) to better understand how diversity has arisen and accumulated within broadly defined regions. There is recent interest in understanding how temporal diversity dynamics vary with ecological or geographic features (e.g., Machac and Graham 2017; Machac et al. 2018). LTSTs offer to link patterns such as slowdowns or speedups in regional lineage accumulation to equilibrium and non-equilibrium diversification dynamics. For example, diversification slowdowns are expected when regions become saturated with diversity (Phillimore and Price 2008). This saturation point (or regional carrying capacity) is expected to be greater in highly productive or larger areas (Rohde 2006; Rabosky and Hurlbert 2015*b*; Storch and Okie 2019). However, if some clades have only recently colonised a region, low diversity may be the result for a lack of time-for-speciation – a non-equilibrium dynamic (Stephens and Wiens 2003; Wiens 2011; Pontarp and Wiens 2017). One way to pull these dynamics apart is by placing diversification in a biogeographic context and incorporating information on range evolution.

Another way to investigate equilibrium and non-equilibrium ecology is to look at patterns of resource use in co-occurring species at finer spatial scales. MacArthur (MacArthur and Levins 1967; MacArthur 1972) developed a framework for equilibrium ecology based on the idea that areas vary in their carrying capacities for species due to differences in the number and kinds of resources available, as well as the way in which species divide these resources. If resources are limiting, then species should partition their ecological niches to restrict resource sharing, while niche overlap might be facilitated if a resource is abundant. Ultimately this idea reduces to how the abiotic environment shapes the competitive landscape. We often do not have direct information on species ecological niches, and instead, competition has traditionally been inferred by investigating local patterns of co-occurrence at a community scale. Integration of phylogenetics and functional trait data (phenotypic, life history, phenology, etc.) into this field

led to the development of testable hypotheses given how we expect the relatedness of species (Webb et al. 2002; Kraft et al. 2007; Cavender-Bares et al. 2009; Graham et al. 2010) and their functional traits (McGill et al. 2006; Spasojevic and Suding 2012; Lamanna et al. 2014) to determine the composition of communities under different ecological assembly mechanisms (e.g., competition vs filtering).

In Chapter Four, I compared patterns of functional divergence amongst ten major clades of lizards, using functional traits, to determine which macroecological diversity hypotheses best explain species richness patterns (Skeels et al. 2019). I found that high species richness was sometimes associated with divergence in traits and sometimes with trait similarities (convergence). I also found idiosyncratic relationships with different environmental variables. In an equilibrium world, we might expect closely related and physiologically similar taxa, like different lizard clades, to show similar drivers of diversity. This is because we expect that resource availability, dictated by environmental conditions, should place the constraints on the number of ecologically similar species that can coexist (MacArthur 1972; Srivastava and Lawton 1998; Storch et al. 2018). Instead it is possible that non-equilibrium dynamics (for example the time-for-speciation effect) may help to explain differences between lizard groups, but more work is required here to untangle the ultimate drivers of lizard diversity patterns.

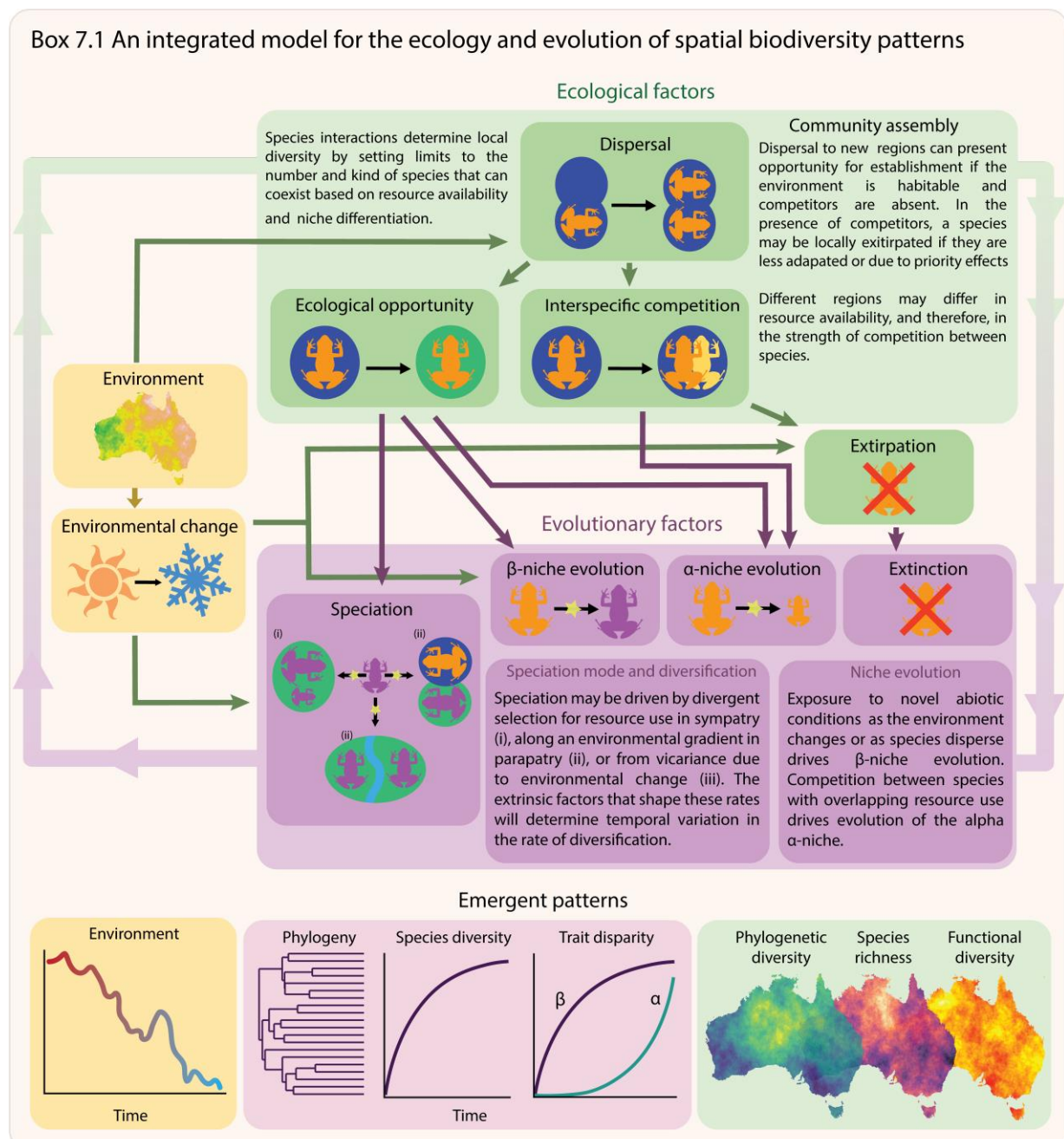
In Chapter Five, I developed a hypothesis testing framework for integrating community ecology with phenotypic evolution and temporal diversification dynamics to understand when equilibrium or non-equilibrium dynamics are important in structuring regional diversity patterns (Skeels and Cardillo 2019a). Here, I estimated which functional traits were involved in environmental filtering or competition between species using methods from community ecology (Cavender-Bares et al. 2004; Silvertown et al. 2006). I then investigated how these different traits evolved over deep time. One expectation is that traits that mediate negative

interspecific interactions, such as competition ( $\alpha$ -niche traits), should diversify as species diversity increases and the potential for ecological interactions between sympatric species also increases - a diversity-dependent model of  $\alpha$ -niche evolution. In Chapter Five, I applied this hypothesis testing framework to the large Australian plant genus, *Hakea*, as a case study. I found that both equilibrium and non-equilibrium dynamics explain spatial diversity patterns in *Hakea* in different regions and at different times throughout the clade's radiation. In Chapter Six, I extended the same framework to floral traits in *Hakea* to answer a related, but more-specific question: have negative interspecific interactions, including reproductive interference and pollinator competition, shaped the evolution of floral traits and pollination ecology of high diversity communities in Southwest Australian *Hakea*? Both chapters show how  $\alpha$ -niche traits tend to evolve in response to competition with sympatric lineages in the later stages of a radiation, when regional diversity is high. Both studies individually highlight how the ecological diversity we observe in communities today is the outcome of varied and complex macroevolutionary histories.

The studies I have presented highlight how combining ecological and evolutionary approaches gives us a richer understanding of biodiversity and reinforces the need for a synthetic approach to biodiversity studies. We are closer to having a more complete framework for integrating different ecological and evolutionary processes to investigate the emergence of spatial diversity patterns (e.g., Pontarp et al. 2019) and different models have been developed which already incorporate multiple ecological and evolutionary processes. For example, spatially explicit, process-based simulation models (PBSM) of evolution have been used to investigate species richness patterns (Rangel et al. 2007, 2018; Gotelli et al. 2009; Colwell and Rangel 2010; Descombes et al. 2018), and in particular, to understand how complex interacting traits, such as dispersal and niche evolution (Qiao et al. 2016), or habitat carrying capacity (Pontarp and

Wiens 2017), affect diversification rates and the spatial distribution of species. PBSMs have also been used to study other biogeographic processes such as the role of competition in community structure (Pontarp et al. 2012), and species range overlap during adaptive radiations (Pontarp et al. 2015).

Box 7.1 An integrated model for the ecology and evolution of spatial biodiversity patterns



PBSMs are an exciting frontier for biodiversity studies as they allow us to parameterize interacting ecological and evolutionary processes that may be too complex for analytical likelihood-based models, allowing us to link process to pattern. A complete model of biodiversity should be able to simultaneously explain a range of patterns, and a much-needed extension of PBSMs is to explain the numerous inter-related patterns discussed throughout this thesis: spatial patterns of species richness, phylogenetic, and functional diversity, as well as macroevolutionary patterns of lineage and trait diversification, and geographic range evolution. This would enable us to tease apart equilibrium and non-equilibrium dynamics governing diversity patterns (Box 7.1 explores a hypothetical PBSM which integrates ecological and evolutionary feedbacks). However, PBSMs are no silver-bullet, and are constrained by a necessary simplification of ecological and evolutionary processes. This is partially due to computational constraints, but also because our understanding of even the most fundamental ecological processes, like competition between species, is still incomplete. PBSMs rely on complex parameterisation of processes that should ideally be grounded in empirical data, but where this is lacking is often derived from verbal or theoretical models which themselves may be imperfect. One benefit of simplifying processes in PBSMs is to be able to detect the minimum number of ecological processes required to generate realistic biodiversity patterns. This, in fact, has been one of the major breakthroughs of the neutral theory of biodiversity (Hubbell 2001), which is able to replicate a wide variety of macroecological patterns despite being an extreme simplification of ecological and evolutionary processes.

The issue regarding uncertainty of fundamental ecological and evolutionary processes raises some more general concerns, not only of PBSMs, but of a purely neontological approach in general, which is largely what the research in this thesis presents. That is that 1) inferring historical ecological and evolutionary processes using only data collected from the present-day

may be insufficient and 2) phylogenetic comparative methods are typically based on a range of assumptions which may not be met by a given dataset.

To the first point, fossil data can inform many procedures used in evolutionary biology, from the calibration of divergence dates in phylogenetic reconstruction, to grounding models of ancestral state reconstructions of geographic ranges and phenotypic traits. Without well sampled fossil data, which may not be present for most clades, inferring evolutionary dynamics from phylogenies needs to be done cautiously. For example, a recent study has shown that any molecular phylogeny might be consistent with an infinite combination of time-varying speciation and extinction rates (Louca and Pennell 2020). Where it has been possible, the inclusion of fossil data has been shown to drastically change the inferences we make (for example the discrepancy between the estimated origin of the mammal radiation from molecular and fossil evidence (Archibald and Deutschman 2001)) and this is partly because fossil data often highlights discontinuities in species diversity and morphology (Gould and Eldredge 1977; Sepkoski 1978) that we could not predict from commonly used models of evolution (e.g., Brownian Motion model of trait evolution or a birth-death model of diversification).

This brings me to the second issue, model misspecification and model assumptions in phylogenetic comparative methods. The toolbox of evolutionary biologists is limited (but always expanding) and many studies of diversification and trait evolution are based on comparisons between a small subset of models (e.g., Brownian Motion (BM) and Ornstein-Uhlenbeck (OU)). Such models assume stationary processes across the phylogeny and through time. However, we know that rates vary stochastically, or systematically with changes in the environment or life history traits (for example diversification rates are higher in mammal species that have large litters (Cardillo et al. 2003)). Some models have been extended to include branch-varying rates. For example, Clavel and morlon (Clavel 2017) developed a time-

varying BM model. While other studies have shown that the underlying model of evolution itself can change over time. For example, (Slater 2013) found that body size evolution in mammals is best predicted by an OU model until the Cretaceous-Paleogene boundary, and a BM model after it. Non-stationarity of rates and model misspecification are problems that also applies to phylogenetic reconstruction, which all phylogenetic comparative methods ultimately rely on, and any biases present in the reconstruction can have downstream effects on many inferences we draw.

An example of this, relevant to the research presented in this thesis, is the inference of adaptive radiation dynamics from an observed slowdown in diversification rates on a phylogenetic tree. While this pattern is expected by theory, slowdowns may also be present due to a number of other factors (reviewed in Moen and Morlon 2014). At least two of these factors are biases introduced during phylogenetic reconstruction. The first is that branch lengths may be underestimated when rates of molecular evolution vary systematically across the tree, for example when speciation rate is related to the rate of molecular evolution (Duchene et al. 2017), and this can cause an artificial slowdown in diversification rates over time (Harmon and Harrison 2015). Secondly, incomplete taxon sampling can lead to an artificially sparse distribution of branches towards the tips of the tree (Harmon and Harrison 2015), again resulting in a slowdown pattern. This means that we need to provide evidence independent of the distribution of branch lengths across a phylogeny to support the role of diversity-dependent processes. In chapter 5 I attempt to do this by showing that regions of high diversity for *Hakea* in Southwest Australia are also places where competition-related traits are more divergent than a null expectation which supports the role of competition driving the observed diversification slowdown. It is also worth noting that a slowdown is not the only expected outcome of adaptive radiation dynamics. For example, some models predict that competition should actually

increase available niche space, facilitating increasing rates of diversification (Fischer 1960). There is also no reason to believe that we exist at a time when most radiations would be in a saturated phase of diversification and based on phylogenetic evidence it appears many clades are still expanding (Machac and Graham 2017*b*). The case of diversification slowdowns highlights how the pitfalls of phylogenetic reconstruction, phylogenetic comparative methods, and predictions from verbal models all need to be considered when drawing inferences about historical processes.

What this means is that many inferences we draw need to be interpreted cautiously and in light of the assumptions of our models and the information content of our data. Phylogenetic comparative methods and phylogenetic reconstruction methods may both be improved (and already have been) by the inclusion of fossil data and by extending current methods or developing new methods to account for rate and model variation over time and across the branches of the tree of life. What is still needed are methods that combine what are currently separate steps, the phylogenetic reconstruction and downstream macroevolutionary analyses, into a unified framework. This may remove some of the circularity and biases involved in estimating a tree when many of its features (e.g., branch lengths) are influenced by macroevolutionary and macroecological dynamics and vis-versa.

Biodiversity is earth's most valuable natural resource, and despite over 150 years of research in the light of evolutionary theory, we still are learning to appreciate and understand the amazing complexity of processes that have shaped the distribution of species around the world. In saying that, it is also worth noting we have come a long way. The development of an array of tools for describing patterns and understanding the processes that shape diversity, from phylogenetic reconstruction methods, to models of phenotypic evolution, have greatly enhanced our ability to link observable, present-day patterns to the deep evolutionary history

of life on earth. We are better equipped today than ever before to understand important concepts in evolution and ecology, such as how ecological interactions shape macroevolutionary and macroecological patterns, and when equilibrium or non-equilibrium dynamics (or both) can explain spatial diversity patterns.

# References

- Abràmoff, M. D., P. J. Magalhães, and S. J. Ram. 2004. Image processing with ImageJ. *Biophotonics international* 11:36–42.
- Ackerly, D. D. 2003. Community assembly, niche conservatism, and adaptive evolution in changing environments. *International Journal of Plant Sciences* 164:S165–S184.
- Adler, P. B., E. W. Seabloom, E. T. Borer, H. Hillebrand, Y. Hautier, A. Hector, W. S. Harpole, et al. 2011. Productivity is a poor predictor of plant species richness. *Science* 333:1750–1753.
- Adolph, S. C., and W. P. Porter. 1993. Temperature, activity, and lizard life histories. *The American Naturalist* 142:273–295.
- Aizen, M. A., and D. P. Vázquez. 2006. Flowering phenologies of hummingbird plants from the temperate forest of southern South America : Is there evidence of competitive displacement? *Ecography* 29:357–366.
- Aldous, D. 1996. Probability Distributions on Cladograms. Pages 1–18 in D. Aldous and R. Pemantle, eds. *Random Discrete Structures*. Springer, New York.
- Anacker, B. L., and S. Y. Strauss. 2014. The geography and ecology of plant speciation: Range overlap and niche divergence in sister species. *Proceedings of the Royal Society B: Biological Sciences* 281:20132980.
- Andrae, J. W., F. A. McInerney, P. J. Polissar, J. M. K. Sniderman, S. Howard, P. A. Hall, and S. R. Phelps. 2018. Initial Expansion of C4 Vegetation in Australia During the Late Pliocene. *Geophysical Research Letters* 45:4831–4840.
- Aragón, P., J. M. Lobo, M. Á. Olalla-Tárraga, and M. Á. Rodríguez. 2010. The contribution of contemporary climate to ectothermic and endothermic vertebrate distributions in a glacial refuge. *Global Ecology and Biogeography* 19:40–49.
- Archibald, J. D., and D. H. Deutschman. 2001. Quantitative analysis of the timing of the origin and diversification of extant placental orders. *Journal of Mammalian Evolution* 8:107–124.
- Armbruster, W. ., M. E. Edwards, and E. . Debevec. 1994. Floral Character Displacement Generates Assemblage Structure of Western Australian. *Ecology* 75:315–329.
- Armbruster, W. S., and N. Muchhal. 2009. Associations between floral specialization and species diversity: Cause, effect, or correlation? *Evolutionary Ecology* 23:159–179.
- Australian, H. W. 2019. FloraBase—the Western Australian Flora. Department of Biodiversity, Conservation and Attractions.

- Baack, E., M. C. Melo, L. H. Rieseberg, and D. Ortiz-Barrientos. 2015a. The origins of reproductive isolation in plants. *New Phytologist* 207:968–984.
- Baack, E., M. C. Melo, L. H. Rieseberg, and D. Ortiz-Barrientos. 2015b. The origins of reproductive isolation in plants. *New Phytologist* 207:968–984.
- Badgley, C. 2010. Tectonics, topography, and mammalian diversity. *Ecography* 33:220–231.
- Badgley, C., T. M. Smiley, R. Terry, E. B. Davis, L. R. G. DeSantis, D. L. Fox, S. S. B. Hopkins, et al. 2017. Biodiversity and topographic complexity: modern and geohistorical perspectives. *Trends in Ecology and Evolution* 32:211–226.
- Barker, R. M., L. Haegi, and W. R. Barker. 1999. Hakea. *Flora of Australia* 17b:31–170.
- Barluenga, M., K. N. Stölting, W. Salzburger, M. Muschick, and A. Meyer. 2006. Sympatric speciation in Nicaraguan crater lake cichlid fish. *Nature* 439:719–723.
- Barraclough, T. G., and A. P. Vogler. 2000. Detecting the geographic pattern of speciation from species level phylogenies. *American Naturalist* 155:419–434.
- Barraclough, T. G., A. P. Vogler, and P. H. Harvey. 1998. Revealing the factors that promote speciation. *Philosophical Transactions of the Royal Society B: Biological Sciences* 353:241–249.
- Beaulieu, J. M., D. C. Jhueng, C. Boettiger, and B. C. O’Meara. 2012. Modeling stabilizing selection: Expanding the Ornstein-Uhlenbeck model of adaptive evolution. *Evolution* 66:2369–2383.
- Beaulieu, J. M., and B. C. O’Meara. 2016. Detecting hidden diversification shifts in models of trait-dependent speciation and extinction. *Systematic Biology* 65:583–601.
- Beerling, D. J., and C. P. Osborne. 2006. The origin of the savanna biome. *Global Change Biology* 12:2023–2031.
- Bertness, M. D., and R. Callaway. 1994. Positive interactions in communities. *Trends in Ecology and Evolution* 9:187–191.
- BirdLife. 2016. Bird species distribution maps of the world Version 6.
- Bivand, R., E. J. Pebesma, and V. Gomez-Rubio. 2013. Applied spatial data analysis with R (second edi.). Springer, NY, New York.
- Bivand, R., and C. Rundel. 2016. rgeos: Interface to Geometry Engine - Open Source (GEOS). R package version 0.3-20. <https://CRAN.R-project.org/package=rgeos>.
- Bivand, R. S., and D. W. S. Wong. 2018. Comparing implementations of global and local indicators of spatial association. *Test* 27:716–748.

- Blackburn, T. M., and K. J. Gaston. 1997. The relationship between geographic area and the latitudinal gradient in species richness in New World birds. *Evolutionary Ecology* 11:195–204.
- Blomberg, S. P., T. Garland, and A. R. Ives. 2003. Testing for phylogenetic signal in comparative data: Behavioral traits are more labile. *Evolution* 57:717–745.
- Blum, M. G. B., and O. Francois. 2005. On statistical tests of phylogenetic tree imbalance : The Sackin and other indices revisited. *Mathematical Biosciences* 195:141–153.
- Blum, M. G. B., and O. François. 2006. Which random processes describe the tree of life? A large-scale study of phylogenetic tree imbalance. *Systematic Biology* 55:685–691.
- Blum, M. G. B., and O. François. 2010. Non-linear regression models for Approximate Bayesian Computation. *Statistics and Computing* 20:63–73.
- Blum, M. G. B., M. A. Nunes, D. Prangle, and S. A. Sisson. 2013. A Comparative Review of Dimension Reduction Methods in Approximate Bayesian Computation. *Statistical Science* 28:189–208.
- Bolnick, D. I., and B. M. Fitzpatrick. 2007. Sympatric speciation: models and empirical evidence. *Annual Review of Ecology, Evolution, and Systematics* 38:459–87.
- Botero, C. A., R. Dor, C. M. McCain, and R. J. Safran. 2014. Environmental harshness is positively correlated with intraspecific divergence in mammals and birds. *Molecular Ecology* 23:259–268.
- Botta-Dukát, Z. 2005. Rao ' s quadratic entropy as a measure of functional diversity based on multiple traits. *Journal of Vegetation Science* 16:533–540.
- Bowman, D. M. J. S., G. K. Brown, M. F. Braby, and J. R. Brown. 2010. Biogeography of the Australian monsoon tropics. *Journal of Biogeography* 37:201–216.
- Bradshaw, S. D. 1988. Desert reptiles: a case of adaptation or pre-adaptation? *Journal of Arid Environments* 14:155–174.
- Breiman, L. 2001. Random forests. *Machine Learning* 45:5–32.
- Brennan, I. G., and P. M. Oliver. 2017. Mass turnover and recovery dynamics of a diverse Australian continental radiation. *Evolution* 71:1352–1356.
- Brown, J. H. 2014. Why are there so many species in the tropics? *Journal of Biogeography* 41:8–22.
- Brown, J. H., and B. A. Maurer. 1989. Macroecology: The Division of Food and Space among Species on Continents. *Science* 243:1145–1150.

- Brown, W. L., and E. O. Wilson. 1956. Character displacement. *Systematic Zoology* 5:49–64.
- Bruggeman, J., J. Heringa, and B. W. Brandt. 2009. PhyloPars: Estimation of missing parameter values using phylogeny. *Nucleic Acids Research* 37:179–184.
- Buckley, L. B., A. H. Hurlbert, and W. Jetz. 2012. Broad-scale ecological implications of ectothermy and endothermy in changing environments. *Global Ecology and Biogeography* 21:873–885.
- Buckley, L. B., and W. Jetz. 2010. Lizard community structure along environmental gradients. *Journal of Animal Ecology* 79:358–365.
- Buckley, L. B., G. H. Rodda, and W. Jetz. 2008. Thermal and energetic constraints on ectotherm abundance: A global test using lizards. *Ecology* 89:48–55.
- Buckley, L. B., and J. Roughgarden. 2006. A hump-shaped density-area relationship for island lizards. *Oikos* 113:243–250.
- Burhenne, S., D. Jacob, and G. P. Henze. 2011. Sampling based on sobol' sequences for monte carlo techniques applied to building simulations. Pages 1816–1823 inProceedings of Building Simulation 2011: 12th Conference of International Building Performance Simulation Association.
- Bush, G. L. 1994. Sympatric speciation in animals: new wine in old bottles. *Trends in Ecology and Evolution* 9:285–288.
- Byrne, M., D. A. Steane, L. Joseph, D. K. Yeates, G. J. Jordan, D. Crayn, K. Aplin, et al. 2011. Decline of a biome: evolution, contraction, fragmentation, extinction and invasion of the Australian mesic zone biota. *Journal of Biogeography* 38:1635–1656.
- Byrne, M., D. Yeates, L. Joseph, M. Kearney, J. Bowler, M. A. J. Williams, S. Cooper, et al. 2008. Birth of a biome: insights into the assembly and maintenance of the Australian arid zone biota. *Molecular Ecology* 17:4398–4417.
- Cabral, J. S., L. Valente, and F. Hartig. 2017. Mechanistic simulation models in macroecology and biogeography: state-of-art and prospects. *Ecography* 40:267–280.
- Cadotte, M. W., T. J. Davies, and P. R. Peres-Neto. 2017. Why phylogenies do not always predict ecological differences. *Ecological Monographs* 87:535–551.
- Caetano, D. S., B. C. O'Meara, and J. M. Beaulieu. 2018. Hidden state models improve state-dependent diversification approaches, including biogeographical models. *Evolution* 1–17.
- Cardillo, M. 2015. Geographic range shifts do not erase the historic signal of speciation in mammals. *The American Naturalist* 185:343–353.
- Cardillo, M., J. S. Huxtable, and L. Bromham. 2003. Geographic range size, life history and rates of diversification in Australian mammals. *Journal of Evolutionary Biology* 16:282–288.

- Cardillo, M., and R. Pratt. 2013. Evolution of a hotspot genus: Geographic variation in speciation and extinction rates in Banksia (Proteaceae). *BMC Evolutionary Biology* 13:155.
- Cardillo, M., and D. Warren. 2016. Analysing patterns of spatial and niche overlap among species at multiple resolutions. *Global Ecology and Biogeography* 25:951–963.
- Cardillo, M., P. H. Weston, Z. K. M. Reynolds, P. M. Olde, A. R. Mast, E. M. Lemmon, A. R. Lemmon, et al. 2017. The phylogeny and biogeography of Hakea (Proteaceae) reveals the role of biome shifts in a continental plant radiation. *Evolution* 71:1928–1943.
- Castiglione, S., G. Tesone, M. Piccolo, M. Melchionna, A. Mondanaro, C. Serio, M. Di Febbraro, et al. 2018. A new method for testing evolutionary rate variation and shifts in phenotypic evolution. *Methods in Ecology and Evolution* 9:974–983.
- Cavender-Bares, J., D. D. Ackerly, D. A. Baum, and F. A. Bazzaz. 2004. Phylogenetic Overdispersion in Floridian Oak Communities. *American Naturalist* 163:823–843.
- Cavender-Bares, J., A. Keen, and B. Miles. 2006. Phylogenetic structure of Floridian plant communities depends on taxonomic and spatial scale. *Ecology* 87:109–122.
- Cavender-Bares, J., K. H. Kozak, P. V. A. Fine, and S. W. Kembel. 2009. The merging of community ecology and phylogenetic biology. *Ecology Letters* 12:693–715.
- Chesser, R. T., and R. M. Zink. 1994. Modes of speciation in birds: a test of Lynch's method. *Evolution* 48:490–497.
- Chesson, P. 2000. Mechanisms of maintenance of species diversity. *Annual Review of Ecology and Systematics* 31:343–66.
- Chevan, A., and M. Sutherland. 2017. Hierarchical partitioning. *The American Statistician* 45:90–96.
- Clavel, J. 2017. Accelerated body size evolution during cold climatic periods in the Cenozoic 114.
- Collins, B. G., and T. Rebelo. 1987. Pollination biology of the Proteaceae in Australia and southern Africa. *Australian Journal of Ecology* 12:387–421.
- Colwell, R. K., and T. F. Rangel. 2010. A stochastic, evolutionary model for range shifts and richness on tropical elevational gradients under Quaternary glacial cycles. *Philosophical Transactions of the Royal Society B: Biological Sciences* 365:3695–3707.
- Colwell, R. K., and D. K. Winkler. 1984. A Null Model for Null Models in Biogeography. Pages 344–359 in *Ecological Communities: Conceptual Issues and the Evidence*. Princeton University Press.
- Condamine, F. L., M. E. Clapham, and G. J. Kergoat. 2016. Global patterns of insect

- diversification: Towards a reconciliation of fossil and molecular evidence? *Scientific Reports* 6:1–13.
- Cook, L. G., N. B. Hardy, M. D. Crisp, and L. G. Cook. 2015. Three explanations for biodiversity hotspots: Small range size, geographical overlap and time for species accumulation. *An Australian case study. New Phytologist* 207:390–400.
- Cooke, R. S. C., A. E. Bates, and F. Eigenbrod. 2019. Global trade-offs of functional redundancy and functional dispersion for birds and mammals. *Global Ecology and Biogeography* 28:484–495.
- Coomes, D. A., and P. J. Grubb. 2003. Colonization, tolerance, competition and seed-size variation within functional groups. *Trends in Ecology and Evolution* 18:283–291.
- Cooper, N., G. H. Thomas, and R. G. FitzJohn. 2016. Shedding light on the ‘dark side’ of phylogenetic comparative methods. *Methods in Ecology and Evolution* 7:693–699.
- Cornell, H. V. 2013. Is regional species diversity bounded or unbounded? *Biological Reviews* 88:140–165.
- Cowie, R. H., and B. S. Holland. 2006. Dispersal is fundamental to biogeography and the evolution of biodiversity on oceanic islands. *Journal of Biogeography* 33:193–198.
- Cowling, R. M., A. J. Potts, P. L. Bradshaw, M. Arianoutsou, S. Ferrier, F. Forest, M. Fyllas, et al. 2015. Variation in plant diversity in mediterranean-climate ecosystems : the role of climatic and topographical stability. *Journal of Biogeography* 42:552–564.
- Cox, C. L., and R. M. Cox. 2015. Evolutionary shifts in habitat aridity predict evaporative water loss across squamate reptiles. *Evolution* 69:2507–2516.
- Coyne, J. A., and H. A. Orr. 2004. Speciation. Sinauer Associates, Inc, Sunderland, Massachusetts.
- Csilléry, K., M. G. B. Blum, O. E. Gaggiotti, and O. François. 2010. Approximate Bayesian Computation (ABC) in practice. *Trends in Ecology and Evolution* 25:410–418.
- Csilléry, K., O. François, and M. G. B. Blum. 2012. Abc: An R package for approximate Bayesian computation (ABC). *Methods in Ecology and Evolution* 3:475–479.
- Currie, D. J., G. G. Mittelbach, H. V Cornell, R. Field, D. M. Kaufman, E. O. Brien, and J. R. Turner. 2004. Predictions and tests of climate-based hypotheses of broad-scale variation in taxonomic richness. *Ecology Letters* 7:1121–1134.
- Darwin, C. 1859. The origin of species by means of natural selection: or, the preservation of favoured races in the struggle for life. John Murray, London.
- Davies, J. T., S. Meiri, T. G. Barraclough, and J. L. Gittleman. 2007. Species co-existence and character divergence across carnivores. *Ecology Letters* 10:146–152.

- Debastiani, V. J., and V. D. Pillar. 2012. Syncsa-R tool for analysis of metacommunities based on functional traits and phylogeny of the community components. *Bioinformatics* 28:2067–2068.
- Descombes, P., T. Gaboriau, C. Albouy, C. Heine, F. Leprieur, and L. Pellissier. 2018. Linking species diversification to palaeo-environmental changes: A process-based modelling approach. *Global Ecology and Biogeography* 27:233–244.
- Diamond, J. M., and T. J. Case. 1986. *Community Ecology*. Harper & Row.
- Dobzhansky, T. 1950. Evolution in the tropics. *American Scientist* 38:209–211.
- Drury, J., J. Clavel, M. Manceau, and H. Morlon. 2016. Estimating the effect of competition on trait evolution using maximum likelihood inference. *Systematic Biology* 65:700–710.
- Drury, J. P., M. Barnes, A. E. Finneran, M. Harris, and G. F. Grether. 2019. Continent-scale phenotype mapping using citizen scientists' photographs. *Ecography* 1436–1445.
- Drury, J. P., J. A. Tobias, K. J. Burns, and N. A. Mason. 2018. Contrasting impacts of competition on ecological and social trait evolution in songbirds. *PLOS Biology* 16:1–23.
- Duchene, D., X. Hua, and L. Bromham. 2017. Phylogenetic estimates of diversification rate are affected by molecular rate variation. *Journal of Evolutionary Biology* 30:1884–1897.
- Dupin, J., N. J. Matzke, T. Särkinen, S. Knapp, R. G. Olmstead, L. Bohs, and S. D. Smith. 2016. Bayesian estimation of the global biogeographical history of the Solanaceae. *Journal of Biogeography* 44:887–899.
- Dyer, A. G., S. Boyd-Gerny, S. McLoughlin, M. G. P. Rosa, V. Simonov, and B. B. M. Wong. 2012. Parallel evolution of angiosperm colour signals: Common evolutionary pressures linked to hymenopteran vision. *Proceedings of the Royal Society B: Biological Sciences* 279:3606–3615.
- Dynesius, M., and R. Jansson. 2000. Evolutionary consequences of changes in species' geographical distributions driven by Milankovitch climate oscillations. *Proceedings of the National Academy of Sciences* 97:9115–9120.
- Eaton, D. A. R., C. B. Fenster, J. Hereford, S. Q. Huang, and R. H. Ree. 2012. Floral diversity and community structure in *Pedicularis* (Orobanchaceae). *Ecology* 93:182–194.
- Egan, S. P., G. J. Ragland, T. H. Q. Lauren Assour, G. R. H. Powell, S. Emrich, P. Nosil, and J. L. Feder. 2015. Experimental evidence of genome-wide impact of ecological selection during early stages of speciation-with-gene-flow. *Ecology Letters* 18:817–825.
- Elton, C. 1946. Competition and the structure of ecological communities. *Journal of Animal Ecology* 15:54–68.

- Elzinga, J. A., A. Atlan, A. Biere, L. Gigord, A. E. Weis, and G. Bernasconi. 2007. Time after time: flowering phenology and biotic interactions. *Trends in Ecology and Evolution* 22:432–439.
- Esquerré, D., I. G. Brennan, R. A. Catullo, F. Torres-Pérez, and J. S. Keogh. 2019. How mountains shape biodiversity: The role of the Andes in biogeography, diversification, and reproductive biology in South America's most species-rich lizard radiation (Squamata: Liolaemidae). *Evolution* 73:214–230.
- Etienne, R. S., A. L. Pigot, and A. B. Phillimore. 2016. How reliably can we infer diversity-dependent diversification from phylogenies? *Methods in Ecology and Evolution* 7:1092–1099.
- Etienne, R. S., and J. Rosindell. 2012. Prolonging the Past Counteracts the Pull of the Present: Protracted Speciation Can Explain Observed Slowdowns in Diversification. *Systematic Biology* 61:204–213.
- Feder, J. L., S. P. Egan, and P. Nosil. 2012. The genomics of speciation-with-gene-flow. *Trends in Genetics* 28:342–350.
- Feder, J. L., S. M. Flaxman, S. P. Egan, A. A. Comeault, and P. Nosil. 2013. Geographic mode of speciation and genomic divergence. *Annual Review of Ecology, Evolution, and Systematics* 44:73–97.
- Feder, J. L., X. Xie, J. Rull, S. Velez, A. Forbes, B. Leung, H. Dambroski, et al. 2005. Mayr, Dobzhansky, and Bush and the complexities of sympatric speciation in *Rhagoletis*. *Proceedings of the National Academy of Sciences* 102:6573–6580.
- Feldman, A., N. Sabath, R. A. Pyron, I. Mayrose, and S. Meiri. 2016. Body sizes and diversification rates of lizards, snakes, amphisbaenians and the tuatara. *Global Ecology and Biogeography* 25:187–197.
- Fine, P. V. A. 2015a. Ecological and Evolutionary Drivers of Geographic Variation in Species Diversity.
- Fine, P. V. A. 2015b. Ecological and evolutionary drivers of geographic variation in species diversity. *Annual Review of Ecology, Evolution, and Systematics* 46:369–392.
- Fischer, A. G. 1960. Latitudinal variations in organic diversity. *Evolution* 14:64–81.
- Fitzpatrick, B. M., J. A. Fordyce, and S. Gavrilets. 2009. Pattern, process and geographic modes of speciation. *Journal of Evolutionary Biology* 22:2342–2347.
- Fitzpatrick, B. M., and M. Turelli. 2006. The geography of mammalian speciation: mixed signals from phylogenies and range maps. *Evolution* 60:601–615.
- Foote, A. D. 2018. Sympatric Speciation in the Genomic Era. *Trends in Ecology & Evolution* 33:85–95.

- Ford, H. A., D. C. Paton, and N. Forde. 1979. Birds as pollinators of Australian plants. *New Zealand Journal of Botany* 17:509–519.
- Forrest, J., and A. J. Miller-Rushing. 2010. Toward a synthetic understanding of the role of phenology in ecology and evolution. *Philosophical Transactions of the Royal Society B: Biological Sciences* 365:3101–3112.
- Freckleton, R. P., P. H. Harvey, and M. Pagel. 2002. Phylogenetic Analysis and Comparative Data: A Test and Review of Evidence. *The American Naturalist* 160:712–726.
- Freschet, G. T., A. T. C. Dias, D. D. Ackerly, R. Aerts, P. M. Van Bodegom, W. K. Cornwell, M. Dong, et al. 2011. Global to community scale differences in the prevalence of convergent over divergent leaf trait distributions in plant assemblages. *Global Ecology and Biogeography* 20:755–765.
- Fritz, S. A., O. R. P. Bininda-Emonds, and A. Purvis. 2009. Geographical variation in predictors of mammalian extinction risk: Big is bad, but only in the tropics. *Ecology Letters* 12:538–549.
- Gaston, K. J. 1998. Species-range size distributions: products of speciation, extinction and transformation. *Philosophical Transactions of the Royal Society B: Biological Sciences* 353:219–230.
- Gaston, K. J. 2003. The structure and dynamics of geographic ranges. Oxford University Press, Oxford; UK.
- Gavrilets, S., and A. Hastings. 1996. Founder effect speciation: A theoretical reassessment. *American Naturalist* 147:466–491.
- Gavrilets, S., H. Li, and M. D. Vose. 2000. Patterns of parapatric speciation. *Evolution* 54:1126–1134.
- Getz, W. M., and C. C. Wilmers. 2004. A local nearest-neighbor convex-hull construction of home ranges and utilization distributions. *Ecography* 27:489–505.
- Gibson, N., G. Keighery, M. Lyons, and A. Webb. 2004. Terrestrial flora and vegetation of the Western Australian wheatbelt. *Records of the Western Australian Museum Supplement* 67:139–189.
- Givnish, T. J. 2015. Adaptive radiation versus ‘radiation’ and ‘explosive diversification’: why conceptual distinctions are fundamental to understanding evolution. *New Phytologist* 207:297–303.
- Goldberg, E. E., L. T. Lancaster, and R. H. Ree. 2011. Phylogenetic inference of reciprocal effects between geographic range evolution and diversification. *Systematic Biology* 60:451–465.

- Gómez, J. M., F. Perfectti, and J. Lorite. 2015. The role of pollinators in floral diversification in a clade of generalist flowers. *Evolution* 69:863–878.
- Gotelli, N. J. 2000. Null model analysis of species co-occurrence patterns. *Ecology* 81:2606–2621.
- Gotelli, N. J., M. J. Anderson, H. T. Arita, A. Chao, R. K. Colwell, S. R. Connolly, D. J. Currie, et al. 2009. Patterns and causes of species richness: A general simulation model for macroecology. *Ecology Letters* 12:873–886.
- Gould, S. J., and N. Eldredge. 1977. Punctuated equilibria: The tempo and mode of evolution reconsidered. *Paleobiology* 2:115–151.
- Graham, C. H., and P. V. A. Fine. 2008. Phylogenetic beta diversity: Linking ecological and evolutionary processes across space in time. *Ecology Letters* 11:1265–1277.
- Graham, C. H., J. L. Parra, C. Rahbek, and J. A. McGuire. 2010. Phylogenetic structure in tropical hummingbird communities. *Proceedings of the National Academy of Sciences* 107:513–513.
- Grant, V. 1949. Pollination Systems as Isolating Mechanisms in Angiosperms. *Evolution* 3:82–97.
- \_\_\_\_\_. 1994. Modes and origins of mechanical and ethological isolation in angiosperms. *Proceedings of the National Academy of Sciences of the United States of America* 91:3–10.
- Grenyer, R., C. D. L. Orme, S. F. Jackson, G. H. Thomas, R. G. Davies, T. J. Davies, K. E. Jones, et al. 2006. Global distribution and conservation of rare and threatened vertebrates. *Nature* 444:93–96.
- Grinnell, J. 2008. The Niche-Relationships of the California Thrasher. *Auk* 34:427–433.
- Gröning, J., and A. Hochkirch. 2008. Reproductive interference between animal species. *Quarterly Review of Biology* 83:257–282.
- Groom, P., and B. Lamont. 2015. Pollination Syndromes. Pages 126–152 in *Plant Life of Southwestern Australia: Adaptations for Survival*. De Gruyter, Berlin.
- Grossenbacher, D. L., S. D. Veloz, and J. P. Sexton. 2014. Niche and range size patterns suggest that speciation begins in small, ecologically diverged populations in north american monkeyflowers (*Mimulus* spp.). *Evolution* 68:1270–1280.
- Guillerme, T. 2018. dispRity: A modular R package for measuring disparity. *Methods in Ecology and Evolution* 9:1755–1763.
- Guisan, A., and U. Hofer. 2003. Predicting reptile distributions at the mesoscale: Relation to climate and topography. *Journal of Biogeography* 30:1233–1243.

- Hanley, M. E., B. B. Lamont, and W. S. Armbruster. 2009. Pollination and plant defence traits co-vary in Western Australian Hakeas. *New Phytologist* 182:251–260.
- Hardy, O. J. 2008. Testing the spatial phylogenetic structure of local communities: Statistical performances of different null models and test statistics on a locally neutral community. *Journal of Ecology* 96:914–926.
- Harmon, L. J., C. S. Andreazzi, F. Débarre, J. Drury, E. E. Goldberg, A. B. Martins, C. J. Melián, et al. 2019. Detecting the Macroevolutionary Signal of Species Interactions. *Journal of Evolutionary Biology* jeb.13477.
- Harmon, L. J., and S. Harrison. 2015. Species Diversity Is Dynamic and Unbounded at Local and Continental Scales. *The American Naturalist* 185:584–593.
- Harmon, L. J., J. B. Losos, T. Jonathan Davies, R. G. Gillespie, J. L. Gittleman, W. Bryan Jennings, K. H. Kozak, et al. 2010. Early bursts of body size and shape evolution are rare in comparative data. *Evolution* 64:2385–2396.
- Harmon, L. J., J. A. Schulte, A. Larson, and J. B. Losos. 2003. Tempo and mode of evolutionary radiation in iguanian lizards. *Science* 301:961–964.
- Harmon, L. J., J. T. Weir, C. D. Brock, R. E. Glor, and W. Challenger. 2008. GEIGER: investigating evolutionary radiations. *Bioinformatics* 24:129–131.
- Harris, D. J., E. N. Arnold, and R. H. Thomas. 1998. Rapid speciation, morphological evolution, and adaptation to extreme environments in South African sand lizards (*Meroles*) as revealed by mitochondrial gene sequences. *Molecular Phylogenetics and Evolution* 10:37–48.
- Hartigan, J. A., and M. A. Wong. 1979. A K-means clustering algorithm. *Applied Statistics* 28:100–108.
- Harvey, P. H., M. R. May, and S. Nee. 1994. Phylogenies without fossils. *Evolution* 48:523–529.
- Hedges, S. B. 1985. The Influence of size and phylogeny on life history variation in reptiles: a response to Stearns. *American Naturalist* 126:258–260.
- Hennig, C. 2015. fpc: flexible procedures for clustering. R package version 2.1-10. <https://CRAN.R-project.org/package=fpc>.
- Hernández-Hernández, T., and J. J. Wiens. n.d. Why are there so many flowering plants? A multi-scale analysis of plant diversification. *American Naturalist* 0–2.
- Hewitt, G. 2000. The genetic legacy of the Quaternary ice ages. *Nature* 405:907–913.
- Heywood, V. H., D. M. Moore, J. Dunkley, and C. King. 1978. Flowering plants of the world (Vol. 336). Oxford University Press Oxford.

- Hijmans, R. J. 2016. Raster: geographic data analysis and modeling. R package version 2.8-19. <https://CRAN.R-project.org/package=raster>.
- Hijmans, R. J., S. E. Cameron, J. L. Parra, P. G. Jones, and A. Jarvis. 2005. Very high resolution interpolated climate surfaces for global land areas. *International Journal of Climatology* 25:1965–1978.
- Hill, R. S. 2004. Origins of the southeastern Australian vegetation. Pages 1537–1549 in *Philosophical Transactions of the Royal Society B: Biological Sciences* (Vol. 359).
- Holt, R. D. 2003. On the evolutionary ecology of species' ranges. *Evolutionary Ecology Research* 5:159–178.
- Holt, R. D. 2009. Bringing the Hutchinsonian niche into the 21st century: Ecological and evolutionary perspectives. *Proceedings of the National Academy of Sciences* 106:19659–19665.
- Hopper, S. D. 1981. Honeyeaters and their winter food plants on granite rocks in the central wheatbelt of Western Australia. *Wildlife Research* 8:187–197.
- Hopper, S. D. 2009. OCBIL theory: Towards an integrated understanding of the evolution, ecology and conservation of biodiversity on old, climatically buffered, infertile landscapes. *Plant and Soil*.
- Hopper, S. D., and P. Gioia. 2004. The Southwest Australian floristic region: Evolution and conservation of a global hot spot of biodiversity. *Annual Review of Ecology, Evolution, and Systematics* 35:623–650.
- Hopper, S. D., F. A. O. Silveira, and P. L. Fiedler. 2016. Biodiversity hotspots and Ocbil theory. *Plant and Soil*.
- Hua, X., S. Greenhill, M. Cardillo, H. Schneeman, and L. Bromham. 2019. The ecological drivers of variation in global language diversity. *Nature Communications* 10:2047.
- Hubbell, S. P. 2001. *The Unified Neutral Theory of Biodiversity and Biogeography*. Princeton University Press, Princeton.
- Hutchinson, G. E. 1959. Homage to Santa Rosalia or Why Are There So Many Kinds of Animals? *The American Naturalist* 93:145–159.
- Hutchinson, G. E. 1978. *An introduction to population ecology*. Yale University Press, Hew Haven, Connecticut.
- Imhoff, M. L., L. Bounoua, T. Ricketts, C. Loucks, R. Harriss, and W. T. Lawrence. 2004a. Global patterns in net primary productivity. Data distributed by the Socioeconomic Data and Applications Center (SEDAC): <http://sedac.ciesin.columbia.edu/es/hanpp.html>.
- Imhoff, M. L., L. Bounoua, T. Ricketts, C. Loucks, R. Harriss, and W. T. Lawrence. 2004b.

- Global patterns in human consumption of net primary production. *Nature* 429:870–873.
- Ingram, T. 2011. Speciation along a depth gradient in a marine adaptive radiation. *Proceedings of the Royal Society B: Biological Sciences* 278:613–618.
- Ingram, T., and Y. Kai. 2014. The geography of morphological convergence in the radiations of Pacific *Sebastes* rockfishes. *American Naturalist* 184:115–131.
- Jackson, S. T., and J. T. Overpeck. 2010. Responses of Plant Populations and Communities to Environmental Changes of the Late Quaternary. *Paleobiology* 26:194–220.
- James, C. D., and R. Shine. 2000. Why are there so many coexisting species of lizards in Australian deserts? *Oecologia* 125:127–141.
- Janzen, T., S. Höhna, and R. S. Etienne. 2015. Approximate Bayesian Computation of diversification rates from molecular phylogenies: Introducing a new efficient summary statistic, the nLTT. *Methods in Ecology and Evolution* 6:566–575.
- Jetz, W., and P. V. A. Fine. 2012. Global Gradients in Vertebrate Diversity Predicted by Historical Area-Productivity Dynamics and Contemporary Environment. *PLoS Biology* 10:e1001292–e1001292.
- Jetz, W., G. H. Thomas, J. B. Joy, K. Hartmann, and A. O. Mooers. 2012. The global diversity of birds in space and time. *Nature* 491:444–448.
- Johnson, S. D. 1993. Climatic and Phylogenetic Determinants of Flowering Seasonality in the Cape Flora. *Journal of Ecology* 81:567–572.
- Jónsson, H., M. Schubert, A. Seguin-orlando, A. Ginolhac, and L. Petersen. 2014. Speciation with gene flow in equids despite extensive chromosomal plasticity. *Proceedings of the National Academy of Sciences* 111:18655–18660.
- Jordan, D. S. 1905. The origin of species through isolation. *Science* 22:545–562.
- Junker, R. R., N. Blüthgen, and A. Keller. 2015. Functional and phylogenetic diversity of plant communities differently affect the structure of flower-visitor interactions and reveal convergences in floral traits. *Evolutionary Ecology* 29:437–450.
- Kantsa, A., R. A. Raguso, A. G. Dyer, S. P. Sgardelis, J. M. Olesen, and T. Petanidou. 2017. Community-wide integration of floral colour and scent in a Mediterranean scrubland. *Nature Ecology and Evolution* 1:1502–1510.
- Kattge, J., S. Díaz, S. Lavorel, I. C. Prentice, P. Leadley, G. Bönnisch, E. Garnier, et al. 2011. TRY - a global database of plant traits. *Global Change Biology* 17:2905–2935.
- Kay, K. M., and R. D. Sargent. 2009. The Role of Animal Pollination in Plant Speciation: Integrating Ecology, Geography, and Genetics. *Annual Review of Ecology, Evolution, and*

Systematics 40:637–656.

Kembel, S. W., P. D. Cowan, M. R. Helmus, W. K. Cornwell, H. Morlon, D. D. Ackerly, S. P. Blomberg, et al. 2010. Picante: R tools for integrating phylogenies and ecology. Bioinformatics 26:1463–1464.

Kennedy, J. D., M. K. Borregaard, P. Z. Marki, A. Machac, J. Fjeldså, and C. Rahbek. 2018. Expansion in geographical and morphological space drives continued lineage diversification in a global passerine radiation. Proceedings of the Royal Society B: Biological Sciences 285:20182181.

Kew, R. B. G. 2018. Seed Information Database (SID). Version 7.1. Available from: <http://data.kew.org/sid/e>.

Kiester, A. R., R. Lande, and D. W. Schemske. 2016. Models of Coevolution and Speciation in Plants and Their Pollinators. American Naturalist 124:220–243.

Klaus, K. V., and N. J. Matzke. 2020. Statistical Comparison of Trait-Dependent Biogeographical Models Indicates That Podocarpaceae Dispersal Is Influenced by Both Seed Cone Traits and Geographical Distance. Systematic Biology 69:61–75.

Kraft, N. J. B., P. B. Adler, O. Godoy, E. C. James, S. Fuller, and J. M. Levine. 2015. Community assembly, coexistence and the environmental filtering metaphor. Functional Ecology 29:592–599.

Kraft, N. J. B., W. K. Cornwell, C. O. Webb, and D. D. Ackerly. 2007. Trait evolution, community assembly, and the phylogenetic structure of ecological communities. American Naturalist 170:271–283.

Kraft, N. J. B., R. Valencia, and D. D. Ackerly. 2008. Functional traits and niche-based tree community assembly in an Amazonian forest. Science 322:580–582.

Kriticos, D. J., V. Jarosik, and N. Ota. 2014. Extending the suite of BIOCLIM variables : a proposed registry system and case study using principal components analysis. Methods in Ecology and Evolution 5:956–960.

Kuhn, M. 2016. Caret: classification and regression training. R package version 6.0-73.

Laliberte, E., J. B. Grace, M. A. Huston, H. Lambers, P. Teste, B. L. Turner, and D. A. Wardle. 2013. How does pedogenesis drive plant diversity ? Trends in Ecology & Evolution 28:331–340.

Laliberte, E., C. J. Kiely, A. F. Carley, P. Landon, G. J. Hutchings, D. W. Goodman, R. Meyer, et al. 2014a. Environmental filtering explains variation in plant diversity along resource gradients. Science 345:1602–1605.

Laliberte, E., and P. Legendre. 2010. A distance-based framework for measuring functional diversity from multiple traits. Ecology 91:299–305.

- Laliberte, E., P. Legendre, and B. Shipley. 2014b. FD: measuring functional diversity from multiple traits, and other tools for functional ecology. R package version 1.0-12.
- Lamanna, C., B. Blonder, C. Viole, N. J. B. Kraft, B. Sandel, J. C. D. Ii, J. Svenning, et al. 2014. Functional trait space and the latitudinal diversity gradient. *Proceedings of the National Academy of Sciences* 111:13745–13750.
- Lamont, B. ., T. He, and S. . Lim. 2016a. Hakea, the world’s most sclerophyllous genus, arose in southwestern Australian heathland and diversified throughout Australia over the past 12 million years. *Australian Journal of Botany* 64:77–88.
- Lamont, B. B., and P. K. Groom. 1998. Seed and Seedling Biology of the Woody-fruited Proteaceae. *Australian Journal of Botany* 46:387–406.
- Lamont, B. B., M. E. Hanley, P. K. Groom, and T. He. 2016b. Bird pollinators, seed storage and cockatoo granivores explain large woody fruits as best seed defense in Hakea. *Perspectives in Plant Ecology, Evolution and Systematics* 21:55–77.
- Lamont, B. B., and T. He. 2017. When did a Mediterranean-type climate originate in southwestern Australia? *Global and Planetary Change*. Elsevier B.V.
- Landis, M. J., N. J. Matzke, B. R. Moore, and J. P. Huelsenbeck. 2013. Bayesian analysis of biogeography when the number of areas is large. *Systematic Biology* 62:789–804.
- Lefcheck, J. S. 2016. piecewiseSEM: Piecewise structural equation modelling in r for ecology, evolution, and systematics. *Methods in Ecology and Evolution* 7:573–579.
- Legendre, P. 1993. Spatial autocorrelation: trouble or new paradigm? *Ecology* 74:1659–1673.
- Levin, D. A. 2006. Ancient dispersals, propagule pressure, and species selection in flowering plants. *Systematic Botany* 31:443–448.
- Levin, D. A., and W. W. Anderson. 1970. Competition for Pollinators between Simultaneously Flowering Species. *The American Naturalist* 104:455–467.
- Li, K., W. Hong, H. Jiao, G. Wang, K. A. Rodriguez, R. Buffenstein, and Y. Zhao. 2015. Sympatric speciation revealed by genome-wide divergence in the blind mole rat *Spalax*. *Proceedings of the National Academy of Sciences* 112:11905–11910.
- Linder, H. P. 2005. Evolution of diversity: the Cape flora. *Trends in Plant Science* 10:536–541.
- Linder, H. P., and Y. Bouchenak-Khelladi. 2015. The causes of southern African spatial patterns in species richness: Speciation, extinction and dispersal in the Danthonioideae (Poaceae). *Journal of Biogeography* 42:914–924.
- Litsios, G., C. A. Sims, R. O. Wüest, P. B. Pearman, N. E. Zimmermann, and N. Salamin.

2012. Mutualism with sea anemones triggered the adaptive radiation of clownfishes. *BMC Ecology* 12:212.
- Losos, J. B., and R. E. Glor. 2003. Phylogenetic comparative methods and the geography of speciation. *Trends in Ecology and Evolution* 18:220–227.
- Louca, S., and M. W. Pennell. 2020. Extant timetrees are consistent with a myriad of diversification histories. *Nature* 580:502–505.
- Luebert, F., P. Jacobs, H. H. Hilger, and L. A. H. Muller. 2013. Evidence for nonallopatric speciation among closely related sympatric *Heliotropium* species in the Atacama Desert. *Ecology and Evolution* 4:266–275.
- Lynch, J. D. 1989. The gauge of speciation: on the frequencies of modes of speciation. Pages 527–553 in D. Otte and J. . Endler, eds. *Speciation and its consequences*. Sinauer Associates, Inc, Sunderland, Massachusetts.
- MacArthur, R. 1965. Patterns of species diversity. *Biological Reviews of the Cambridge Philosophical Society* 40:510–530.
- MacArthur, R. H. 1972. *Geographical ecology: patterns in the distribution of species*. Princeton University Press, Princeton, New Jersey.
- MacArthur, R., and R. Levins. 1967. The limiting similarity, convergence, and divergence of coexisting species. *American Naturalist* 101:377–385.
- Machac, A., and C. H. Graham. 2017a. Regional diversity and diversification in mammals. *American Naturalist* 189:E1–E13.
- Machac, A., and C. H. Graham. 2017b. Regional diversity and diversification in mammals. *American Naturalist* 189:E1–E13.
- Machac, A., C. H. Graham, and D. Storch. 2018. Ecological controls of mammalian diversification vary with phylogenetic scale. *Global Ecology and Biogeography* 27:32–46.
- MacNally, R. 2000. Regression and model-building in conservation biology , biogeography and ecology : The distinction between – and reconciliation of – ‘predictive’ and ‘explanatory’ models. *Biodiversity and Conservation* 9:655–671.
- Maddison, W. P., P. E. Midford, and S. P. Otto. 2007. Estimating a binary character’s effect on speciation and extinction. *Systematic Biology* 56:701–710.
- Maestri, R., L. R. Monteiro, R. Fornel, N. S. Upham, B. D. Patterson, T. Renato, and O. De Freitas. 2017. The ecology of a continental evolutionary radiation: Is the radiation of sigmodontine rodents adaptive? *Evolution* 71:610–632.
- Mahler, D. L., L. J. Revell, R. E. Glor, and J. B. Losos. 2010. Ecological opportunity and the rate of morphological evolution in the diversification of the Greater Antillean anoles.

Evolution 64:2731–2745.

Maliet, O., F. Hartig, and H. Morlon. 2019. A model with many small shifts for estimating species-specific diversification rates. *Nature Ecology and Evolution* 3:1086–1092.

Marki, P. Z., K. A. Jønsson, M. Irestedt, J. M. T. Nguyen, C. Rahbek, and J. Fjeldså. 2017. Supermatrix phylogeny and biogeography of the Australasian Meliphagidae radiation (Aves: Passeriformes). *Molecular Phylogenetics and Evolution* 107:516–529.

Marki, P. Z., J. D. Kennedy, C. R. Cooney, C. Rahbek, and J. Fjeldså. 2019. Adaptive radiation and the evolution of nectarivory in a large songbird clade. *Evolution* 73:1226–1240.

Marshall, C. R. 2017. Five palaeobiological laws needed to understand the evolution of the living biota. *Nature Ecology & Evolution* 1:1–6.

Marshall, C. R., and T. B. Quental. 2016. The uncertain role of diversity dependence in species diversification and the need to incorporate time-varying carrying capacities. *Philosophical Transactions of the Royal Society of London B* 371:20150217.

Mason, N. W. H., P. Irz, C. Lanoiselée, D. Mouillot, and C. Argillier. 2008. Evidence that niche specialization explains species-energy relationships in lake fish communities. *Journal of Animal Ecology* 77:285–296.

Mason, N. W. H., D. Mouillot, W. G. Lee, and J. B. Wilson. 2005. Functional richness, functional evenness and functional divergence: the primary components of functional diversity. *Oikos* 111:112–118.

Mast, A. R., E. F. Milton, E. H. Jones, R. M. Barker, W. R. Barker, and P. H. Weston. 2012. Time-calibrated phylogeny of the woody Australian genus Hakea (Proteaceae) supports multiple origins of insect-pollination among bird-pollinated ancestors. *American Journal of Botany* 99:472–487.

Matzke, N. J. 2013a. Probabilistic historical biogeography: new models for founder-event speciation, imperfect detection, and fossils allow improved accuracy and model-testing. *Frontiers of Biogeography* 5:242–248.

———. 2013b. BioGeoBEARS: BioGeography with Bayesian (and likelihood) evolutionary analysis in R Scripts. R package, version 0.2 1:2013.

Matzke, N. J. 2014. Model selection in historical biogeography reveals that founder-event speciation is a crucial process in island clades. *Systematic Biology* 63:951–970.

Mayr, E. 1942. Systematics and the origin of species, from the viewpoint of a zoologist. Harvard University Press, Cambridge, Massachusetts.

———. 1963. Animal species and evolution. Harvard University Press, Cambridge, Massachusetts.

- McEwen, J. R., and J. C. Vamosi. 2010. Floral colour versus phylogeny in structuring subalpine flowering communities. *Proceedings of the Royal Society B: Biological Sciences* 277:2957–2965.
- McGill, B. J. 2019. The what, how and why of doing macroecology. *Global Ecology and Biogeography* 28:6–17.
- McGill, B. J., J. M. Chase, J. Hortal, I. Overcast, A. J. Rominger, J. Rosindell, P. A. V. Borges, et al. 2019. Unifying macroecology and macroevolution to answer fundamental questions about biodiversity. *Global Ecology and Biogeography* 28:1925–1936.
- McGill, B. J., B. J. Enquist, E. Weiher, and M. Westoby. 2006. Rebuilding community ecology from functional traits. *Trends in Ecology and Evolution* 21:178–185.
- McWilliam, M., M. O. Hoogenboom, A. H. Baird, C.-Y. Kuo, J. S. Madin, and T. P. Hughes. 2018. Biogeographical disparity in the functional diversity and redundancy of corals. *Proceedings of the National Academy of Sciences* 115:3084–3089.
- Meiri, S. 2010. Length weight allometries in lizards. *Journal of Zoology* 281:218–226.
- Meiri, S. 2018. Traits of lizards of the world : Variation around a successful evolutionary design. *Global Ecology and Biogeography* 27:1168–1172.
- Metallinou, M., E. N. Arnold, P. Crochet, P. Geniez, J. C. Brito, P. Lymberakis, S. Baha, et al. 2012. Conquering the Sahara and Arabian deserts: systematics and biogeography of *Stenodactylus* geckos (Reptilia: Gekkonidae). *BMC Evolutionary Biology* 12:258.
- Miller, E. C., K. T. Hayashi, D. Song, and J. J. Wiens. 2018. Explaining the ocean's richest biodiversity hotspot and global patterns of fish diversity. *Proceedings of the Royal Society B: Biological Sciences* 285:20181314.
- Miller, E. T., D. R. Farine, and C. H. Trisos. 2017a. Phylogenetic community structure metrics and null models : a review with new methods and software. *Ecography* 40:461–477.
- Miller, E. T., S. K. Wagner, L. J. Harmon, and R. E. Ricklefs. 2017b. Radiating despite a Lack of character: ecological divergence among closely related, morphologically similar honeyeaters (Aves: Meliphagidae) co-occurring in arid Australian environments. *American Naturalist* 189:14–30.
- Mittelbach, G. G., and D. W. Schemske. 2015. Ecological and evolutionary perspectives on community assembly. *Trends in Ecology & Evolution* 30:241–247.
- Moen, D., and H. Morlon. 2014. Why does diversification slow down ? *Trends in Ecology & Evolution* 29:190–197.
- Moreira-Hernández, J. I., and N. Muchhal. 2019. Importance of Pollinator-Mediated Interspecific Pollen Transfer for Angiosperm Evolution. *Annual Review of Ecology, Evolution, and Systematics* 50:191–217.

- Morlon, H. 2014. Phylogenetic approaches for studying diversification. *Ecology Letters* 17:508–525.
- Mouchet, M. A., S. Villeger, N. W. H. Mason, and D. Mouillot. 2010. Functional diversity measures: an overview of their redundancy and their ability to discriminate community assembly rules. *Functional Ecology* 24:867–876.
- Muchhalal, N., S. Johnsen, and S. D. Smith. 2014. Competition for hummingbird pollination shapes flower color variation in andean solanaceae. *Evolution* 68:2275–2286.
- Nee, S., A. O. Mooers, and P. H. Harvey. 1992. Tempo and mode of evolution revealed from molecular phylogenies. *Proceedings of the National Academy of Sciences* 89:8322–8326.
- Neilson, K. A. 2002. Evaporative water loss as a restriction on habitat use in endangered New Zealand endemic skinks. *Journal of Herpetology* 36:342–348.
- Niet, T. Van Der, and S. D. Johnson. 2009. Molecular Phylogenetics and Evolution Patterns of plant speciation in the Cape floristic region. *Molecular Phylogenetics and Evolution* 51:85–93.
- Nosil, P. 2008. Speciation with gene flow could be common. *Molecular ecology* 17:2006–2008.
- Nychka, D., R. Furrer, J. Paige, and S. Sain. 2017. Fields: Tools for spatial data. R package version 9.6.
- O’Meara, B. C., S. D. Smith, W. S. Armbruster, L. D. Harder, C. R. Hardy, L. C. Hileman, L. Hufford, et al. 2016. Non-equilibrium dynamics and floral trait interactions shape extant angiosperm diversity. *Proceedings of the Royal Society B: Biological Sciences* 283.
- Oliveira, B. F., A. Machac, G. C. Costa, T. M. Brooks, A. D. Davidson, C. Rondinini, and C. H. Graham. 2016. Species and functional diversity accumulate differently in mammals. *Global Ecology and Biogeography* 25:1119–1130.
- Onstein, R. E., R. J. Carter, Y. Xing, and H. P. Linder. 2014. Perspectives in Plant Ecology , Evolution and Systematics Diversification rate shifts in the Cape Floristic Region : The right traits in the right place at the right time. *Perspectives in Plant Ecology, Evolution and Systematics* 16:331–340.
- Onstein, R. E., G. J. Jordan, H. Sauquet, P. H. Weston, Y. Bouchenak-Khelladi, R. J. Carpenter, and H. P. Linder. 2016. Evolutionary radiations of Proteaceae are triggered by the interaction between traits and climates in open habitats. *Global Ecology and Biogeography* 25:1239–1251.
- Ordonez, A., and J. C. Svenning. 2018. Greater tree species richness in eastern North America compared to Europe is coupled to denser, more clustered functional trait space filling, not to trait space expansion. *Global Ecology and Biogeography* 27:1288–1299.

- Orme, C. D. L., R. P. Freckleton, G. H. Thomas, T. Petzoldt, S. A. Fritz, N. Isaac, and W. D. Pearse. 2018. *caper*: Comparative Analyses of Phylogenetics and Evolution in R. R package version 1.0.1.
- Pagel, M. 1999. Inferring historical patterns of biological evolution. *Nature* 401:877–884.
- Pake, C., and D. L. Venable. 1996. Seed banks in desert annuals 77:1427–1435.
- Paradis, E., J. Claude, and K. Strimmer. 2004. APE: analyses of phylogenetics and evolution in R language. *Bioinformatics* 20:289–290.
- Parmesan, C. 2006. Ecological and evolutionary responses to recent climate change. *Annual Review of Ecology, Evolution, and Systematics* 37:637–671.
- Pärtel, M., J. A. Bennett, and M. Zobel. 2016. Macroecology of biodiversity : disentangling local and regional effects. *New Phytologist* 211:404–410.
- Pastro, L. A., C. R. Dickman, and M. Letnic. 2013. Effects of wildfire, rainfall and region on desert lizard assemblages: the importance of multi-scale processes. *Oecologia* 173:603–614.
- Pauw, A. 2013. Can pollination niches facilitate plant coexistence? *Trends in Ecology and Evolution* 28:30–37.
- . 2019. A Bird ' s-Eye View of Pollination : Biotic Interactions as Drivers of Adaptation and Community Change. *Annual Review of Ecology, Evolution, and Systematics* 50:1–26.
- Peakall, R., D. Ebert, J. Poldy, R. A. Barrow, W. Francke, C. C. Bower, and F. P. Schiestl. 2010. Pollinator specificity, floral odour chemistry and the phylogeny of Australian sexually deceptive Chiloglottis orchids: implications for pollinator-driven speciation. *New Phytologist* 188:437–450.
- Pebesma, E. J. 2004. Multivariable geostatistics in S: the gstat package. *Computers & Geosciences* 30:683–691.
- Penone, C., A. D. Davidson, K. T. Shoemaker, M. Di Marco, T. M. Brooks, B. E. Young, C. H. Graham, et al. 2014. Imputation of missing data in life-history trait datasets : which approach performs the best? *Methods in Ecology and Evolution* 5:961–970.
- Phillimore, A. B., C. D. L. Orme, G. H. Thomas, T. M. Blackburn, P. M. Bennett, K. J. Gaston, and I. P. F. Owens. 2008. Sympatric speciation in birds is rare: insights from range data and simulations. *The American Naturalist* 171:646–657.
- Phillimore, A. B., and T. D. Price. 2008. Density-dependent cladogenesis in birds. *PLoS Biology* 6:0483–0489.
- Pianka, E. R. 1973. The structure of lizard communities. *Annual Review of Ecology and Systematics* 4:53–74.

- Pianka, E. R., and L. J. Vitt. 2003. Lizards: windows to the evolution of diversity. University of California Press, USA.
- Pie, M. R., L. L. F. Campos, A. L. S. Meyer, and A. Duran. 2017. The evolution of climatic niches in squamate reptiles. *Proceedings of the Royal Society B: Biological Sciences* 284:20170268.
- Pigot, A. L., and R. S. Etienne. 2015. A new dynamic null model for phylogenetic community structure. *Ecology Letters* 18:153–163.
- Pigot, A. L., W. Jetz, C. Sheard, and J. A. Tobias. 2018. The macroecological dynamics of species coexistence in birds. *Nature Ecology & Evolution* 2:1112–1119.
- Pigot, A. L., A. B. Phillimore, I. P. F. Owens, and C. D. L. Orme. 2010. The shape and temporal dynamics of phylogenetic trees arising from geographic speciation. *Systematic Biology* 59:660–673.
- Pigot, A. L., and J. A. Tobias. 2013. Species interactions constrain geographic range expansion over evolutionary time. *Ecology Letters* 16:330–338.
- . 2014. Dispersal and the transition to sympatry in vertebrates. *Proceedings of the Royal Society B: Biological Sciences* 282:20141929.
- Pigot, A. L., C. H. Trisos, and J. A. Tobias. 2016. Functional traits reveal the expansion and packing of ecological niche space underlying an elevational diversity gradient in passerine birds. *Proceedings of the Royal Society B: Biological Sciences* 283:1–9.
- Pincheira-Donoso, D., D. J. Hodgson, and T. Tregenza. 2008. The evolution of body size under environmental gradients in ectotherms: why should Bergmann's rule apply to lizards? *BMC Evolutionary Biology* 8:68.
- Pinho, C., and J. Hey. 2010. Divergence with gene flow: models and data. *Annual Review of Ecology, Evolution, and Systematics* 41:215–230.
- Pirie, M. D., E. G. H. Oliver, A. M. De Kuppler, B. Gehrke, N. C. Le Maitre, M. Kandziora, and D. U. Bellstedt. 2016. The biodiversity hotspot as evolutionary hot-bed: spectacular radiation of Erica in the Cape Floristic Region. *BMC Evolutionary Biology* 16:1–11.
- Pitteloud, C., N. Arrigo, T. Suchan, A. Mastretta-yanes, J. Herna, E. Brockmann, R. Vila, et al. 2017. Climatic niche evolution is faster in sympatric than allopatric lineages of the butterfly genus Pyrgus. *Proceedings of the Royal Society B: Biological Sciences* 284:20170208.
- Podani, J. 1999. Extending Gower's general coefficient of similarity to ordinal characters. *Taxon* 48:331–340.
- Poelstra, J. W., E. J. Richards, and C. H. Martin. 2018. Speciation in sympatry with ongoing

- secondary gene flow and a potential olfactory trigger in a radiation of Cameroon cichlids. *Molecular Ecology* 27:4270–4288.
- Pontarp, M., L. Bunnefeld, J. S. Cabral, R. S. Etienne, S. A. Fritz, R. Gillespie, C. H. Graham, et al. 2019. The Latitudinal Diversity Gradient: Novel Understanding through Mechanistic Eco-evolutionary Models. *Trends in Ecology and Evolution* 34:211–223.
- Pontarp, M., J. Ripa, and P. Lundberg. 2012. On the origin of phylogenetic structure in competitive metacommunities. *Evolutionary Ecology Research* 14:269–284.
- . 2015. The Biogeography of Adaptive Radiations and the Geographic Overlap of Sister Species. *The American Naturalist* 186:565–581.
- Pontarp, M., and J. J. Wiens. 2017. The origin of species richness patterns along environmental gradients: uniting explanations based on time, diversification rate and carrying capacity. *Journal of Biogeography* 44:722–735.
- Powney, G. D., R. Grenyer, C. D. L. Orme, I. P. F. Owens, and S. Meiri. 2010. Hot, dry and different: Australian lizard richness is unlike that of mammals, amphibians and birds. *Global Ecology and Biogeography* 19:386–396.
- Preston, F. W. 1948. The Commonness, And Rarity, of Species. *Ecology* 29:254–283.
- Pudlo, P., J.-M. Marin, A. Estoup, J. Cornuet, M. Gauthier, and P. Robert, Christian. 2016. Reliable ABC model choice via random forests. *Bioinformatics* 32:859–866.
- Purvis, A., J. Gittleman, and T. Brooks. 2005. Phylogeny and Conservation. *Conservation Biology*. Cambridge University Press, Cambridge.
- Pybus, O. G., and P. H. Harvey. 2000. Testing macro-evolutionary models using incomplete molecular phylogenies. *Proceedings of the Royal Society B: Biological Sciences* 267:2267–2272.
- Pyron, A. R., and J. J. Wiens. 2013. Large-scale phylogenetic analyses reveal the causes of high tropical amphibian diversity. *Proceedings of the Royal Society B: Biological Sciences* 280:20131622.
- Pyron, R. ., F. T. Burbrink, and J. J. Wiens. 2013. A phylogeny and revised classification of Squamata , including 4161 species of lizards and snakes. *BMC Evolutionary Biology* 13:93.
- Pyron, R. A. 2014. Temperate extinction in squamate reptiles and the roots of latitudinal diversity gradients. *Global Ecology and Biogeography* 23:1126–1134.
- Qiao, H., E. E. Saupe, J. Soberón, A. T. Peterson, and C. E. Myers. 2016. Impacts of niche breadth and dispersal ability on macroevolutionary patterns. *The American Naturalist* 188:149–162.
- Rabosky, D. L. 2013a. Ecological Speciation , and the Role of Competition in

Macroevolution.

Rabosky, D. L. 2013b. Diversity-dependence, ecological speciation, and the role of competition in macroevolution. *Annual Review of Ecology, Evolution, and Systematics* 44:481–502.

Rabosky, D. L., and A. H. Hurlbert. 2015a. Species Richness at Continental Scales Is Dominated by Ecological Limits. *The American Naturalist* 185:572–583.

Rabosky, D. L., and A. H. Hurlbert. 2015b. Species richness at continental scales Is dominated by ecological limits. *American Naturalist* 185:572–583.

Rahbek, C. 2005. The role of spatial scale and the perception of large-scale species-richness patterns. *Ecology Letters* 8:224–239.

Rangel, T. F., A. F. Diniz-filho, and R. K. Colwell. 2007. Species richness and evolutionary niche dynamics: a spatial pattern-oriented simulation experiment. *American Naturalist* 170:602–616.

Rangel, T. F., N. R. Edwards, P. B. Holden, J. A. F. Diniz-Filho, W. D. Gosling, M. T. P. Coelho, F. A. S. Cassemiro, et al. 2018. Modeling the ecology and evolution of biodiversity: Biogeographical cradles, museums, and graves. *Science* 361:5452.

Raup, D. ., and J. J. Sepkoski. 1982. Mass Extinctions in the Marine Fossil Record. *Science* 215:1501–1504.

Raup, D. M., S. J. Gould, T. J. Schopf, and D. S. Simberloff. 1973. Stochastic Models of Phylogeny and the Evolution of Diversity. *Journal of Geology* 81:525–542.

Ree, R. H., and S. A. Smith. 2008. Maximum Likelihood Inference of Geographic Range Evolution by Dispersal, Local Extinction, and Cladogenesis. *Systematic Biology* 57:4–14.

Rees, M., and M. Westoby. 1997. Game-Theoretical Evolution of Seed Mass in Multi-Species Ecological Models. *Oikos* 78:116–126.

Revell, L. J. 2009. Size-correction and principal components for interspecific comparative studies. *Evolution* 63:3258–3268.

Revell, L. J. 2012. Phytools: an R package for phylogenetic comparative biology (and other things). *Methods in Ecology and Evolution* 3:217–223.

Reyes, E., H. Morlon, and H. Sauquet. 2015. Presence in Mediterranean hotspots and floral symmetry affect speciation and extinction rates in Proteaceae. *New Phytologist* 207:401–410.

Ricklefs, R. E. 2004. A comprehensive framework for global patterns in biodiversity. *Ecology Letters*.

- Ricklefs, R. E., and D. Schlüter. 1993. Species diversity in ecological communities : historical and geographical perspectives. (R. E. Ricklefs & D. Schlüter, eds.). University of Chicago Press, Chicago.
- Rieseberg, L. H., and J. H. Willis. 2007. Plant speciation. *Science*.
- Rodríguez-Gironés, M. A., and L. Santamaría. 2004. Why are so many bird flowers red? *PLoS Biology* 2.
- Rohde, K. 2006. Nonequilibrium ecology. Cambridge University Press, Cambridge, United Kingdom.
- Rohde, R. A., and R. A. Muller. 2005. Cycles in fossil diversity. *Nature* 434:208–210.
- Roll, U., A. Feldman, M. Novosolov, A. Allison, A. M. Bauer, R. Bernard, M. Böhm, et al. 2017. The global distribution of tetrapods reveals a need for targeted reptile conservation. *Nature Ecology and Evolution* 1:1677–1682.
- Rolshausen, G., T. J. Davies, and A. P. Hendry. 2018. Evolutionary Rates Standardized for Evolutionary Space: Perspectives on Trait Evolution. *Trends in Ecology and Evolution* 33:379–389.
- Roncal, J., A. Henderson, F. Borchsenius, S. R. S. Cardoso, and H. Balslev. 2012. Can phylogenetic signal, character displacement, or random phenotypic drift explain the morphological variation in the genus Geonoma (Arecaceae)? *Biological Journal of the Linnean Society* 106:528–539.
- Ronquist, F. 1997. Dispersal-vicariance analysis: a new approach to the quantification of historical biogeography. *Systematic Biology* 46:195–203.
- Rosauer, D. A. N., S. W. Laffan, M. D. Crisp, and S. C. Donnellan. 2009. Phylogenetic endemism : a new approach for identifying geographical concentrations of evolutionary history. *Molecular Ecology* 18:4061–4072.
- Rosenzweig, M. L. 1978. Geographical speciation: on range size and the probability of isolate formation. Pages 172–194 in D. Wollkind, ed. *Proceedings of the Washington State University Conference on Biomathematics and Biostatistics*. Washington State University, Pullman, WA.
- Rosser, N., K. M. Kozak, A. B. Phillimore, and J. Mallet. 2015. Extensive range overlap between heliconiine sister species: evidence for sympatric speciation in butterflies? *BMC Evolutionary Biology* 15:125.
- Roy, K., and E. E. Goldberg. 2007. Origination, extinction, and dispersal: Integrative models for understanding present-day diversity gradients. *American Naturalist* 170:S71–S85.
- Rundell, R. J., and T. D. Price. 2009. Adaptive radiation, nonadaptive radiation, ecological speciation and nonecological speciation. *Trends in Ecology & Evolution* 24:394–399.

- Rundle, H., and P. Nosil. 2005. Ecological speciation. *Ecology Letters* 8:336–352.
- Sabath, N., E. E. Goldberg, L. Glick, M. Einhorn, T. Ashman, R. Ming, S. P. Otto, et al. 2016. Dioecy does not consistently accelerate or slow lineage diversification across multiple genera of angiosperms. *New Phytologist* 209:1290–1300.
- Sargent, R. D., and D. D. Ackerly. 2008. Plant-pollinator interactions and the assembly of plant communities. *Trends in Ecology and Evolution* 23:123–130.
- Sauquet, H., and S. Magallón. 2018. Key questions and challenges in angiosperm macroevolution. *New Phytologist* 219:1170–1187.
- Sauquet, H., P. H. Weston, C. L. Anderson, N. P. Barker, D. J. Cantrill, A. R. Mast, and V. Savolainen. 2009. Contrasted patterns of hyperdiversification in Mediterranean hotspots. *Proceedings of the National Academy of Sciences of the United States of America* 106:221–225.
- Savolainen, V., M. Anstett, C. Lexer, I. Hutton, J. J. Clarkson, M. V Norup, M. P. Powell, et al. 2006. Sympatric speciation in palms on an oceanic island. *Nature* 441:9–12.
- Schemske, D. W., G. G. Mittelbach, H. V. Cornell, J. M. Sobel, and K. Roy. 2009. Is there a latitudinal gradient in the importance of biotic interactions? *Annual Review of Ecology, Evolution, and Systematics* 40:245–269.
- Schiestl, F. P., and S. D. Johnson. 2013. Pollinator-mediated evolution of floral signals. *Trends in Ecology and Evolution* 28:307–315.
- Schiestl, F. P., and P. M. Schlüter. 2009. Floral Isolation, Specialized Pollination, and Pollinator Behavior in Orchids. *Annual Review of Entomology* 54:425–446.
- Schlüter, D. 2000. *The Ecology of Adaptive Radiation*. OUP Oxford.
- Schnitzler, J., T. G. Barraclough, J. S. Boatwright, P. Goldblatt, J. C. Manning, M. P. Powell, T. Rebelo, et al. 2011. Causes of plant diversification in the cape biodiversity hotspot of South Africa. *Systematic Biology* 60:343–357.
- Seehausen, O., R. K. Butlin, I. Keller, C. E. Wagner, J. W. Boughman, P. A. Hohenlohe, C. L. Peichel, et al. 2014. Genomics and the origin of species. *Nature Reviews Genetics* 15:176–192.
- Seehausen, O., Y. Terai, I. S. Magalhaes, K. L. Carleton, H. D. J. Mross, R. Miyagi, I. Van Der Sluijs, et al. 2008. Speciation through sensory drive in cichlid fish. *Nature* 455:620–626.
- Sepkoski, J. J. 1978. A kinetic model of Phanerozoic taxonomic diversity I. Analysis of marine orders. *Paleobiology* 4:223–251.
- Sexton, J. P., P. J. McIntyre, A. L. Angert, and K. J. Rice. 2009. Evolution and ecology of

- species range limits. *Annual Review of Ecology, Evolution, and Systematics* 40:415–436.
- Shine, R. 1985. The evolution of viviparity in reptiles: an ecological analysis. Pages 605–694 in C. Gans and F. Billet, eds. *Biology of the Reptilia*. Volume 15. Development B. John Wiley & Sons, New York.
- Shine, R. 2004. Does viviparity evolve in cold climate reptiles because pregnant females maintain stable (not high) body temperatures? *Evolution* 58:1809–1818.
- Shipley, B. 2000. A New Inferential Test for Path Models Based on Directed Acyclic Graphs. *Structural Equation Modeling: A Multidisciplinary Journal* 7:206–218.
- Silvertown, J., M. E. Dodd, D. J. G. Gowing, and J. O. Mountford. 1999. Hydrologically defined niches reveal a basis for species richness in plant communities. *Nature* 400:61–63.
- Silvertown, J., M. Dodd, D. Gowing, C. Lawson, and K. McConway. 2006. Phylogeny and the hierarchical organization of plant diversity. *Ecology* 87:39–49.
- Simberloff, D. 1976. Experimental Zoogeography of Islands: Effects of Island Size. *Ecology* 57:629–648.
- Simões, M., L. Breitkreuz, M. Alvarado, S. Baca, J. C. Cooper, L. Heins, K. Herzog, et al. 2016. The Evolving Theory of Evolutionary Radiations. *Trends in Ecology & Evolution* 31:27–34.
- Simpson, G. G. 1953. The major features of evolution. Columbia biological series no. 17. Columbia University Press, New York.
- Skeels, A. 2019. Lineages through space and time plots: Visualising spatial and temporal changes in diversity. *Frontiers of Biogeography* 11:0–6.
- Skeels, A., and M. Cardillo. 2017. Environmental niche conservatism explains the accumulation of species richness in Mediterranean-hotspot plant genera. *Evolution* 71:582–594.
- Skeels, A., and M. Cardillo. 2019a. Equilibrium and non-equilibrium phases in the radiation of Hakea and the drivers of diversity in Mediterranean-Type Ecosystems. *Evolution* 73:1392–1410.
- Skeels, A., and M. Cardillo. 2019b. Reconstructing the geography of speciation from contemporary biodiversity data. *American Naturalist* 193:240–255.
- Skeels, A., D. Esquerré, and M. Cardillo. 2019. Alternative pathways to diversity across ecologically distinct lizard radiations. *Global Ecology and Biogeography* 454–469.
- Slater, G. J. 2013. Phylogenetic evidence for a shift in the mode of mammalian body size evolution at the Cretaceous-Palaeogene boundary. *Methods in Ecology and Evolution* 4:734–744.

- Smith, J. R., A. D. Letten, P.-J. Ke, C. B. Anderson, J. N. Hendershot, M. K. Dhami, G. A. Dlott, et al. 2018. A global test of ecoregions. *Nature Ecology & Evolution* 2:1889–1896.
- Sniderman, J. M. K., G. J. Jordan, and R. M. Cowling. 2013. Fossil evidence for a hyperdiverse sclerophyll flora under a non-Mediterranean-type climate. *Proceedings of the National Academy of Sciences of the United States of America* 110:3423–3428.
- Spasojevic, M. J., and K. N. Suding. 2012. Inferring community assembly mechanisms from functional diversity patterns : the importance of multiple assembly processes 652–661.
- Srivastava, D. S., and J. H. Lawton. 1998. Why more productive sites have more species: an experimental test of theory using tree-hole communities. *The American Naturalist* 152:510–529.
- Stekhoven, D. J., and P. Bühlmann. 2012. MissForest - non-parametric missing value imputation for mixed-type data. *Bioinformatics* 28:112–118.
- Stephens, P. R., and J. J. Wiens. 2003. Explaining species richness from continents to communities: The time-for-speciation effect in emydid turtles. *American Naturalist* 161:112–128.
- Storch, D., E. Bodhalkova, and J. Okie. 2018. The more-individuals hypothesis revisited : the role of community abundance in species richness regulation and the productivity – diversity relationship. *Ecology Letters* 21:920–937.
- Storch, D., and J. G. Okie. 2019. The carrying capacity for species richness. *Global Ecology and Biogeography* 28:1519–1532.
- Stroud, J. T., and J. B. Losos. 2016. Ecological opportunity and adaptive radiation. *Annual Review of Ecology, Evolution, and Systematics* 47:507–532.
- Sukumaran, J., E. P. Economo, and L. Lacey Knowles. 2016. Machine learning biogeographic processes from biotic patterns: A new trait-dependent dispersal and diversification model with model choice by simulation-Trained discriminant analysis. *Systematic Biology* 65:525–545.
- Tallowin, O., A. Allison, A. C. Algar, F. Kraus, and S. Meiri. 2017. Papua New Guinea terrestrial-vertebrate richness: elevation matters most for all except reptiles. *Journal of Biogeography* 44:1734–1744.
- Thiele, K., and S. Prober. 2014. Progress and prospects for understanding evolution and diversity in the Southwest Australian flora. *Journal of the Royal Society of Western Australia* 97:35–45.
- Thomas, G. H., K. Hartmann, W. Jetz, J. B. Joy, A. Mimoto, and A. O. Mooers. 2013. PASTIS: An R package to facilitate phylogenetic assembly with soft taxonomic inferences. *Methods in Ecology and Evolution* 4:1011–1017.

- Tiefeldorf, M., D. A. Griffith, and B. Boots. 1999. A variance-stabilizing coding scheme for spatial link matrices. *Environment and Planning A* 31:165–180.
- Title, P. O., and J. B. Bemmels. 2018. ENVIREM: an expanded set of bioclimatic and topographic variables increases flexibility and improves performance of ecological niche modeling. *Ecography* 41:291–307.
- Tonini, J. F. R., K. H. Beard, R. B. Ferreira, W. Jetz, and R. A. Pyron. 2016. Fully-sampled phylogenies of squamates reveal evolutionary patterns in threat status. *Biological Conservation* 204:23–31.
- Troyanskaya, O., M. Cantor, G. Sherlock, P. Brown, T. Hastie, R. Tibshirani, D. Botstein, et al. 2001. Missing value estimation methods for DNA microarrays . *Bioinformatics* 17:520–525.
- Turelli, M., N. H. Barton, and J. A. Coyne. 2001. Theory and speciation. *Trends in Ecology and Evolution* 16:330–343.
- Uetz, P., and J. Hošek. 2019. The reptile database. <http://www.reptile-database.org>.
- Valente, L. M., G. Reeves, J. Schnitzler, I. P. Mason, M. F. Fay, T. G. Rebelo, M. W. Chase, et al. 2009. Diversification of the African genus Protea (Proteaceae) in the Cape biodiversity hotspot and beyond: equal rates in different biomes. *Evolution* 64:745–760.
- Vamosi, J. C., S. Magallón, I. Mayrose, S. P. Otto, and H. Sauquet. 2018. Macroevolutionary Patterns of Flowering Plant Speciation and Extinction. *Annual Review of Plant Biology* 69:685–706.
- Vamosi, J. C., and S. M. Vamosi. 2010. Key innovations within a geographical context in flowering plants: Towards resolving Darwin’s abominable mystery. *Ecology Letters* 13:1270–1279.
- Van Dam, M. H., and N. J. Matzke. 2016. Evaluating the influence of connectivity and distance on biogeographical patterns in the south-western deserts of North America. *Journal of Biogeography* 43:1514–1532.
- Van der Niet, T., and S. D. Johnson. 2012. Phylogenetic evidence for pollinator-driven diversification of angiosperms. *Trends in Ecology and Evolution* 27:353–361.
- Via, S. 2001. Sympatric speciation in animals:the ugly duckling grows up. *Trends in Ecology and Evolution* 16:381–390.
- Vidal-García, M., P. G. Byrne, J. D. Roberts, and J. S. Keogh. 2014. The role of phylogeny and ecology in shaping morphology in 21 genera and 127 species of Australo-Papuan myobatrachid frogs. *Journal of Evolutionary Biology* 27:181–192.
- Vidan, E., A. M. Bauer, F. C. Herrera, L. Chirio, C. de Campos Nogueira, T. M. Doan, M. S. Hoogmoed, et al. 2019. The biogeography of lizard functional groups. *Journal of*

Biogeography 00:1–12.

Vilela, B., and F. Villalobos. 2015. LetsR: A new R package for data handling and analysis in macroecology. *Methods in Ecology and Evolution* 6:1229–1234.

Villeger, S., N. W. H. Mason, and D. Mouillot. 2008. New multidimensional functional diversity indices for a multifaceted framework in functional ecology. *Ecology* 89:2290–2301.

von Humboldt, A. 1807. *Essay on the Geography of Plants*.

Waide, R. B., M. R. Willig, C. F. Steiner, G. Mittelbach, L. Gough, S. I. Dodson, G. P. Juday, et al. 1999. The relationship between productivity and species richness. *Annual Review of Ecology and Systematics* 30:257–300.

Wallace, A. R. 1876. *The Geographical Distribution of Animals: With a Study of the Relations of Living and Extinct Faunas as Elucidating the Past Changes of the Earth's Surface*. Cambridge University Press, Cambridge.

Walsh, C., and R. MacNally. 2013. *hier.part: hierarchical partitioning*. R package version 1.0-4. <https://CRAN.R-project.org/package=hier.part>.

Warren, D. L., M. Cardillo, D. F. Rosauer, and D. I. Bolnick. 2014. Mistaking geography for biology: Inferring processes from species distributions. *Trends in Ecology and Evolution* 29:572–580.

Webb, C. O. 2000. Exploring the phylogenetic structure of ecological communities: An example for rain forest trees. *American Naturalist* 156:145–155.

Webb, C. O., D. D. Ackerly, M. A. Mcpeak, and M. J. Donoghue. 2002. Phylogenies and community ecology. *Annual Review of Ecology and Systematics* 33:475–505.

Weber, M. G., N. I. Cacho, M. J. Q. Phan, C. Disbrow, S. R. Ramírez, and S. Y. Strauss. 2018. The evolution of floral signals in relation to range overlap in a clade of California Jewelflowers (*Streptanthus* s.l.). *Evolution* 72:798–807.

Weber, M. G., L. Mitko, T. Eltz, and S. R. Ramírez. 2016. Macroevolution of perfume signalling in orchid bees. *Ecology Letters* 19:1314–1323.

Weber, M. G., and S. Y. Strauss. 2016. Coexistence in Close Relatives : Beyond Competition and Reproductive Isolation in Sister Taxa. *Annual Review of Ecology, Evolution, and Systematics* 47:359–381.

Weber, M. G., S. Y. Strauss, C. E. Wagner, R. J. Best, L. J. Harmon, and B. Matthews. 2017. Evolution in a community context: on integrating ecological interactions and macroevolution. *Trends in Ecology and Evolution* 32:291–304.

Weiher, E., G. D. P. Clarke, P. A. Keddy, E. Weiher, G. D. P. Clarke, P. A. Keddy, and P. A.

- Community. 1998. Community Assembly Rules , Morphological Dispersion , and the Coexistence of Plant Species. *Oikos* 81:309–322.
- Weihs, C., U. Ligges, K. Luebke, and N. Raabe. 2005. *klaR* Analyzing German Business Cycles. Pages 335–343 in D. Baier, R. Decker, and L. Schmidt-Thieme, eds. *Data Analysis and Decision Support*. Springer-Verlag, Berlin.
- Weller, H. I., and M. W. Westneat. 2019. Quantitative color profiling of digital images with earth mover’s distance using the R package *colordistance*. *PeerJ* 7:e6398.
- Westoby, M., M. Leishman, and J. Lord. 1996. Comparative ecology of seed size and dispersal. *Philosophical Transactions of the Royal Society B: Biological Sciences* 351:1309–1318.
- Wiens, J. J. 2004. Speciation and ecology revisited: phylogenetic niche conservatism and the origin of species. *Evolution* 58:193–197.
- Wiens, J. J. 2011. The Causes Of Species Richness Patterns Across Space, Time, And Clades And The Role Of “Ecological Limits.” *The Quarterly Review of Biology* 86:75–96.
- Wiens, J. J., and M. J. Donoghue. 2004. Historical biogeography, ecology and species richness. *Trends in Ecology and Evolution* 19:639–644.
- Wiens, J. J., N. Engstrom, Tag, and T. Chippindale, Paul. 2006. Rapid diversification, incomplete isolation, and the “speciation clock” in North American salamanders (genus *Plethodon*): testing the hybrid swarm hypothesis of rapid radiation. *Evolution* 60:2585–2603.
- Wiens, J. J., and C. H. Graham. 2005. Niche conservatism: Integrating evolution, ecology, and conservation biology. *Annual Review of Ecology, Evolution, and Systematics* 36:519–539.
- Wiens, J. J., K. H. Kozak, and N. Silva. 2013. Diversity and niche evolution along aridity gradients in north american lizards (phrynosomatidae). *Evolution* 67:1715–1728.
- Winkelmann, K., M. J. Genner, T. Takahashi, and L. Rüber. 2014. Competition-driven speciation in cichlid fish. *Nature Communications* 5.
- Wisz, M. S., J. Pottier, W. D. Kissling, L. Pellissier, C. F. Damgaard, C. F. Dormann, M. C. Forchhammer, et al. 2013. The role of biotic interactions in shaping distributions and realised assemblages of species: Implications for species distribution modelling. *Biological Reviews* 88:15–30.
- Wolf, J. B. W., and H. Ellegren. 2016. Making sense of genomic islands of differentiation in light of speciation. *Nature Reviews Genetics* 18:87–100.
- Zatsepina, O. G., K. A. Ulmasov, S. F. Beresten, V. B. Molodtsov, S. A. Rybtsov, and M. B. Evgen’ev. 2000. Thermotolerant desert lizards characteristically differ in terms of heat-shock system regulation. *Journal of Experimental Biology* 203:1017–1025.

